

SYSTEMS INFORMATICS AND ANALYSIS FOR
OPTIMIZATION OF BIOMASS FEEDSTOCK PROVISION

BY

TAO LIN

DISSERTATION

Submitted in partial fulfillment of the requirements
for the degree of Doctor of Philosophy in Agricultural and Biological Engineering
in the Graduate College of the
University of Illinois at Urbana-Champaign, 2013

Urbana, Illinois

Doctoral Committee:

Associate Professor Luis F. Rodríguez, Chair
Professor K.C. Ting
Professor Hayri Onal
Professor Shaowen Wang

ABSTRACT

Biofuels are a promising renewable transportation fuel that can improve energy security and rural economics. How to develop an efficient and effective biomass production and provision system is important for successful large-scale biofuels production. The overall objective of this dissertation is to develop multiple-scale supply chain optimization models and decision support tools to facilitate biomass production and provision. An interdisciplinary approach, Concurrent Science Engineering and Technology (ConSEnT), was applied to facilitate systems informatics and analysis for optimization of biomass feedstock provision. The ConSEnT approach for large-scale biomass supply chain management was developed through the integration of operations research, geographic information systems (GIS), processing modeling, techno-economic analysis, and cyberinfrastructure.

In this dissertation, three optimization modeling tools and a CyberGIS-enabled biomass feedstock provision decision support platform have been developed to facilitate large-scale biomass feedstock provision.

BioScope model, a strategic planning model, was developed to optimize long-term decisions, such as facility numbers, locations, capacities, and biomass distribution patterns, for a three-stage biomass-biofuel production system. The model was implemented to evaluate Illinois Miscanthus based biofuel supply chain system through minimizing annual Miscanthus-ethanol production costs at different scenarios. The results showed that biorefinery related costs are the most important factor, followed by biomass procurement, transportation, and centralized storage

and preprocessing (CSP) related costs. Cropland usage rate, biomass demand, transportation mode, and facility capacity limit are the key factors affecting the production costs.

To better understand the development of biofuel production, Dynamic BioScope model, a multi-period strategic planning model, was developed to address how a biomass provision system would be best evolved to meet the increasing biofuels production demand over time. The model minimizes total production costs throughout the planning period by optimizing decisions including building and expansion timings, numbers, locations, and capacities of facilities and biomass distribution patterns within the system. The model was applied to evaluate the systems performance of Miscanthus-ethanol production in Illinois from 2012 to 2022. The results showed that Miscanthus-ethanol production costs will be reduced as the system evolved, mainly due to the achievement of the economies of scale through building larger biorefineries and better biomass supply chain infrastructure.

To better understand the interactions between strategic and tactical decisions, an integrated biomass supply chain optimization model was developed to minimize annual biomass-ethanol production costs by optimizing both strategic and tactical planning decisions simultaneously. The numbers, locations, and capacities of facilities as well as biomass and ethanol flow patterns are the key strategic decisions; while biomass production, delivery, and operating schedules as well as inventory monitoring are the key tactical decisions. The model comprises four modules including farm management, logistics planning, facility allocation, and ethanol distribution. The activities optimized by the model range from biomass harvesting, packing, in-field transportation, stacking, transportation, preprocessing, storage, to ethanol production and distribution. The model was implemented to study the Miscanthus-ethanol supply

chain in Illinois. Among the biomass production activities, biomass baling and harvesting are the two most expensive operations. The biomass delivery schedules showed seasonal variations. Sensitivity analysis showed a 50% reduction in biomass yield would increase biofuels production costs by 11%.

A CyberGIS-enabled biomass supply chain decision support platform was developed to improve the accessibility and computing performance of the BioScope model. The platform includes four major components: BioScope optimization model, an interactive CyberGIS Gateway interface, GISolve middleware, and high-performance cyberinfrastructure (CI). The workflow and functions of each component were provided to illustrate the development and usage of the platform. Empowered by high performance CI, the platform improved the computing performance for both single and multiple job submissions. This implementation example could serve as a protocol for further integration development of cyberinfrastructure, operations research, and geospatial analysis.

Keywords: biomass, supply chain optimization, decision support, systems analysis, informatics

To my family

ACKNOWLEDGEMENTS

First and foremost, at the risk of forgetting someone important to me, I would like to acknowledge all the people who helped bring this dissertation to fruition. A project of this magnitude could not possibly have been completed in solitude. I sincerely thank to all of you for the guidance, encouragement, comments, and suggestions.

Dr. Luis F. Rodríguez has been my mentor for six years now. I have been working with him since my first day in the U.S. He has contributed so much to my growth throughout the years, not only on the improvement of my technique skills such as oral and written language, programming skill, research thinking and proposal writing skills, but also on the transferable skills such as communication, collaboration, and project management skills. His consistent encouragement, guidance, and support have led me from the initial to the final level of my dissertation. I can only hope for an opportunity to repay him one day.

Thanks to Dr. K.C. Ting, who has also advised me for six years now. I learned a lot from his passion and vision on agricultural engineering. His solid scientific knowledge, wisdom thinking, and hardworking attitude always inspire me to be a better person.

Thanks to the other two committee members Drs. Shaowen Wang and Hayri Onal for their continuous support and guidance throughout my Ph.D. period. It is my great honor to work with them to gain multi-disciplinary knowledge. This dissertation could not have been possible without both of their inputs.

Thanks to my colleagues working on the project “Engineering Solutions for Biomass Feedstock Production” at the Energy Bioscience Institute, including Drs. Alan Hansen, Yogendra

Shastri, Steven Eckhoff, Tony Grift, Grace-Mary Danao, Zewei Miao, Sunil Mathankar, Liujun Li, and Shih-Fang Chen, and Mr. Yung-Chen Liao. The dissertation would not have been completed without their help, comments, and suggestions.

Thanks to all the members at the BIOMASS Laboratory, especially Glen Menezes, Tong Liu, Graham Kent, Brett Ramirez, Wei-Ting Liao, and Sijie Shi for their help and support.

I would also like to take this opportunity to thank my undergraduate advisor, Dr. Yibin Ying, who always trusts and encourages me to be a better scholar. Without his encouragement and recommendations, this six-year journey at ABE of the University of Illinois might not even be possible. Thank you very much for your trust and support.

Lastly, I would like to thank my family and friends, especially my parents and my wife Lijun Xia who have all been there throughout this long journey. I love you very much.

TABLE OF CONTENTS

CHAPTER 1: INTRODUCTION	1
CHAPTER 2: LITERATURE REVIEW	7
CHAPTER 3: STRATEGIC BIOMASS-ETHANOL SUPPLY CHAIN OPTIMIZATION	17
CHAPTER 4: DYNAMIC BIOMASS-ETHANOL SUPPLY CHAIN OPTIMIZATION	58
CHAPTER 5: INTEGRATED STRATEGIC AND TACTICAL BIOMASS SUPPLY CHAIN OPTIMIZATION	79
CHAPTER 6: CYBERGIS-ENABLED DECISION SUPPORT PLATFORM FOR BIOMASS SUPPLY CHAIN OPTIMIZATION	112
CHAPTER 7: CONCLUSIONS	134
CHAPTER 8: FUTURE WORK	137
REFERENCES	142
APPENDIX A: SUPPLEMENTARY MATERIALS FOR BIOSCOPE MODEL	154
APPENDIX B: SUPPLEMENTARY MATERIALS FOR DYNAMIC BIOSCOPE MODEL	160
APPENDIX C: SUPPLEMENTARY MATERIALS FOR INTEGRATED OPTIMIZATION MODEL	167

CHAPTER 1

INTRODUCTION

Biofuels are a promising renewable transportation fuel under consideration, which can improve energy security, reduce greenhouse gas (GHG) emissions, and develop rural economics (EPA, 2010). With the utilization of renewable biomass feedstock, cellulosic biofuels are considered a major potential component of a future fuel system. To meet the target of 16 billion gallons of cellulosic ethanol production in 2022 (EPA, 2010), more than 200 million Mg of biomass will be required annually; however, few commercial cellulosic ethanol facilities exist due to a lack of a cost-effective technology and reliable feedstock supply. Further, biomass is produced in a distributed manner within a limited harvesting window each year. It is expected that biomass feedstock provision will be a key limiting factor for large-scale biofuels production. Moreover, whether or not the existing supply chain infrastructure is efficient and effective to support large-scale biofuels production remains unknown. There is therefore an urgent need to develop a systems-level decision support platform to optimize both long-term supply chain configurations and short-term operations management for large-scale biofuels production.

The objective of this dissertation is to improve efficiency and effectiveness of large-scale biofuels production through the optimization of biomass supply chain configurations and operations management. For the development of an effective and efficient biomass supply chain, there is a critical need for a new systems modeling approach to integrate and optimize all the components within a biomass provision system. An interdisciplinary approach, Concurrent Science Engineering and Technology (ConSEnT), was proposed to evaluate the performance of complex systems (Liao, 2011). Although ConSEnT was proposed recently, the idea of an

integrated systems thinking approach had been presented before, where the purposes are: 1) to integrate information and knowledge related to the systems under study from various sources in a real-time fashion; 2) to perform systems analysis; and 3) to deliver the results of analysis based on the most updated information (Ting et al., 2003). Similar concepts have been implemented for systems analyses of controlled phytomation systems (Fleisher et al., 2002), advanced life support systems (Rodríguez et al., 2003), and forest (Church et al., 2000) and agricultural residual management (Perimenis et al., 2011; Shastri et al., 2010).

Systems informatics, modeling and analysis, and decision support system are the three components of ConSEnT (Figure 1.1). Systems informatics provides means of transferring both experimental and modeling data to information that could be used for further modeling and systems analysis. It starts with defining the system scope and boundary based on the research objective, followed by the system component identification, data collection and management. Design and development of database is crucial to facilitate information management and sharing. Modeling and analysis aims to develop qualitative and quantitative computational analysis tools to evaluate and optimize systems performance under different scenarios. The key performance indicators of the system are to be defined by decision makers, which may include economic, environmental, and social impacts. Development of decision support platform provides accesses to decision makers through the interactive web interfaces. The computational performance could be further improved through the integration of web interface, cyberinfrastructure, and high-performance distributed computing.

In this study, the ConSEnT approach is applied for large-scale biomass feedstock provision management through the integration of geographic information systems (GIS), operations research, processing modeling, techno-economic analysis, and cyberinfrastructure.

Most agricultural systems are spatial explicit. GIS is used to collect and manage spatial explicit data of biomass feedstock. Operations research provides fundamental methodologies to develop systems optimization and simulation analysis tools. Process modeling is adopted to simulate commercial-scale operating performances (e.g. energy and water usage and equipment capacity) based on the lab-scale biomass preprocessing or conversion experimental data. Techno-economic analysis provides cost-benefit evaluations for different biofuels production technologies under different financial scenarios. Cyberinfrastructure and high-performance distributed computing are incorporated to improve computational efficiency and throughput performance. It is expected that this approach could be expanded to evaluate the system performance for many biomass feedstocks, in many regions, and many end-uses.

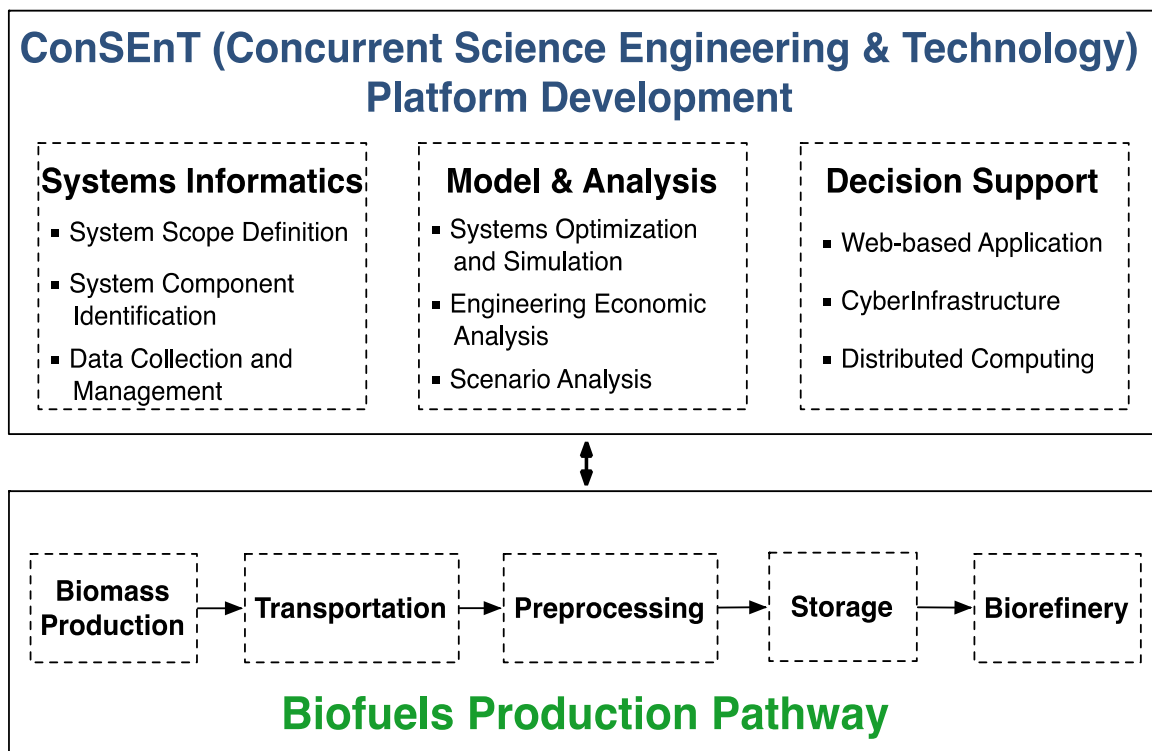


Figure 1.1: The application of the ConSEnT principle on sustainable biofuels pathways

This study will evaluate multiple biofuels production pathways through systems informatics and analysis, primarily through applications of optimization, and identify opportunities and challenges for large-scale biomass feedstock provision. By leveraging high performance distributed cyberinfrastructures, the development of a decision support platform could improve computational efficiency and throughput for large scale applications. The platform will help create an understanding of the complexity of the system and quantify the impact of emerging technologies on the system with web-based spatial visualization. This study contributes to interdisciplinary research collaborations and public knowledge sharing of biofuels production.

The proposed work aims to advance our understandings on large-scale cellulosic biofuels production from engineering and economic perspectives. The following key systems-level questions have been answered:

1. What are the major cost components of cellulosic biofuels production?
2. How do we analyze the interactions between strategic and tactical decisions and how these interactions affect the system performance?
3. How do we quantify the impact of emerging technologies on a large-scale biofuels production system?
4. How do we improve model accessibility and computing performance to improve model applications?

To better answer these key systems-level questions, the dissertation is designed to address the following objectives:

Objective 1: Develop a regional scale biomass supply chain optimization model to address long-term strategic planning challenges.

Objective 2: Integrate both strategic and tactical planning tools to optimize long-term supply chain configurations with the support of short-term operations management.

Objective 3: Establish a CyberGIS enabled decision support platform to facilitate decision-making and knowledge sharing in the context of biofuels production.

The dissertation is organized as follows. Chapter 2 provides a literature review on systems modeling and analysis studies, which includes three parts: 1) an overview of a cellulosic biofuel production system; 2) existing modeling studies on biomass supply chain optimization; and 3) studies on the existing web-based spatial supported decision support platform.

Chapters 3 and 4 focus on strategic biomass supply chain optimization, aiming to identify the major cost components of cellulosic biofuels production by optimizing long-term decisions. Chapter 3 describes the development of a strategic supply chain optimization model, BioScope. The BioScope model is a GIS-enabled mixed integer linear programming model, which minimizes annual biofuel production costs through optimizing the number, location, and capacity of facilities as well as biomass flow patterns. Detailed constraints and objective functions are provided. Several case studies of Miscanthus-ethanol production in Illinois are provided to illustrate the application of the model.

To meet a target of 16 billion gallons of cellulosic ethanol production in 2022 (EPA, 2010), biofuel production infrastructure will undergo significant development. Dynamic, multi-period, strategic supply chain optimization provides an effective tool to evaluate the system development during the rapid development phase. Chapter 4 describes the development of multi-period supply chain optimization for large-scale biofuels production. The model minimizes the total biofuels production costs throughout the planning period by optimizing production timings, numbers, locations, and capacities of facilities and annual biomass procurement and delivery

patterns. The model is implemented to optimize Miscanthus-ethanol production in Illinois from 2012 to 2022 given the projected changes of biomass supply and demand.

Biomass is produced within a limited time but needs to be processed all year round. Understanding how to harvest, store, and deliver biomass to support processing activities is vital to an optimized biomass supply chain. Chapter 5 describes the development of an integrated strategic and tactical biomass supply chain optimization model. The integrated model coordinates and optimizes the interactions between strategic decisions, such as facility location and capacity, and tactical decisions, such as biomass production and delivery schedules. Several case studies of Miscanthus production in Illinois are presented to illustrate the usage of the model.

Model accessibility and computational efficiency are the major limitations for a wide application of developed optimization models. Chapter 6 describes the development of a CyberGIS-enabled decision support platform for biomass supply chain optimization. The platform provides web-based services to support large group applications through the integration of three layers: web-based user interface, CyberGIS middleware, and high-performance distributed cyberinfrastructure. Detailed descriptions of key components and workflow development are presented to illustrate the development cycle. Case studies are presented to show how this platform could improve model computing efficiency for single and multiple job submissions.

Finally, we will summarize the dissertation in Chapter 7 and discuss future research directions in Chapter 8.

CHAPTER 2

LITERATURE REVIEW

Systems informatics, modeling and analysis, and decision support platform development are three components that facilitate complex systems analyses. It is critical to define the scope of a biofuel production system to be modeled prior to systems abstraction and information retrieval. To that end, a literature review of biofuel production systems is presented to illustrate the system components, existing technologies, possible scenarios, and the data describing these components and scenarios. Because of the complexity of a biofuel production system, supply chain optimization is proposed to facilitate effective biomass provision and, generally, three levels of decision-making are considered: strategic, tactical, and operational decisions. A literature review is presented here to describe the existing modeling approaches and tools for strategic and tactical planning of biofuel production. Model accessibility and results visualization are key factors for a good decision support platform. A literature review of spatial supported decision support platform development is also presented.

2.1 BIOMASS-BIOFUEL PRODUCTION SYSTEM

Cellulosic ethanol is considered an important component of a sustainable fuel system (EPA, 2010). However, due to low energy density and distributed supply of biomass, ensuring effective biomass feedstock provision is one of many challenges for large-scale cellulosic biofuels production (Hess et al., 2007). From a systems perspective, a biofuel production system includes the following parts: biomass farm production, transportation, storage, preprocessing, conversion, ethanol distribution and blending, and end consumption (Figure 2.1).



Figure 2.1: The scope of a biofuel production system

Biomass farm production is to grow, harvest, and produce deliverable biomass for processing facilities, which includes the following major steps: biomass planting, harvesting, packing, in-field transportation, handling, and storage. Biomass yield, availability, and its associated production costs are the key factors affecting biomass procurement costs. Because of spatial differences in weather and soils, biomass availability, quality, and production costs vary geographically. Geographical Information Systems (GIS) have been applied to estimate the yields, supplies, and production costs for different feedstocks, including Miscanthus (Khanna et al., 2008), switchgrass (Perrin et al., 2008), and corn stover (Kadam et al., 2003).

Biomass transportation is one of the major challenges of large-scale biofuels production. As compared with other energy resources, biomass has a relatively lower energy and physical

density and is collected from a more distributed manner. Biomass can be transported by truck, train, barge, pipeline, and/or a combination of these transportation modes (Miao et al., 2012). For any single transportation mode, transportation costs are usually composed of distance independent fixed costs and variable distance dependent costs (Mahmudi and Flynn, 2006). Fixed costs are related to biomass loading and unloading costs, which will vary based on the specific form of biomass; while variable distance related costs are dependent on the distance of biomass travelled (Searcy et al., 2007). Among the three transportation modes, truck usually incurs the lowest fixed cost but the highest unit distance related costs; whereas barge usually incurs the highest fixed cost and lowest unit distance related costs. Because of these tradeoffs, studies have been presented to compare the biomass transportation costs by different transportation modes (Mahmudi and Flynn, 2006) and different types of feedstocks (Miao et al., 2012).

Biomass storage is a very critical link in biofuels production system, which serves as a buffer between a short-time window of biomass production and a year-around continuous biomass processing. Biomass can be stored on farm fields, intermediate centralized locations, or next to refineries. Ambient and covered storage are two major storage methods, whereas moisture content and dry matter loss are the key performance indicators for storage (Ebadian et al., 2012). Covered storage incurs higher costs but could reduce annual dry matter loss to 2%, lower than the 15% loss using ambient storage (Brummer et al., 2000). The decisions on the selection of storage location are dependent on the systems demand, facility location, storage method selection, and biomass formats.

Biomass preprocessing, or biomass physical densification, reduces logistics burdens and provides uniform biomass feedstock format for ethanol conversion. Size reduction and

mechanical densification are the two major steps. Depending on the differences of ground particle size and densification pressure, ground biomass with compaction (Hess et al., 2007), briquette (Sokhansanj and Turhollow, 2004), and pellet (Campbell, 2007) are the three major biomass forms after physical densification. The biomass bulk density can be improved from less than approximately 100 kg m^{-3} at a loose condition to a range of 320 to 700 kg m^{-3} given different densification levels. Because of the low energy and physical density of loose biomass, many researchers have been working on the feasibility of developing regional biomass storage and preprocessing depots for large-scale biofuels production (Sokhansanj et al., 2009; Eranki et al., 2011; Shastri et al., 2012a).

Cellulosic biorefineries are to produce renewable fuels from cellulose, hemicellulose, or lignin biomass. High capital investment costs and production costs as well as low conversion efficiency are considered the major challenges for scaling up biofuels production. Although there exists no commercial cellulosic biofuel facility currently, more than ten commercial projects are under development (Brown and Brown, 2013). The current cellulosic ethanol conversion technologies can be grouped into two broad categories: hydrolytic and thermochemical, where a detailed description of each conversion technology and their production and cost status can be found in Dwivedi et al (2009). A process simulation model had been developed to estimate a commercial scale biorefinery using dilute acid pretreatment and enzymatic hydrolysis and co-fermentation (Humbird et al., 2011). The model showed that it would require a capital investment of 422.5 million dollars to build a refinery at annual capacity of 61 million gallons and it would cost \$2.15 per gallon of ethanol production assuming a 76% of conversion efficiency (Humbird et al., 2011).

After production, ethanol will be distributed to blending stations to mix with gasoline for end uses. Ethanol is shipped mainly via truck across the United States (Morrow et al., 2006). Because of its high energy density, ethanol distribution costs were estimated at a \$0.01-0.02 per liter of ethanol, which remains a relatively small fraction of total fuel cost (Morrow et al., 2006).

2.2 BIOMASS SUPPLY CHAIN MANAGEMENT

Supply chain management has been proposed to facilitate effective biomass provision and, generally, three levels of decision-making are considered: strategic, tactical, and operational decisions; we seek to focus in the interplay between strategic and tactical decision-making.

Strategically, biomass resource evaluation and selection of facility location and capacity are important long-term decisions. On the supply side, biomass availability and associated production costs have been evaluated for feedstocks including Miscanthus (Khanna et al., 2008), switchgrass (Perrin et al., 2008), and corn stover (Kadam et al., 2003). On the biomass end-use side, biofuels producers prefer to maintain constant quantity and uniform quality of feedstock (Hess et al., 2007). Large biorefineries could reduce ethanol production costs by \$0.05-0.08 L⁻¹ (\$0.2-0.3 gal⁻¹) as a result of the economies of scale (Kocoloski et al., 2011). However, the larger the biorefinery production capacity, the larger the biomass feedstock supply region, and accordingly the higher the transportation costs. Biomass transportation and storage costs accounted for more than half of biomass (corn stover) costs at biorefinery gate and farmer participation had a significant impact on the total production costs (Leboreiro and Hilaly, 2011). Balancing the trade-off between transportation costs and unit production costs is important for an efficient biomass supply chain design.

Considering the spatial variances of biomass availability and production costs as well as facility economies of scale, optimal facility location and capacity selection and optimal biomass source pattern are key decisions of strategic supply chain optimization. Several models have been presented to optimize strategic planning decisions given a single biomass resource (Panichelli and Gnansounou, 2008; Kim et al., 2011; Lin et al., 2013) and multiple renewable resources (Parker et al., 2010). Most of the previous studies have optimized the biomass supply chain that only includes two stages: biomass suppliers and biorefineries. However, the two-stage supply chain may not be effective for large-scale biofuel production (Hess et al., 2007). Several optimization models have been developed to evaluate the system performance of adopting a three-stage supply chain (Parker et al., 2010; Lin et al., 2013). These strategic planning models provide decision support based on the annual biomass delivery estimations, without much consideration on the tactical planning details.

Tactically, biomass can only be harvested within a limited window due to its standing dry matter loss. Biomass production, delivery, and operating schedules and inventory monitoring are key tactical decisions. Biomass procurement consists of multiple unit operations including biomass harvesting, packing, in-field transportation, and handling. Several biomass supply chain simulation and optimization models have been developed to manage biomass production and delivery activities for different feedstocks, including Miscanthus (Shastri et al., 2010), switchgrass (Kumar and Sokhansanj, 2007; Zhu et al., 2011), corn stover (Sokhansanj et al., 2006; Leboreiro and Hilaly, 2011), and cotton stalks (Tatsiopoulos and Tolis, 2003). These models, however, are based on the given strategic decisions, such as previously determined facility locations and capacities.

Strategic decisions regarding biomass supply chain will impact subsequent tactical decisions. Without the support of biomass delivery, the processing facility cannot achieve its designed operating capacity. Few multi-scale supply chain optimization models have been developed to solve processing facility locations and capacities as well as biomass delivery schedules simultaneously (Eksioglu et al., 2009; Zhang et al., 2013). However, these two studies did not consider other important tactical decisions simultaneously, such as biomass production schedules and farm management issues.

Biomass is harvested within a limited window but needs to be processed all year round. Determining how to harvest, store, and deliver biomass to support the processing activities is vital to optimizing biomass supply chains. Therefore, it is important to coordinate and optimize linkages between biomass production, logistics, and processing on both strategic and tactical levels simultaneously.

In the long run, biofuels production system infrastructure will be expanded in response to its growing demand, expanding from zero to an estimated production volume of 16 billions of gallons in 2022. In addition to the annual biofuel production optimization for strategic and tactical planning, facility construction and expansion timing as well as resource competition are key issues for dynamic system changes. Given the changes of supply and demand in the planning period, dynamic optimization was applied to address facility location and resource allocation issues for biomass-methanol production (Leduc et al., 2010), synthetic biodiesel production (Walther et al., 2012), and biofuels production from multiple feedstock resources (Huang et al., 2010; Chen and Fan, 2012).

2.3 WEB-BASED DECISION SUPPORT SYSTEMS

Decision support systems (DSS) are considered to facilitate management decision making. Data, models and analysis tools, and user interface compromise the major parts for a DSS. With the development of internet and spatial understanding, web-based and spatial-supported are the major improvements for DSS. The development of spatial supported decision support systems (SDSS) origins from the integration of two sources: geographic information systems, which is good at managing and displaying spatial related data, and decision support tools, which is good at providing analytic tools for complex problem solving (Suguraman and Suguraman, 2007). A SDSS incorporates both geographic information systems (GIS) functionalities such as spatial data management, cartographic display, etc., as well as analytical modeling capabilities, a flexible user interface, and complex spatial data structures (Goodchild, 2000). However, model accessibility remains a major bottleneck for the implementation because of hardware and software requirements.

The recent progresses on web technologies have transformed the design, development, implementation, deployment of DSS (Bhargava et al., 2007). The web-based SDSS uses the Web as a medium to collect spatial input information and deploy spatial analysis tools for a much broader audience of decision makers, without any limits on space and time (Bhargava et al., 2007). Web-based SDSS were initially applied to solve material distribution (Prindezis and Kiranoudis, 2005), vehicle routing problems (Ray, 2007; Santos et al., 2011), Recently, it has been applied to renewable energy development, including strategic planning of wind farm (Simao et al., 2009; Mari et al., 2011) and woody based biomass logistics (Frombo et al., 2009), and tactical planning of biomass provision (Liao, 2011). However, these platforms are

concentrated on data analysis and visualization, without much emphasis on harnessing high-performance distributed computing network. Computational efficiency could be a potential bottleneck for large-scale group applications.

Cyberinfrastructure (CI) is designed to integrate computing systems, data storage systems, advanced instruments, and visualization environments together by software and high performance networks to facilitate complex problem solving (Stewart et al., 2010).

Cyberinfrastructure based GIS (CyberGIS) provides a seamless integration of CI, GIS, and spatial modeling analysis, which is becoming important to facilitate large-scale problem solving, model accessibility, and visualization capabilities (Wang et al., 2013). The GISolve Toolkit is one of representative CyberGIS software, which is composed of service-oriented GIS components, spatial middleware, a suite of parallel and distributed GIS algorithms, and a set of user-interface and collaboration services (Wang, 2010). GISolve has been applied to various research areas, including ecological analysis (Wang and Zhu, 2008), geostatistical modeling (Yan et al., 2007), and a spatially explicit agent-based model (Tang and Wang, 2009).

2.4 CONCLUSIONS

The nature of biomass production imposes spatial and temporal constraints that must be considered for successful biofuels production and delivery. A typical cellulosic-ethanol production pathway ranges from biomass growing, harvesting, packing, storage, pre-processing, transportation, to ethanol production and distribution. The components within the system interact with each other. Supply chain optimization has been applied to facilitate the efficiency and effectiveness of biomass feedstock provision. Most studies however focus on strategic level planning optimization given the general assumption of tactical plans, without much emphasis on

the optimization of detailed tactical level planning. In order to facilitate decision making, there is a need to develop an integrated strategic and tactical modeling tool to understand, evaluate, and optimize both strategic planning, such as technology selection, facility locations, and resource allocations, to tactical planning decision, such as day-to-day decision making and scheduling.

The development of spatial supported web decision support systems facilitates decision making. Through the integration of cyber infrastructure (CI), GIS, and spatial modeling analysis, CyberGIS could facilitate large-scale problem solving, data management, model accessibility, and visualization. Supported by the high performance CI and service oriented middleware, integrating CyberGIS and biomass supply chain optimization models will facilitate decision making on biomass feedstock provision.

CHAPTER 3

STRATEGIC BIOMASS-ETHANOL SUPPLY CHAIN OPTIMIZATION*

This chapter describes the development of a strategic biomass supply chain optimization model, the BioScope model. The development of BioScope model aims to optimize long-term strategic biomass provision decisions including the components of biomass-biofuel production costs, optimal facility locations and capacities, and optimal biomass distribution patterns. The detailed constraint equations, variables, and input data parameters are provided to better understand the component of a biomass supply chain system. Several case studies of Miscanthus production in Illinois are presented to illustrate the usage of the model. Cropland usage rate, biomass demand, preprocessing technology selection are key factors affecting biomass production costs.

This chapter cannot be realized without successful teamwork, where the team members are Tao Lin, Luis Rodríguez, Yogendra Shastri, Alan Hansen, and K.C. Ting. Mr. Lin led the overall research, collected data, developed the model, and drafted the manuscript. Dr. Rodríguez, Shastri, Hansen, and Ting participated the research design and the draft revision.

The primary tasks conducted by Mr. Lin include: 1) development of constraint and objective equations that are listed in the chapter, 2) design of the proposed input-output model workflow, and 3) design of spatial related maps for results visualization. The content of this chapter has been published in a journal paper (Lin et al., 2013).

*Reprint, with permission, from Lin et al., 2013, "GIS-enabled biomass-ethanol supply chain optimization: model development and Miscanthus application," *Journal of Biofuels, Bioproducts & Biorefining* 7(3): 314-333.

Abstract. *To ensure effective biomass feedstock provision for large-scale ethanol production, a three-stage supply chain was proposed to include biomass supply sites, centralized storage and preprocessing (CSP) sites, and biorefinery sites. A GIS-enabled biomass supply chain optimization model (BioScope) was developed to minimize annual biomass-ethanol production costs by selecting the optimal numbers, locations, and capacities of farms, CSPs, and biorefineries as well as identifying the optimal biomass flow pattern from farms to biorefineries. The model was implemented to study the Miscanthus-ethanol supply chain in Illinois. The results of the baseline case, assuming 2% of cropland is allocated for Miscanthus production, showed that unit Miscanthus-ethanol production costs were \$220.6 Mg⁻¹, or \$0.74 L⁻¹. Biorefinery related costs are the largest cost component, accounting for 48% of the total costs, followed by biomass procurement, transportation, and CSP related costs. The unit Miscanthus-ethanol production costs could be reduced to \$198 Mg⁻¹ using 20% of cropland, primarily due to savings in transportation costs. Sensitivity analyses showed that the optimal supply chain configurations, including the numbers and locations of supply sites, CSP facilities, and biorefineries, changed significantly for different cropland usage rates, biomass demands, transportation means, and preprocessing technologies. A supply chain composed of large biorefineries with the support of distributed CSP facilities was recommended to reduce biofuels production costs. Rail outperformed truck transportation to ship preprocessed biomass. Ground biomass with tapping is the suggested biomass format for the case study in Illinois, while high-density biomass formats are suggested for long distance transportation.*

Keywords. Supply chain, optimization, GIS, facility location, biomass, biofuels

3.1 INTRODUCTION

The development of renewable fuels can help reduce greenhouse gas (GHG) emissions, reduce petroleum imports, and improve energy security (EPA, 2010). Cellulosic ethanol is expected to be an important component of a future renewable fuel system and its production has been targeted to be 16 billion gallons in 2022 (EPA, 2010). The advantage of cellulosic ethanol is that it uses renewable biomass as the primary feedstock, which does not compete with food supply as compared with corn ethanol production. However, due to low energy density and distributed supply of biomass, ensuring effective biomass feedstock provision is one of many challenges anticipated for large-scale ethanol production. Strategic design of the biomass supply chain will be essential to overcoming this challenge. From a systems perspective, facility capital related costs, facility operating costs, biomass procurement costs, and biomass transportation costs are major cost categories for cellulosic ethanol production (Hess et al. 2007; Humbird et al., 2011).

On the supply side, biomass availability, quality, and production costs vary geographically because of the spatial differences in weather and soils. Therefore, Geographical Information System (GIS) has been applied to estimate biomass yields, supplies, and production costs (Graham et al., 2000; Noon et al., 2002; Khanna et al., 2008). Due to spatial variation of biomass availability and its production cost, optimal facility location selection is important for ensuring the most efficient biomass supply. Previous studies have applied GIS and mixed integer linear programming (MILP) on facility location optimization for single biomass resource (Panichelli and Gnansounou, 2008; Kim et al., 2011) and multiple renewable resources (Parker et al., 2010).

On the biorefinery side, producers prefer to maintain constant quantity and uniform quality of input materials and to exploit the economies of scale (Hess et al., 2007). A previous study has shown that large facilities could decrease ethanol production costs by \$0.05-0.08 L⁻¹ (\$0.2-0.3 gal⁻¹) due to the economies of scale (Kocoloski et al., 2011). However, the larger the biorefinery production capacity, the larger the biomass feedstock supply area, and accordingly the higher the transportation related costs. Therefore, large-scale cellulosic ethanol biorefineries can reduce the unit production costs, but require higher biomass provision costs. Biomass transportation and storage costs accounted for more than half of biomass (corn stover) costs at the biorefinery gate and farmer participation had a significant impact on the total production costs (Leboreiro and Hilaly, 2011). Balancing the trade-off between transportation costs and unit production costs will be important for an efficient biomass supply chain design.

Large-scale biorefineries not only incur high biomass transportation costs, but also face significant challenges with logistics, delivery schedules, and inconsistent feedstock formats (Hess et al., 2007). By shifting preprocessing from biorefineries to storage sites, biorefineries will receive feedstock with the same format and thus can reduce potential operating problems. Furthermore, preprocessed biomass requires lower biomass transportation costs due to the increased biomass density (Shastri et al., 2012a; Sokhansanj et al., 2009; Eranki et al., 2011). Therefore, in order to meet the processing demand and minimize production costs, the optimal biomass supply chain design should not only consider the optimal locations and capacities of facilities, but also the sourcing of consistent biomass supply. Most of the previous studies have optimized the biomass supply chain that only includes two stages: biomass suppliers and biorefineries (Panichelli and Gnansounou, 2008; Kim et al., 2011; Parker et al, 2010; Kocoloski et al., 2011; Leboreiro and Hilaly, 2011). However, the two-stage supply chain may not be

effective for large-scale biofuel production. To provide consistent quality and format of feedstock and reduce logistics burdens, centralized storage and preprocessing were proposed to provide services to store, handle, and preprocess biomass (Hess et al., 2007; Eranki et al., 2011). This leads to a three-stage supply system including several biomass suppliers, centralized storage and preprocessing sites, and biorefineries, with potentially different capacities at different locations (Figure 3.1).

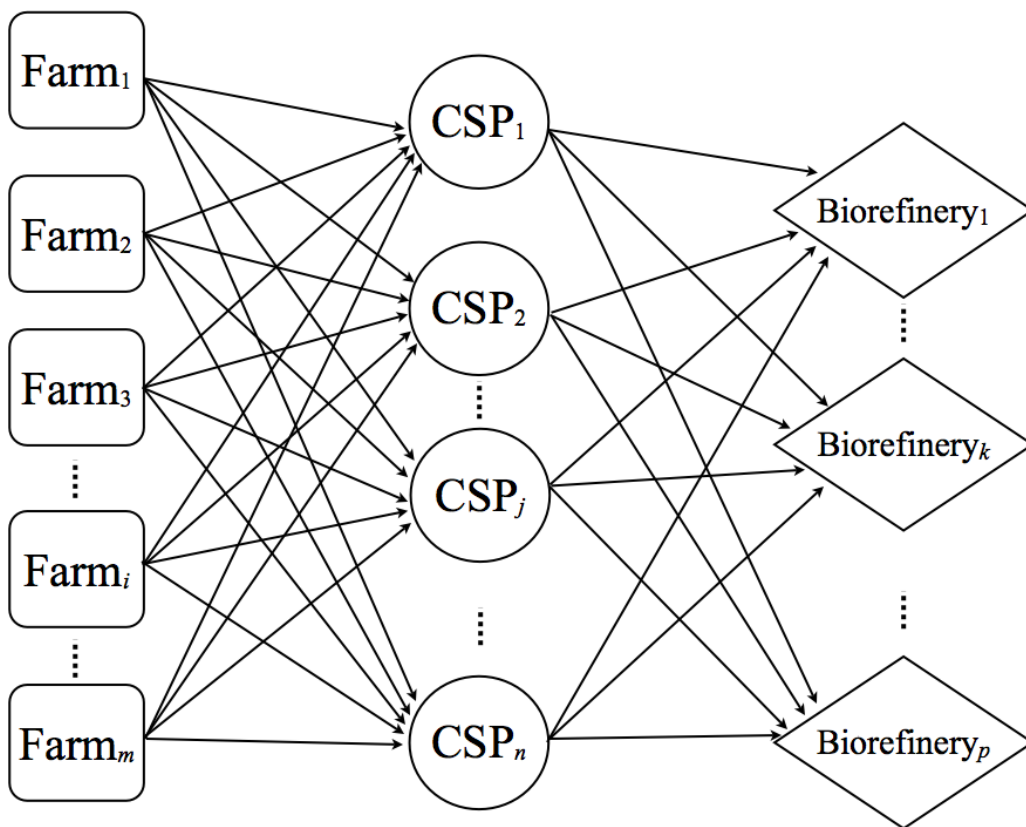


Figure 3.1: Farms, centralized storage and preprocessing (CSP) sites, and biorefineries make up a three-stage biomass-ethanol supply chain. The associated costs include biomass purchase costs, transportation costs, CSP operating costs, CSP capital related costs, biorefinery operating costs, and biorefinery capital related costs.

To minimize annual biomass-ethanol production costs within the three-stage biomass supply chain, a GIS-enabled optimization model, BioScope, was developed to select the optimal numbers, locations, and capacities of the biomass supply sites, centralized storage and preprocessing sites, and biorefineries and to identify the most efficient biomass flow patterns within the system. GIS was used to store, manage, and retrieve geospatial related information, including county level biomass availability, biomass production costs, and transportation distances between facilities in the supply chain.

3.2 OVERVIEW OF THE BIOSCOPE MODEL

The BioScope model was developed by integrating geographical information and optimization tools to provide decision support on biomass supply chain configurations. Biomass availability and farm-gate prices, transportation distances, annual facility capital costs, and annual facility operating costs were the five major inputs for the BioScope optimization model (Figure 3.2). Biomass availability was estimated by using biomass yield and cropland area (USDA, 2010) at the county level. For example, Miscanthus yield data could be predicted via the MISCANMOD tool (Jain et al., 2010). The optimal biomass farm-gate prices were composed of biomass establishment and production costs, and land opportunity costs. To assemble a distance matrix between facilities, ArcGIS (ESRI, 2013) was used to calculate the shortest transportation distances between facilities using the existing road network (US Census Bureau, 2011). Based on data describing the capital investment costs for centralized storage and preprocessing site (Hess et al., 2007) and biorefinery (Humbird et al., 2011) at one capacity level, a facility cost estimation model was developed to estimate annual capital related costs for CSPs and biorefineries at various capacities.

Subject to user defined scenarios, spatial data, such as biomass availability, production costs, and distances, can be managed using GIS tools to generate input data that can be stored in a spreadsheet file format. The BioScope model can read spreadsheet files to instantiate parameters and constraints for analyses. The BioScope model is a mixed integer linear programming model that was developed on the GAMS platform and solved using the CPLEX solver (GAMS, 2013). The results are exported into an Excel spreadsheet and can be further visualized on the maps via ArcGIS.

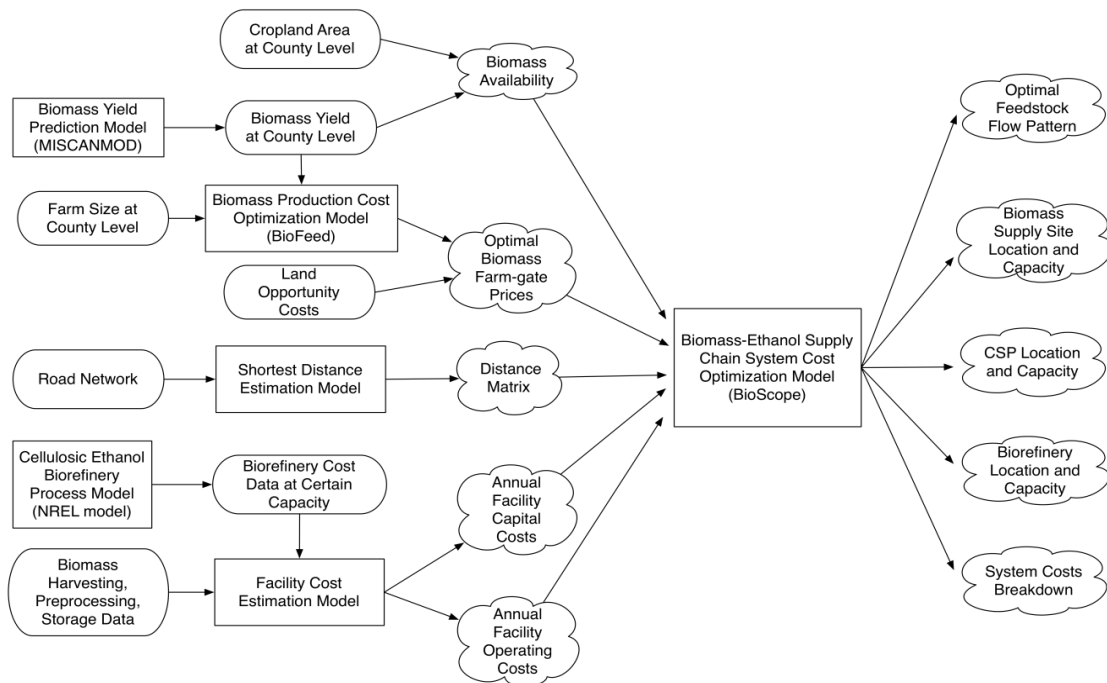


Figure 3.2: The components of the BioScope model and their data flow. The rounded rectangles represent source data (biomass harvesting, preprocessing, and storage (Hess et al., 2007), land opportunity costs (Jain et al., 2010), county level farm size and cropland area (USDA, 2010), county level biomass yield (Jain et al., 2010), road networks (US Census Bureau, 2011)) the rectangles represent the models used in the system (MISCANMOD (Jain et al., 2010), BioFeed (Shastri et al., 2010), and the NREL model (Humbird et al., 2011)). BioScope, Shortest Distance Estimation Model, and Facility Cost Estimation Model were developed in this study), and clouds represent processed input and output data.

3.2.1 Spatial Elements of the System

Biomass availability varies at the county level because of the spatial differences in weather, soil condition, growing area, and biomass yield. Biomass availability is estimated based on the biomass yield predicted at the county level and the cropland area to be allocated to growing biomass. For example, Miscanthus yield rates, as predicted by the MISCANMOD model (Jain et al., 2010), have been shown to vary at the county level (Khanna et al., 2008), as does the cropland area (USDA, 2010). Therefore, assuming 2% of cropland was allocated for growing Miscanthus, its availability at each county of Illinois was estimated (Figure 3.3).

Biomass farm-gate prices, or biomass procurement costs, are composed of land opportunity costs, biomass establishment, and production costs. Biomass production costs, include harvesting, baling, infield transportation, and transportation within the county, are a function of not only biomass yield but also farm size (Shastri et al., 2010). By integrating a previously developed biomass production optimization model, BioFeed (Shastri et al., 2010), with typical county-level farm size distributions from USDA (2010) and county-level Miscanthus yield data (Jain et al., 2010) in Illinois, Miscanthus harvestable yield and its production costs can be estimated. The sum of production costs and establishment (Jain et al., 2010) and land opportunity costs (Jain et al., 2010), is the biomass farm-gate price, which can be estimated for each county in Illinois (Figure 3.4).

Biomass transportation costs are correlated to the distance between facilities. To integrate feedstock resource data with transportation network data, it was assumed that all the feedstock produced in a county was available at the biggest city of each county. The transportation distance within each county was approximated as the radius of a circle with the same area as the county.

Interstate and state highway road networks were considered for biomass transportation between facilities. Given the existing road network data (US Census Bureau, 2011), ArcGIS was used to calculate the shortest pathway between any potential biomass supply sites, CSP sites, and biorefinery sites.

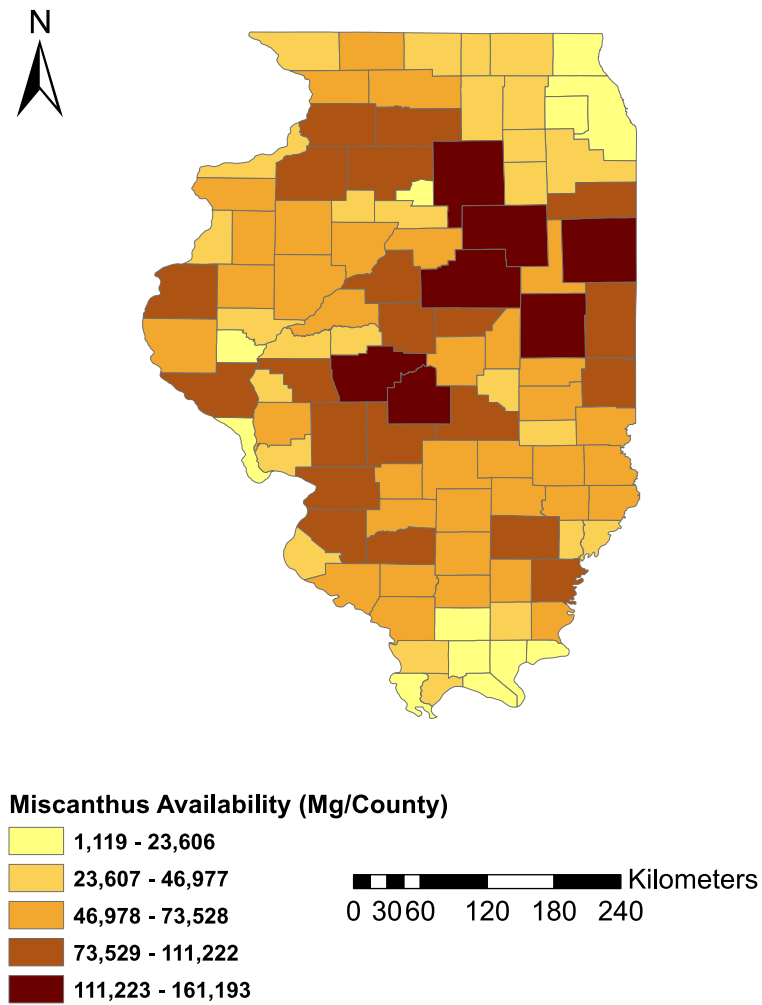


Figure 3.3: The quantity of available Miscanthus in each county of Illinois given 2% of cropland is allocated for Miscanthus production. County level cropland area is from USDA (2010) and Miscanthus harvestable yield data is based on the MISCANMOD model (Jain et al., 2010) and the BioFeed Model (Shastri et al., 2010).

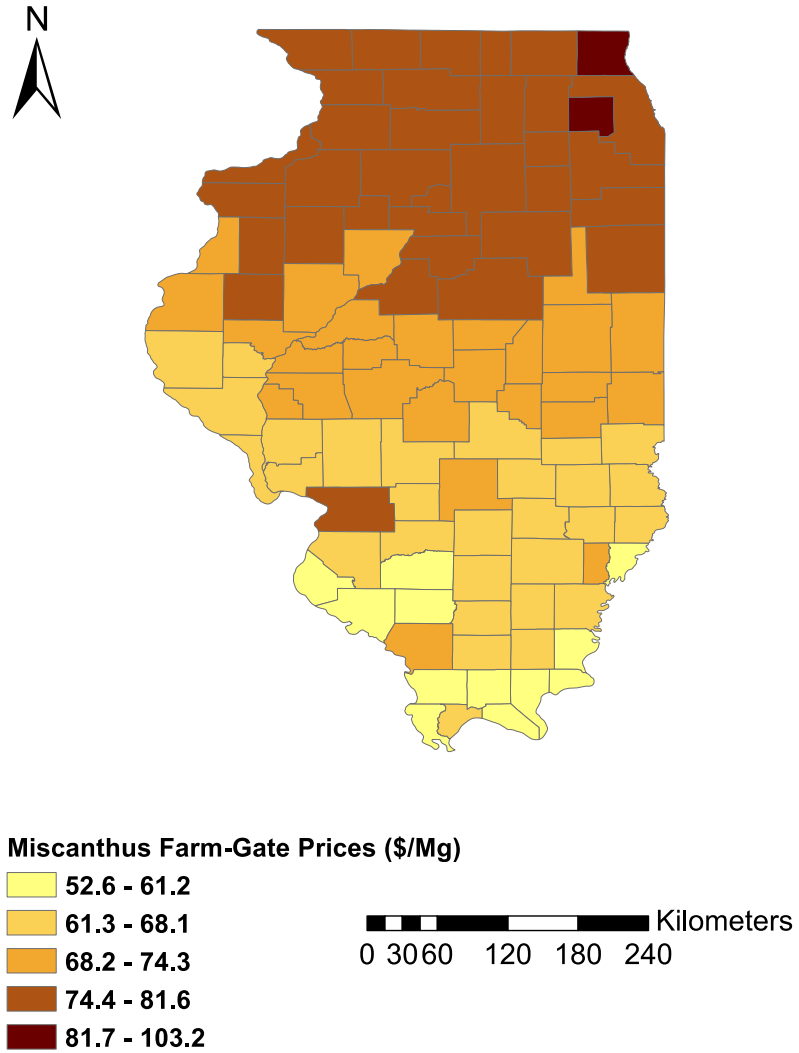


Figure 3.4: The optimal farm-gate prices of Miscanthus in each county of Illinois. The Miscanthus farm-gate prices are composed of land opportunity (Jain et al., 2010), establishment, and production costs. Miscanthus production costs include harvesting, baling, and infield transportation, and within county transportation costs were estimated based on the BioFeed model (Shastri et al., 2010).

3.2.2 Facility Capital Related Costs for Biorefineries and CSP Sites

Facility capital investment costs are the most significant costs for cellulosic ethanol production. To estimate the economies of scale of processing facilities, the power law has been applied to predict capital investment costs based on the costs of a baseline case; scaling factors are typically selected ranging from 0.6 to 0.7 for biomaterial and chemical processing facilities (Peters and Timmerhaus, 1991; Park, 1984). The capital investment costs of a biorefinery have increased significantly in the last decade (Humbird et al., 2011; Aden et al., 2002), largely due to the cost increase of the raw materials. In this study, a baseline case of biorefinery was assumed to be 772,000 Mg y⁻¹ with capital investment costs of \$422 million (Humbird et al., 2011). A scaling factor of 0.7 was used to estimate the capital costs at other capacities (Figure 3.5A).

Because a linear programming model is computationally efficient and can provide a guaranteed optimum result, a piecewise linear approximation of the power law nonlinear equation was used to estimate the economies of scale of the facility predicted by the power law. To improve the estimation resolution, we proposed three facility capacity levels of biorefineries in this study, namely small (50,000-600,000 Mg y⁻¹), medium (600,000-1,300,000 Mg y⁻¹), and large (1,300,000-1,900,000 Mg y⁻¹) (Figure 3.5A). The largest single biorefinery facility was set at 1,900,000 Mg y⁻¹ (150 million gallons of ethanol per year) for this study. Within each segment, there exists a separate linear equation to estimate the capital investment costs: the slope of the line represents the unit variable capital related costs and the intercept value represents the fixed capital related costs (Figure 3.5A). The larger the facility capacity, the higher will be the fixed capital investment costs, but the unit variable capital investment costs will be lower.

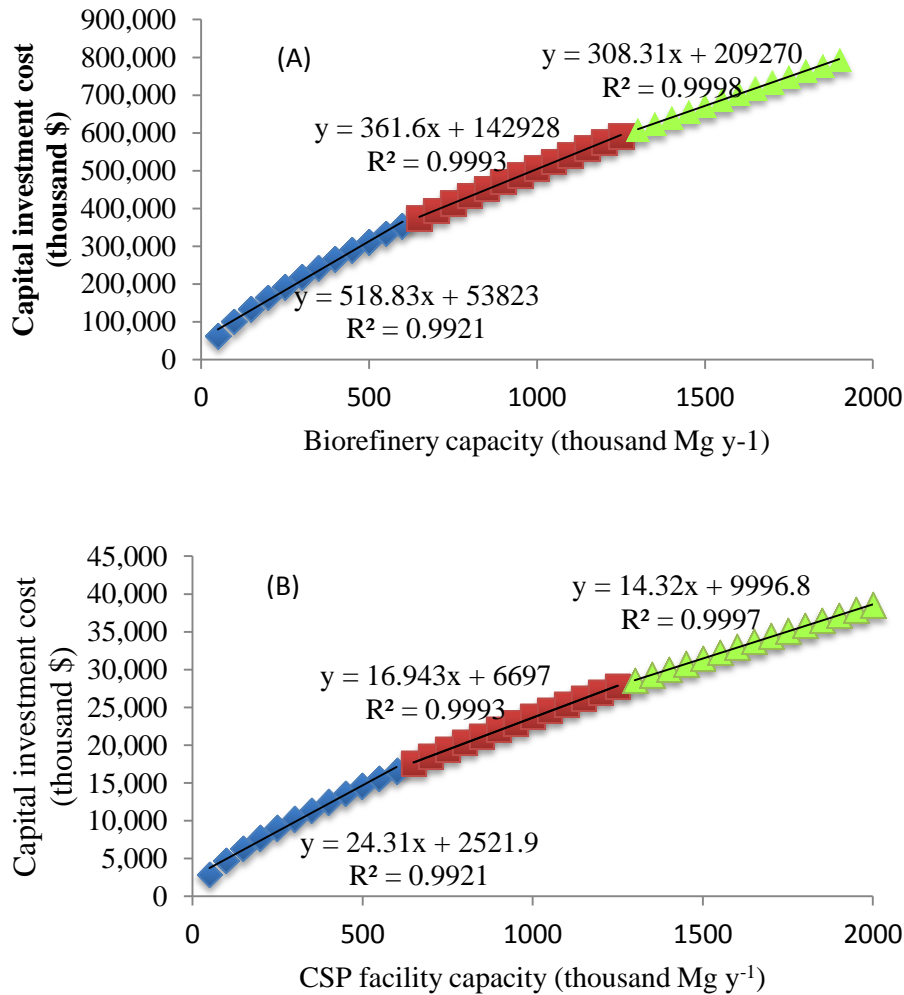


Figure 3.5: Biorefinery capital investment cost estimation at small, medium, and large facility capacity levels for biorefineries (A) and centralized storage and preprocessing (CSP) facilities (B). The curves were generated using a scaling factor of 0.7 with the base-case costs. The base-case costs for biorefineries are \$422 million at a capacity of 772,000 Mg y⁻¹ from NREL (Humbird et al., 2011) and for CSPs are \$19 million at a capacity of 726,000 Mg y⁻¹ from INL (Hess et al., 2007). The piecewise approximation method was applied to generate linear equations to estimate capital investment costs at three facility capacity levels for both biorefineries and CSPs.

Annual capital related costs include depreciation, amortized loan payments, and the internal return requirement for investors. It was assumed that the facility has a 15-year life span

with zero salvage value. Annual depreciation costs were calculated using the straight-line depreciation method. The facility investors owned 40% equity and required 10% of internal return rate for their investment. The remaining 60% of the total capital investment costs were from a loan with an annual 5% interest rate. Given these assumptions, the annual facility capital related costs were \$57.8 million for the baseline case (772,000 Mg y⁻¹). The annual facility capital costs accounted for 13.7% of the facility capital investment costs (Table 3.1).

Table 3.1: Annual biorefinery capital costs are listed, given the baseline case biorefinery at a cost of \$422 million with a capacity of 772,000 Mg y⁻¹ (Humbird et al., 2011). It is assumed that investors own 40% of the facility with the internal return rate of 10%. 60% of the capital investment costs are from a loan at the interest rate of 5% with 15-year payback period. The facility has a 15-year life span with zero salvage value.

Description	Value
Capital investment costs (A)	\$422,500,000
Principal (60% of A)	\$253,500,000
Equity (40% of A)	\$169,000,000
Annual dividends (10% IRR for investors) (B)	\$22,173,232
Annual depreciation (15-year facility life span with zero salvage value) (C)	\$11,266,667
Amortized payment (5% interest rate with 15-year payback period) (D)	\$24,422,770
Annual facility related costs (E=B+C+D)	\$57,862,669
The ratio of annual facility capital costs to capital investment costs (E/A)	13.7%

Centralized storage and preprocessing (CSP) facilities were proposed to receive, handle, store, and preprocess biomass. Tub-grinding was considered for biomass size reduction at CSP facilities in the current study. It was estimated to cost \$19 million to build a CSP facility with a capacity of 726,000 Mg y⁻¹ (Hess et al., 2007). Three facility capacity levels of CSP facilities were proposed, namely: small (50,000-600,000 Mg y⁻¹), medium (600,000-1,300,000 Mg y⁻¹), and large (1,300,000 – 2,000,000 Mg y⁻¹) (Figure 3.5B). A scaling factor of 0.7 was applied to estimate the capital investment costs of CSPs at various capacities, and a similar linear approximation method was used for CSPs, resulting in three cost estimation equations (Figure 3.5B). Further, a factor of 13.7% was also applied to estimate annual facility capital costs based on the capital investment costs of each CSP facility.

3.2.3 Optimization Model Formulation

The objective of the optimization model is to minimize annual biomass-ethanol production costs (Z) that are comprised of four costs: biomass purchase costs (C_B), transportation related costs (C_T), CSP site related costs (C_S), and biorefinery related costs (C_E) (Eq. 3.1).

$$\text{Minimize } Z = C_B + C_T + C_S + C_E \quad (3.1)$$

In the current study, let i represent any element in the set I that is composed of m possible biomass supply counties, j represent any element in the set J that is composed of n potential CSP sites, k represent any element in the set K that is composed of p potential biorefinery sites (see Figure 3.1), and l represent any possible facility capacity level.

3.2.3.1 Biomass Supply

Biomass purchase costs (C_B) are a function of the optimal biomass flow pattern ($f^{i,j}$) from supply sites to CSP sites and the county-level biomass production costs at the sourcing site (c^i) (Eq. 3.2). The decision variable related to biomass purchase costs is the amount of biomass flow from each supply site to each CSP site ($f^{i,j}$). County-level biomass production costs (c^i) and biomass availability (b^i) are two inputs related to biomass supply (i.e. Figure 3.3 and 3.4 for the baseline case analysis). Since both inputs vary by county, it is important to optimize the supply site selection as well as the quantity of biomass to purchase from each site to meet the total biomass demand (P) (Eq. 3.3). Moreover, the total amount of biomass output from a biomass supply site should not exceed its biomass availability (Eq. 3.4).

$$C_B = \sum_i \sum_j c^i f^{i,j} \quad (3.2)$$

$$\sum_i \sum_j f^{i,j} = P \quad (3.3)$$

$$\sum_j f^{i,j} \leq b^i \quad (3.4)$$

3.2.3.2 Biomass Transportation

Biomass transportation costs (C_T) are composed of variable transportation costs (T_v) and fixed transportation costs (T_f) (Eq. 3.5). There are two transportation stages: the transportation before CSP sites and the transportation after CSP sites. The decision variables related to total biomass purchase costs are the amount of biomass flow from supply sites to CSP sites ($f^{i,j}$) and the amount of preprocessed biomass flow from CSP sites to biorefineries ($f^{j,k}$). Variable transportation costs are a function of the unit variable transportation cost (t_{v1}, t_{v2}), which will

vary depending on the form of the biomass (i.e. baled and ground as considered in the case study), amount of biomass being transported ($f^{i,j}$, $f^{j,k}$), and the transportation distance ($d^{i,j}$, $d^{j,k}$) (Eq. 3.6). Fixed transportation costs that include loading and unloading costs depend on the unit fixed transportation cost (t_{f1} , t_{f2}) and the amount of biomass being transported ($f^{i,j}$, $f^{j,k}$) (Eq. 3.7). Unit variable and fix transportation costs are inputs that can be decided by users. The shortest distances between the facilities within the system ($d^{i,j}$, $d^{j,k}$) are inputs calculated via ArcGIS using the existing road network.

$$C_T = T_v + T_f \quad (3.5)$$

$$T_v = \sum_i \sum_j (t_{v1} \times f^{i,j} \times d^{i,j}) + \sum_j \sum_k (t_{v2} \times f^{j,k} \times d^{j,k}) \quad (3.6)$$

$$T_f = \sum_i \sum_j (t_{f1} \times f^{i,j}) + \sum_j \sum_k t_{f2} \times f^{j,k} \quad (3.7)$$

3.2.3.3 Centralized Storage and Preprocessing

The costs related to CSP facilities (C_C) are composed of annual operating costs (S_o) and annual capital related costs (S_c) (Eq. 3.8). Annual operating costs include the costs for utilities, maintenance, labor, supervision, insurance, laboratory charges, and waste treatment. In this study, it is assumed that CSP facilities with different capacities incur the same unit operating costs (s_{op}). Therefore, annual operating costs are linearly dependent on the demand of biomass for CSP facilities (P) (Eq. 3.9).

Annual capital costs are linearly dependent on the capital investment costs where a factor α (13.7%) is used to represent its relationship. To improve the accuracy, the model adopts a piecewise linear approximation to estimate the capital investment costs for three different levels

of facility capacity. Therefore, annual capital related costs are linearly dependent on the sum of fixed (s_f^l) and variable (s_v^l) capital related costs at every level of capacity at each potential location (Eq. 3.10). The binary decision variable o_s^j controls whether there exists a CSP facility located in county j . The binary decision variable $o_s^{j,l}$ controls the capacity level l of the CSP facility located in county j . And the variable $p^{j,l}$ represents the specific capacity of the CSP in county j at the capacity level l .

$$C_S = S_o + S_c \quad (3.8)$$

$$S_o = s_{op} \times P \quad (3.9)$$

$$S_c = \alpha \times \left(\sum_j \sum_l s_v^l \times p^{j,l} + s_f^l \times o_s^{j,l} \right) \quad (3.10)$$

The total capacities of all CSP facilities should be equal to the amount of the total biomass required for processing (Eq. 3.11). Eq. 3.12 to 3.14 describe the capacity range of the facility at small ($l = 1$), medium ($l = 2$), and large ($l = 3$) facility capacity levels (Figure 3.5A). The minimum (λ_s^0) and maximum (λ_s^l) capacities of each facility capacity level for CSP facilities are inputs decided by users. If there exists a facility in county j , the binary variable o_s^j will be set equal to one. In order to ensure there exists exactly one facility in county j , exactly one binary variable $o_s^{j,l}$ must be equal to one (Eq. 3.15). Alternatively, if no facility exists in county j , o_s^j will be set equal to zero. Thus, no facility is located in county j at any capacity levels, as all binary variables $o_s^{j,l}$ must be equal to zero (Eq. 3.15). Therefore, the sum of the capacities of CSP at all levels should be the same as the CSP capacity for that county (Eq. 3.16). Considering the mass balance, the CSP capacity in county j should be equal to the total amount of biomass

transported to county j from all supply sites (Eq. 3.17). The model also considers the biomass loss at the CSP stage (Eq. 3.18). Biomass loss rate (β) is an input parameter decided by users.

$$\sum_j \sum_l p^{j,l} = P \quad (3.11)$$

$$\lambda_s^0 \times o_s^{j,1} \leq p^{j,1} \leq \lambda_s^1 \times o_s^{j,1} \quad (3.12)$$

$$\lambda_s^1 \times o_s^{j,2} \leq p^{j,2} \leq \lambda_s^2 \times o_s^{j,2} \quad (3.13)$$

$$\lambda_s^2 \times o_s^{j,3} \leq p^{j,3} \leq \lambda_s^3 \times o_s^{j,3} \quad (3.14)$$

$$\sum_l o_s^{j,l} = o_s^j \quad (3.15)$$

$$\sum_l p^{j,l} = p^j \quad (3.16)$$

$$\sum_i f^{i,j} = \sum_l p^{j,l} \quad (3.17)$$

$$\sum_k f^{j,k} \leq \sum_l p^{j,l} \times (1 - \beta) \quad (3.18)$$

3.2.3.4 Biorefinery

Similar to CSP facilities, the costs related to biorefineries (C_E) are composed of annual biorefinery operating costs (E_o) and annual biorefinery capital costs (E_c), as shown in Eq. 3.19.

In this study, it is assumed that the unit operating costs for the biorefinery (e_{op}) are constant for any capacity. Therefore, annual operating costs are linearly dependent on the demand of processed biomass for ethanol production at biorefineries (Q), which is an input parameter

decided by users (Eq. 3.20). Annual biorefinery capital costs have a linear relationship ($\alpha = 13.7\%$ in the current study) with biorefinery capital investment costs, which are the sum of fixed and variable capital related costs at every level of capacity at each potential location (Eq. 3.21). The binary variable $o_e^{k,l}$ indicates whether there exists a biorefinery at capacity level l located in county k , and the variable $q^{k,l}$ represents the biorefinery with the capacity at level l located in county k . As in the case of the CSP facilities, a piecewise linear approximation method for biorefinery capacity and capacity level identification was implemented (Eq. 3.22-3.26). Regarding mass balance, the amount of all the preprocessed biomass flow into the biorefinery located in county k from all CSPs should be equal to the biorefinery facility capacity (Eq. 3.27). The total capacity of all biorefineries should meet the given demand of processed biomass for ethanol production (Eq. 3.28).

$$C_E = E_o + E_c \quad (3.19)$$

$$E_o = e_{op} \times Q \quad (3.20)$$

$$E_c = \alpha \times \left(\sum_j \sum_l e_v^l \times q^{k,l} + e_f^l \times o_e^{k,l} \right) \quad (3.21)$$

$$\lambda_e^0 \times o_e^{k,1} \leq q^{k,1} \leq \lambda_e^1 \times o_e^{k,1} \quad (3.22)$$

$$\lambda_e^1 \times o_e^{k,2} \leq q^{k,2} \leq \lambda_e^2 \times o_e^{k,2} \quad (3.23)$$

$$\lambda_e^2 \times o_e^{k,3} \leq q^{k,3} \leq \lambda_e^3 \times o_e^{k,3} \quad (3.24)$$

$$\sum_l o_e^{k,l} = o_e^k \quad (3.25)$$

$$\sum_l q^{k,l} = q^k \quad (3.26)$$

$$\sum_j f^{j,k} = \sum_l q^{k,l} \quad (3.27)$$

$$\sum_k \sum_l q^{k,l} = Q \quad (3.28)$$

3.3 CASE STUDY OF MISCANTHUS APPLICATION IN ILLINOIS

3.3.1 Baseline case

To illustrate the use of the BioScope model, we chose a Miscanthus-ethanol supply chain in Illinois for the baseline case study. Each county in Illinois was a candidate location. Thus, each of the three stages in the supply chain had 102 potential candidates for consideration. In the baseline case, 2% of cropland was assumed allocated for Miscanthus production, and the total Miscanthus processing demand was 2,000,000 Mg y⁻¹. Biomass loss rate (β) of 5% was assumed at centralized storage and preprocessing (CSP) sites, and therefore the total amount of preprocessed biomass available for ethanol conversion was 1,900,000 Mg y⁻¹. Assuming that one Mg of Miscanthus could produce 300 liters (79 gallons) of ethanol (Humbird et al., 2011), the total ethanol production capacity was 570 million liters per year (150 million gallons per year) for the baseline case.

There existed a relatively wide range of unit transportation costs for baled biomass (Table 2) (Kumar et al., 2005), and the costs at the high estimate level were used as inputs in the baseline case study. Size reduction processes have been proposed to reduce biomass transportation costs and logistics burdens (Sokhansanj et al., 2009; Eranki et al., 2011). The density of ground biomass with tapping is 200 kg m⁻³, higher than 150 kg m⁻³ for baled biomass (Sokhansanj et al., 2009). Further, ground biomass has better flowability than baled biomass,

which would reduce loading and unloading costs (fixed transportation costs). In this study, CSP facilities were designed to preprocess baled biomass to provide ground biomass with tapping. Therefore, the unit variable and fixed transportation costs from CSP facilities to biorefineries were lower than the costs before preprocessing. The unit transportation costs after preprocessing (t_{v2}, t_{f2}) were assumed to be 80% of the costs before preprocessing (t_{v1}, t_{f1}) (Table 3.2).

Table 3.2: Transportation cost data before and after preprocessing used in the baseline case study

Symbol	Description	Unit	Value (High estimate)	Value (Low estimate)
t_{v1}	Variable transportation cost before preprocessing (bale)	$\$ \text{Mg}^{-1} \text{km}^{-1}$	0.15	0.073
t_{v2}	Variable transportation cost after preprocessing (ground)	$\$ \text{Mg}^{-1} \text{km}^{-1}$	0.12	0.058
t_{f1}	Fixed transportation cost (including loading and unloading) before preprocessing	$\$ \text{Mg}^{-1}$	5.42	7.08
t_{f2}	Fixed transportation cost (including loading and unloading costs) after preprocessing	$\$ \text{Mg}^{-1}$	4.34	5.67

The estimation of the facility capital investment costs for biorefineries and CSP facilities was conducted using a scaling factor of 0.7 (Figure 3.5). The baseline case costs were \$422 million at a capacity of 772,000 Mg y⁻¹ for biorefineries (Humbird et al., 2011) and \$19 million at a capacity of 726,000 Mg y⁻¹ for CSP facilities (Hess et al., 2007). An annualized cost factor

of 13.7% (α) was used to estimate the annualized capital related costs. The unit operating costs of a biorefinery (e_{op}) were considered constant at \$48 Mg⁻¹ at any capacity level (Humbird et al., 2011), while the unit operating costs of a CSP facility (s_{op}) were \$9.95 Mg⁻¹ at any capacity level (Hess et al., 2007).

All the costs used in this study have been converted to year 2007 using three cost indices. The costs of equipment related to farm operating and biomass size reduction (tub grinder) were adjusted through the Index of prices paid by growers for farm machinery in the USDA's Agricultural Prices (USDA, 2007). For the equipment related to biomass handling and storage at CSP and all the equipment at the biorefinery, the Chemical Engineering Plant Cost Index (Chemical Engineering, 2010) was used to adjust the prices. Labor costs were adjusted according to the Bureau of Labor Statistics index (US Department of Labor, 2010). A complete list of input parameters and decision variables for the baseline case is provided in Tables A.1 to A.4 in Appendix A.

3.3.2 Scenario Analyses of Cropland Usage Rate

A sensitivity analysis was conducted to illustrate how the optimal biomass supply chain configuration changed to provide the same total biomass processing demand at eight different cropland usage rates. The cropland usage rate was considered from 2, 3, 4, 5, 7, 10, 15, to 20% for each county in Illinois.

3.3.3 Scenario Analyses of Biomass Demand Changes

A scenario analysis was conducted to assess the impact of biomass processing demand changes on the optimal biomass supply chain configuration, where two levels of biomass demand,

2,000,000 and 10,000,000 Mg y⁻¹, were analyzed. To ensure sufficient biomass supply in both scenarios, 5% of cropland in Illinois was allocated for growing Miscanthus.

3.3.4 Scenario Analyses of Transportation Cost Changes

Scenario analysis was conducted to identify how the supply chain network design changed at two different levels of truck transportation costs (Table 3.2). In both scenarios, 5% of cropland was allocated to produce Miscanthus to meet the demand of 10,000,000 Mg y⁻¹.

3.3.5 Scenario Analyses of Variable Cropland Usage Rates

A case study was conducted to allow the farmer participation rate to vary within specified distances served by CSP facilities. Farmers near CSP facilities require lower transportation costs and would likely allocate more land to grow energy crops than those are further away. The systems processing demand was set at 10,000,000 Mg y⁻¹. Additional decision variables and constraints are necessary to the study of variable cropland usage rates (Table A.5 and Eq. A.4a-A.4f of Appendix A).

3.3.6 Scenario Analyses of Biorefinery Capacity Limit

A scenario analysis was conducted to identify the impact of biorefinery capacity on the biomass supply chain configuration. As compared to the base case where maximum biorefinery capacity was limited to 1,900,000 Mg per year (570 million liters per year), no capacity limit was imposed on a biorefinery for the new scenario. The biomass supply and demand requirements remained the same as those in Scenario 3.3.4.

3.3.7 Scenario Analyses of Preprocessing Technology and Transportation

Modes

A scenario analysis was conducted to evaluate the system performance of utilizing different transportation modes and preprocessing technologies. Truck and rail are the possible modes to transport. Truck is used from biomass supply sites to CSP facilities, whereas rail car is considered as an option from CSPs to biorefineries. At the CSP facilities grinding with tapping as opposed to pelletization were considered. Pelletization produces biomass with higher density and could reduce the unit transportation costs (Table 3.3), but requires higher capital investment and operating costs (Table 3.4) (Campell, 2007). The biomass supply and demand requirements remained the same as those in Scenario 3.3.4; no capacity limit was imposed for a biorefinery.

Table 3.3: The cost of shipping varies depending on preprocessing technology and form of transport. Fixed and variable cost assumptions for transport of preprocessed biomass are listed for ground and pelletized biomass using truck and rail.

	Ground Biomass with Tapping		Biomass Pellets	
	Truck	Rail	Truck	Rail
Fixed transportation costs (\$ Mg ⁻¹)	4.34	6.98	4.34	6.98
Variable transportation costs (\$ Mg ⁻¹ km ⁻¹)	0.12	0.05	0.1	0.02

Table 3.4: The cost, density, and capacity assumptions for biomass grinding and pelletization technologies

Description	Grinding	Pelletization
Base case capacity (Mg y ⁻¹)	726,000	100,000
Capital investment costs	\$18,586,800	\$7,261,600
Operating costs (\$ Mg ⁻¹)	9.95	15
Density (kg m ⁻³)	200	550

3.4 RESULTS AND DISCUSSION

3.4.1 Baseline Case Analysis

The results showed that 35 counties were selected to produce 2,000,000 Mg of biomass annually; 13 centralized storage and preprocessing (CSP) facilities were selected with capacities ranging from 82,000 to 376,000 Mg y⁻¹; one biorefinery was selected with the capacity of 1,900,000 Mg y⁻¹ (Figure 3.6). The southern Illinois counties were selected as biomass supply sites because of their relatively low biomass procurement costs and high yields. The optimal Miscanthus-ethanol production costs were \$220.6 Mg⁻¹ of biomass, or \$0.74 L⁻¹ (\$2.79 gal⁻¹) of ethanol. Among the costs, biorefinery related costs were the most significant costs, accounting for 47.9% of the system costs, followed by biomass procurement, transportation, and CSP related costs (Figure 3.7). Because biorefinery related costs have a significant impact on the total costs, it is worthwhile to build a large-scale centralized facility take advantage of the economies of scale. The results showed that all 13 CSPs were located around the biorefinery. The largest CSP site

was situated at the same location as the biorefinery, which reduced the biomass transportation costs from CSP to biorefinery.

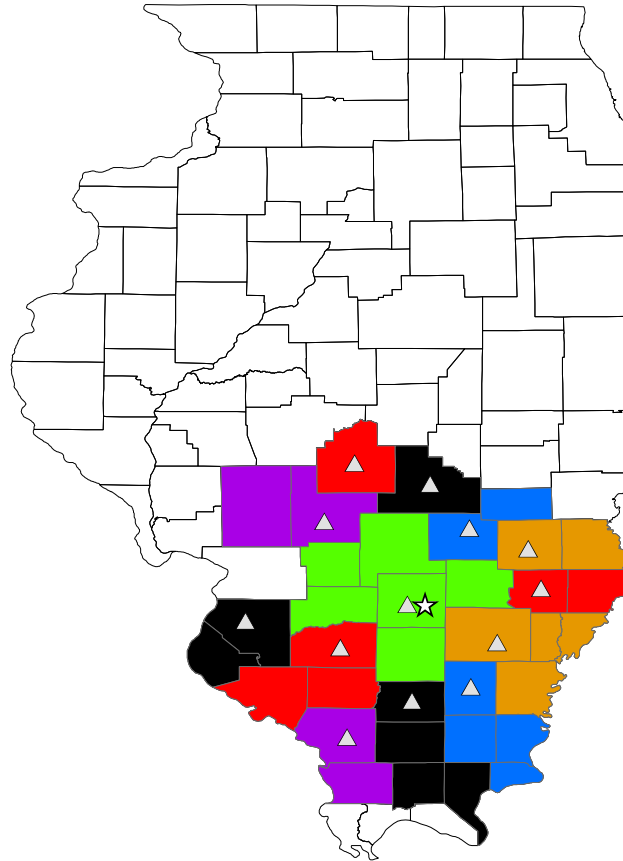


Figure 3.6: The optimal 3-stage biomass-ethanol supply chain configuration when 2% of cropland is allocated for Miscanthus production and the biomass processing demand is 2,000,000 Mg y⁻¹. Colors signify a biomass supply region serving the CSP (marked by the triangle) contained within that region. Stars represent the location of the biorefinery.

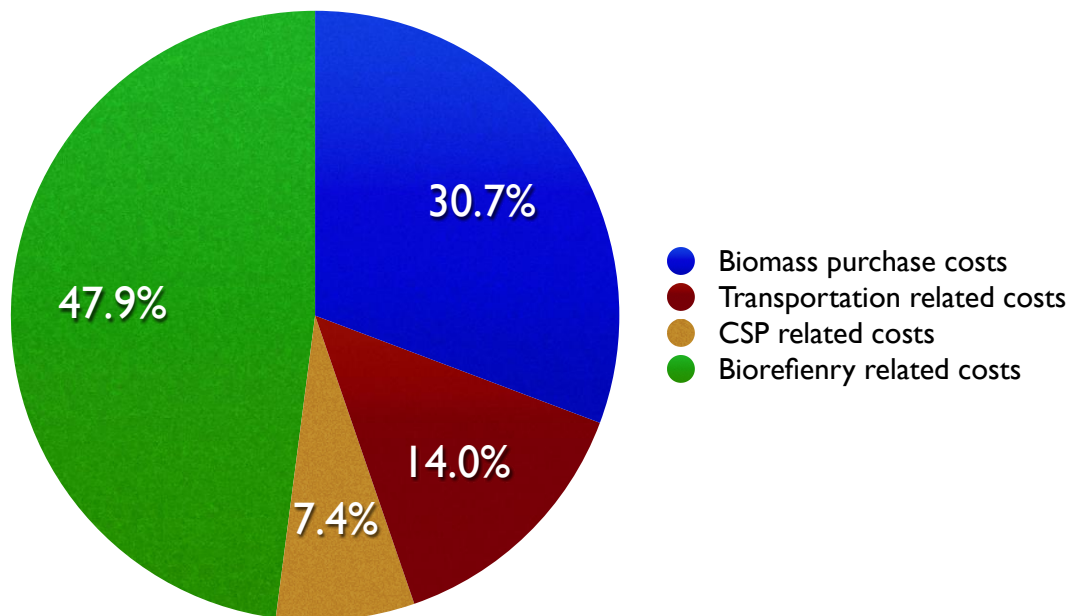


Figure 3.7: Cost breakdown of biomass-ethanol production systems when 2% of cropland is allocated for Miscanthus production in Illinois and total biomass processing demand is 2,000,000 Mg y⁻¹. The unit Miscanthus-ethanol production costs are \$220.6 Mg⁻¹ (\$0.74 L⁻¹ or \$2.8 gal⁻¹).

The optimal cellulosic-ethanol production costs in this study (\$0.74 L⁻¹) were higher than the cost of \$0.55 L⁻¹ given in a recent NREL study (Humbird et al., 2011), which considered corn stover as feedstock. The cost increase was largely due to the difference of biomass costs at the biorefinery gate. Miscanthus procurement, handling, and transportation costs were \$0.39 L⁻¹ in the current study, higher than the \$0.2 L⁻¹ for corn stover (Humbird et al., 2011). Since only 2% of cropland in each county was allocated for Miscanthus production, it required a large number of biomass supply sites to meet the annual demand of 2,000,000 Mg y⁻¹. Therefore, transportation costs were substantial and accounted for 14% of total ethanol production cost (\$0.11 L⁻¹).

3.4.2 Scenario Analysis of Cropland Usage Rate

To quantify the impact of cropland usage rate on the optimal biomass supply chain configuration, 8 different cropland usage rates, ranging from 2% to 20%, were selected. The optimal configuration of the supply chain was changed significantly at different cropland usage rates, including capacities and locations of supply counties, CSP sites, and biorefineries (Figure 3.8). With higher cropland usage rate for Miscanthus production, fewer biomass supply sites were required to meet the biomass demand. The optimal numbers of biomass supply sites reduced from 35 to 3 counties, when the cropland usage rate increased from 2 to 20%. The number of CSP facilities also decreased with the higher cropland usage rate, while the average capacity of the CSP facility increased. A single centralized biorefinery facility was suggested in all scenarios.

The optimal Miscanthus-ethanol production costs decreased from \$220.6 to \$198 Mg^{-1} when the cropland usage rates increased from 2 to 20%, largely due to the savings of transportation costs (Figure 3.9). The share of transportation related costs decreased from 14% to 7% when the cropland usage for Miscanthus production increased from 2% to 20%. Biorefinery related costs remained constant because one biorefinery with the same capacity was selected in all scenarios. Biomass procurement costs changed slightly with higher cropland usage rates, which indicates that the selected biomass supply region has biomass production costs similar to the baseline case. As a result of lower transportation costs, biorefinery related costs and biomass procurement costs exert higher impact on the biofuels production costs with a higher cropland usage rate.

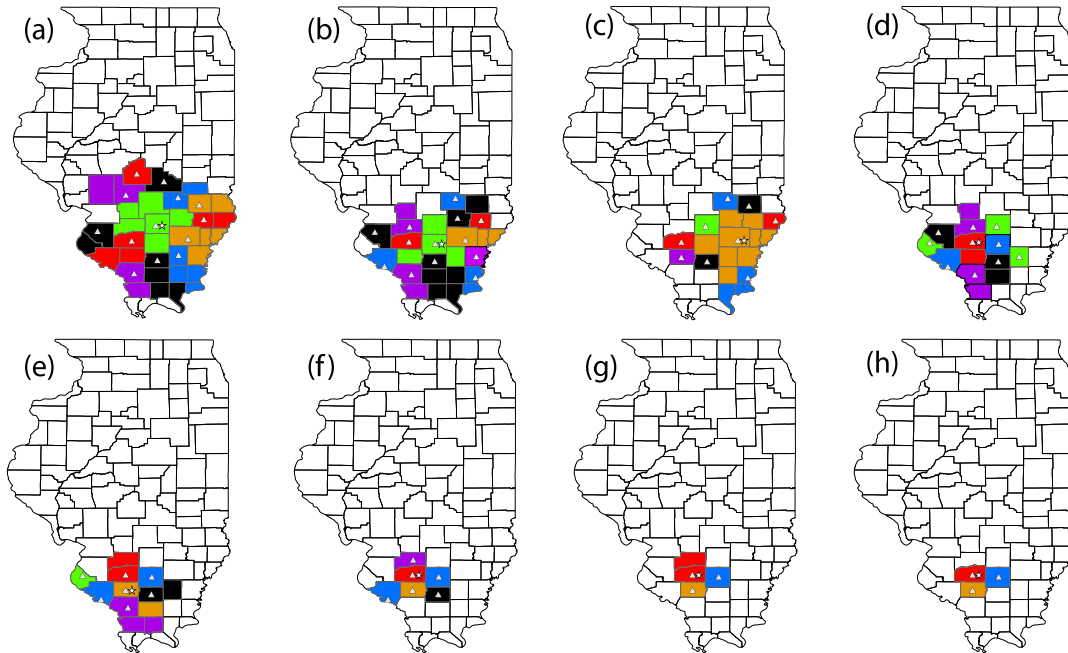


Figure 3.8: The optimal 3-stage biomass-ethanol supply chain configuration at various cropland usage rates: (a) 2%; (b) 3%; (c) 4%; (d) 5%; (e) 7%; (f) 10%; (g) 15%; (h) 20%. Each colored area represents one biomass supply region for one CSP facility. Triangles represent CSP facilities and stars represent biorefinery facilities.

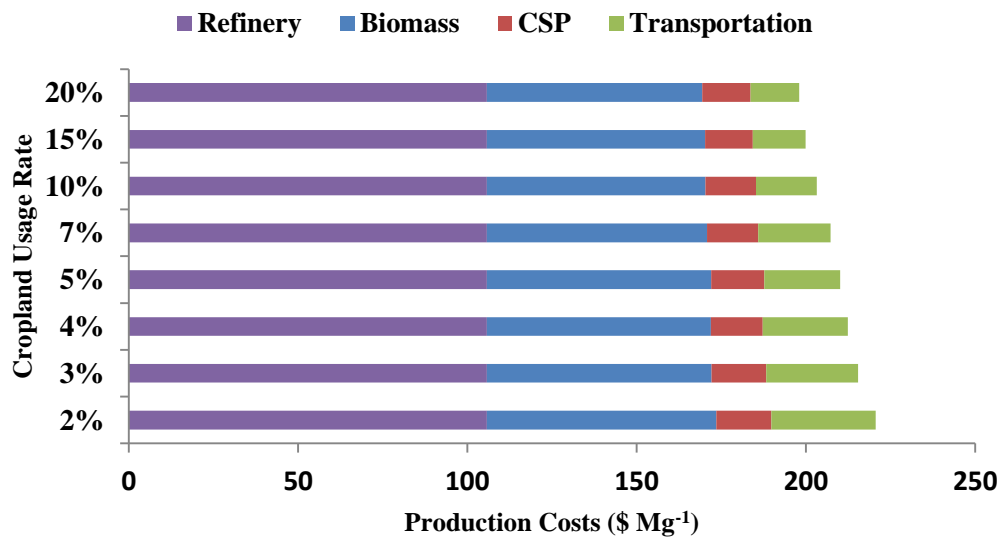


Figure 3.9: The impact of changing cropland usage rates on the optimal Miscanthus-ethanol production costs.

3.4.3 Scenario Analysis of Biomass Demand Changes

Two biomass demand scenarios, 2,000,000 and 10,000,000 Mg y⁻¹, were selected to quantify the impact of biomass demand changes on the optimal biomass supply chain configurations. 5% of cropland was allocated for Miscanthus production. The results showed that the number of suggested supply counties increased from 14 to 66 in the high demand scenario; the number of CSP facilities increased from 10 to 40; and the number of biorefineries increased from one to five (Figure 3.10). The proposed biomass supply region for the high demand scenario included all counties selected for the low demand scenario. All the selected biorefineries in both scenarios reached the capacity limit, 1,900,000 Mg y⁻¹. Ethanol producers should build large biorefineries to take advantage of economies of scale. The optimal Miscanthus-ethanol production costs changed slightly, increasing from \$210.1 to \$215.6 Mg⁻¹ at the high biomass demand. The increase of biomass procurement costs was the major contributing factor for the increase of biofuels production costs. The increased demand for biomass would cause processing facilities to source biomass from the areas that require relatively high production costs.

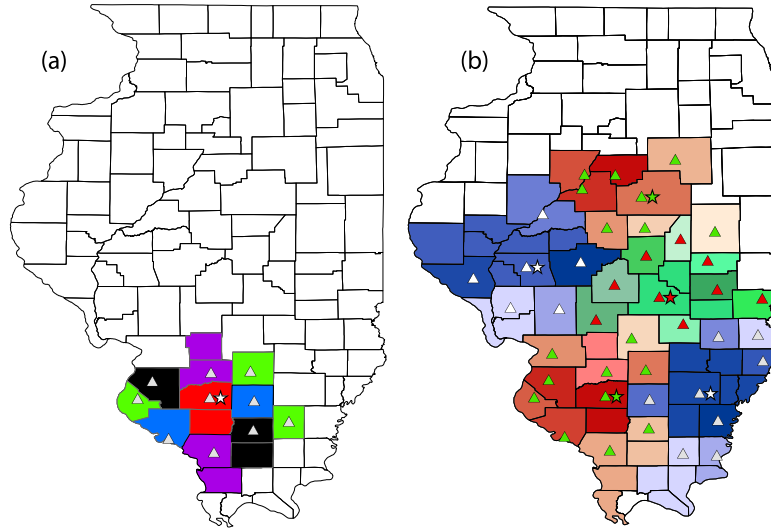


Figure 3.10: The impact of biomass demand change on the optimal biomass supply chain configuration: (a) 2,000,000 Mg y⁻¹; (b) 10,000,000 Mg y⁻¹. 5% of cropland is allocated for Miscanthus production in both scenarios. Triangles represent CSP facilities and stars represent biorefinery facilities. Each colored area represents one biomass supply region serving by a CSP facility. Biorefineries source biomass from CSPs of the same color.

3.4.4 Scenario Analysis of Transportation Cost Changes

Given the same biomass supply and demand, two transportation cost scenarios (Table 3.2) were selected to quantify the impact of transportation costs on the optimal biomass supply chain configuration. The results showed that the optimal supply chain in each scenario requires the same biomass supply sites but different numbers and capacities of CSP facilities (Figure 3.11). 41 CSPs were suggested in the base transportation cost scenario, whereas 12 CSPs were suggested in the low transportation cost scenario. Among the 12 CSP facilities, five CSP facilities had a capacity larger than 1,250,000 Mg y⁻¹, whereas all 41 CSP facilities in the base transportation cost scenario operated below 800,000 Mg y⁻¹. In the base transportation cost

scenario, the savings of transportation costs by preprocessing biomass locally outweighed the increased unit CSP related costs due to small capacities. The results conceptually agree with what previous work that suggested distributed preprocessing at farms and centralized storage sites was cost effective for biomass provision (Shastri et al., 2012). Therefore, a distributed biomass supply chain with more CSP facilities is suggested when transportation costs are high.

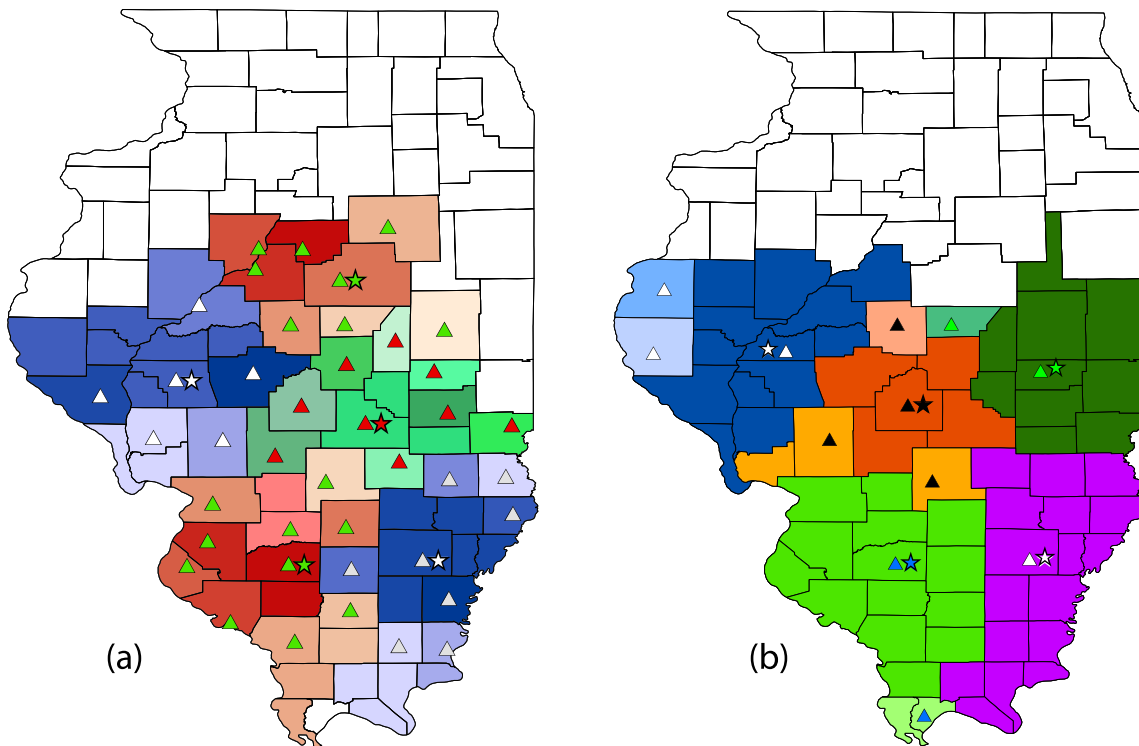


Figure 3.11: The impact of transportation costs on the optimal biomass supply chain configuration: (a) high estimate of transportation costs; (b) low estimate of transportation costs (Table 2). Five percent of cropland is allocated for Miscanthus production in both scenarios. The biomass processing demand is 10,000,000 Mg y⁻¹.

Triangles represent CSP facilities and stars represent biorefinery facilities. A commonly shaded area represents one biomass supply region served by a CSP. Biorefineries source from biomass CSPs of the same color.

3.4.5 Scenario Analysis of Variable Cropland Usage Rates

Cropland usage rates could be varied related to the transportation distances between supply sites and CSP facilities. The results suggest that supply chain would be composed of five biorefineries, 35 CSP facilities, and 37 supply counties (Figure 3.12). All the selected supply counties are located within a distance of 80 km to the CSP facilities they serve, and therefore 10% of cropland was allocated for Miscanthus production in these counties. The number of biomass supply counties decreased significantly from 60 counties using the constant cropland usage rate (Figure 3.10). The optimal Miscanthus-ethanol production costs were reduced from \$215.6 to \$207.3 Mg⁻¹, largely due to the savings of biomass transportation and procurement costs (Table 3.5).

Table 3.5: A breakdown of biofuels production costs considering a variable cropland usage rate, with and without biorefinery capacity limit. Annual biomass demand is 10,000,000 Mg y⁻¹. All values are in terms of \$ Mg⁻¹.

	With Biorefinery Capacity Limit		Without Biorefinery Capacity Limit
	Constant 5% Cropland Usage Rate	Variable Cropland Usage Rate	Variable Cropland Usage Rate
Biomass costs	71.9	67.7	67.7
CSP related costs	15.3	15	15
Transportation costs	22.6	18.8	24.4
Biorefinery related costs	105.7	105.7	96.7
Total production costs	215.6	207.3	203.8

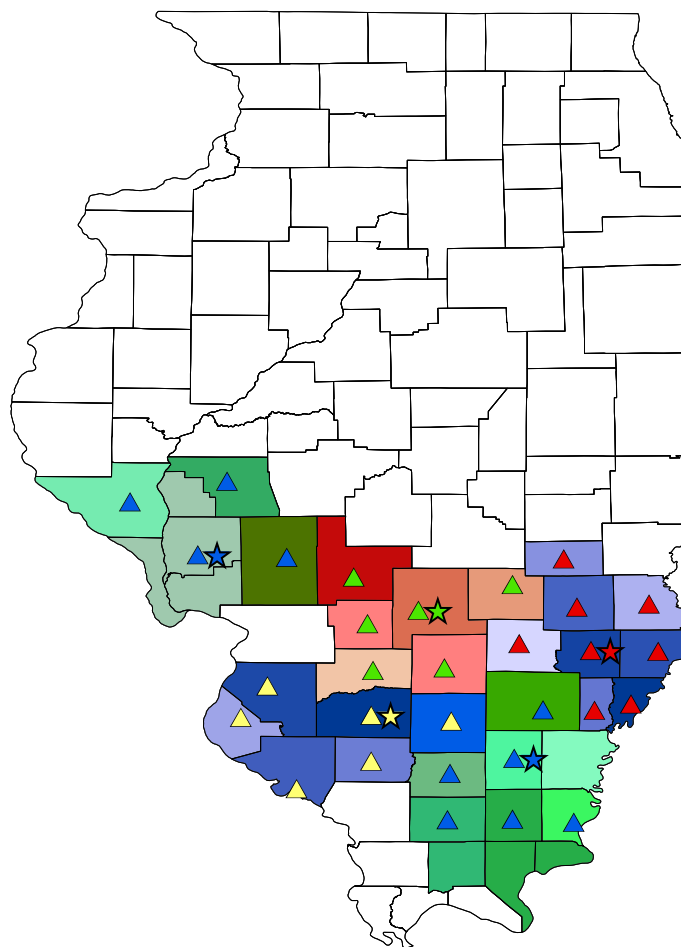


Figure 3.12: The optimal 3-stage biomass-ethanol supply chain configuration considering a variable cropland usage rate as a function of distance from centralized storage and preprocessing (CSP) facilities. The biomass processing demand is 10,000,000 Mg y⁻¹. Triangles represent CSP facilities and stars represent biorefinery facilities. Commonly shaded areas represents one biomass supply region served by a CSP. Biorefineries source biomass from CSPs of the same color. All the selected biomass supply counties are within a distance of 80 km served by CSP facilities.

3.4.6 Scenario Analysis of Biorefinery Capacity Limit

Without any capacity limit on a biorefinery, the optimal supply chain for conversion of 10,000,000 Mg of biomass per year was composed of two biorefineries, 30 CSP facilities, and 36 supply counties (Figure 3.13). As compared to the case with biorefinery capacity limit imposed (Figure 3.12), the new supply chain required fewer, though larger, biorefineries. The capacity of two refineries in the new scenario was 5,560,000 and 3,940,000 Mg y⁻¹, respectively. The optimal Miscanthus-ethanol production costs were reduced from \$207.3 to \$203.8 Mg⁻¹ (Table 3.5). The savings of unit biorefinery related costs outweighed the increased transportation costs, which recommended a supply chain that is composed of large biorefineries with the support of distributed, small CSP facilities. Furthermore, the system suggested building two large biorefineries instead of a single centralized biorefinery. This indicates that there is a maximum biorefinery capacity, given regional biomass availability, where reduced unit biorefinery related costs are not sufficient to offset the increased truck transportation costs, given longer distance transportation.

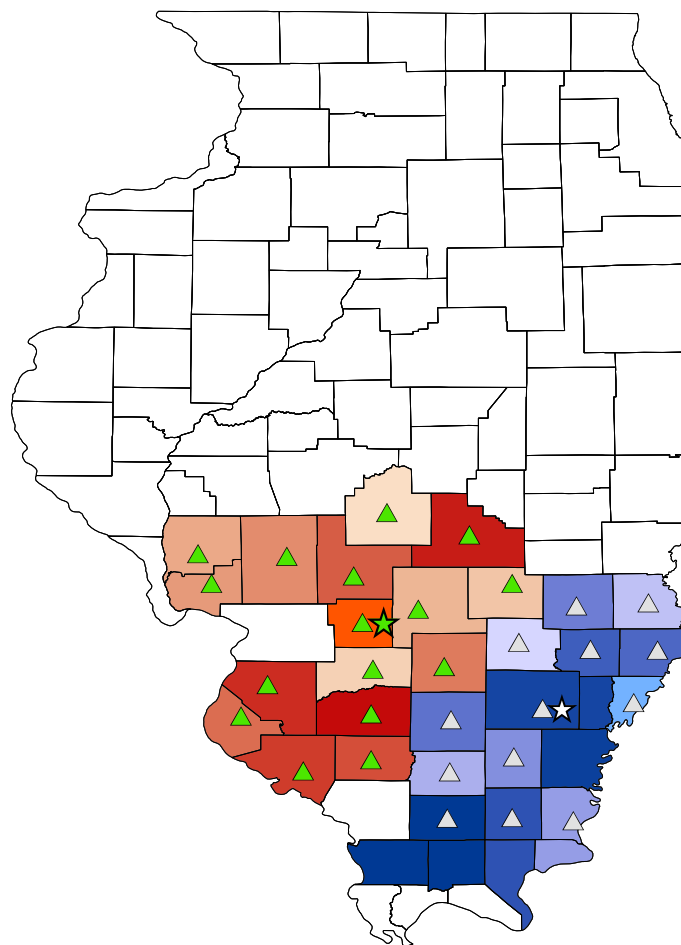


Figure 3.13: The optimal 3-stage biomass-ethanol supply chain configuration when no biorefinery capacity limit is imposed. The cropland usage rate changes at different levels of distance from centralized storage and preprocessing (CSP) facilities. The biomass processing demand is $10,000,000 \text{ Mg y}^{-1}$. Triangles represent CSP facilities and stars represent biorefinery facilities. Commonly shaded areas represents one biomass supply region served by a CSP. Biorefineries source biomass from CSPs of the same color.

3.4.7 Scenario Analysis of Preprocessing Technology and Transportation

Modes

To quantify the impact of preprocessing and transportation modes we considered pelletization and rail transport. The results showed that the optimal supply chain configuration was dependent on the selection of the transportation mode (Figure 3.14). One biorefinery was selected in scenarios including rail transport, while two biorefineries were selected using truck transport. Further, all scenarios suggest that there are benefits to distributed preprocessing of biomass. All the selected biomass supply sites are within 80 km of the CSP facilities they serve. The results recommended ground biomass with rail transportation, where the optimal biofuel production costs could be reduced to \$198.4 Mg⁻¹ (Table 3.6).

Table 3.6: The breakdown of biofuels production costs considering different preprocessing technologies and transportation means. All the numbers in the table are in terms of \$ Mg⁻¹.

	Ground Biomass with Tapping		Biomass Pellets	
	Truck + Truck	Truck + Rail	Truck + Truck	Truck + Rail
Biomass costs	67.7	67.2	67.6	67
CSP related costs	15	15.2	22.8	23.1
Transportation costs	24.4	22.4	22.2	16.8
Biorefinery related costs	96.7	93.7	96.7	93.7
Total production costs	203.8	198.4	209.3	200.6

Rail transportation provides a better transportation means for preprocessed biomass between CSPs and biorefineries. Biomass pellets gained higher savings of transportation costs using rail transportation, due to its higher density. The relatively low variable (distance related)

costs for rail transportation makes it effective to source biomass pellets from further away areas where biomass procurement costs are low (Figure 3.14b and 14d). The reduced transportation costs using biomass pellets, however, could not offset increased preprocessing costs—approximately \$8 Mg⁻¹ higher than ground biomass. This is because the current study of biomass supply chain is considered within Illinois, where average transportation distance is about 140 km for both rail transportation scenarios. The longer distance biomass transported, the more savings could be gained by biomass pellets. It is therefore anticipated that biomass pellets could be a recommended format for long distance transportation.

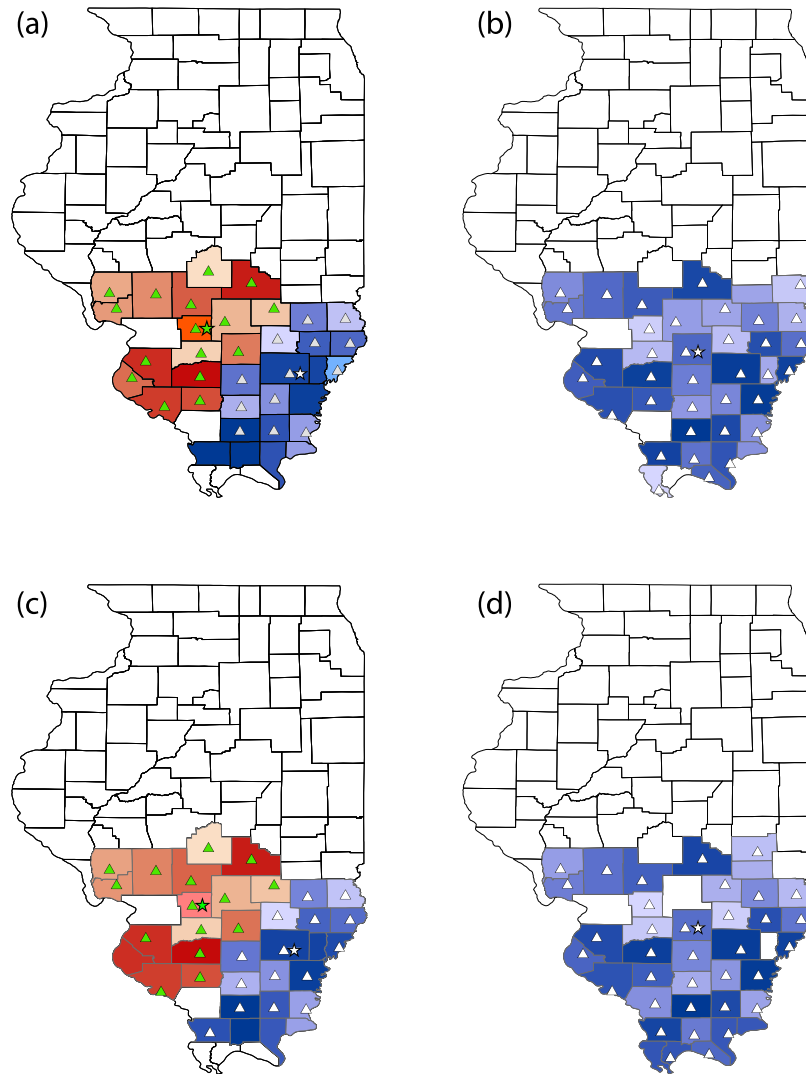


Figure 3.14: The impact of preprocessing technology and transportation mode on the biomass supply chain configuration: (a) ground biomass with tapping and truck transportation, (b) ground biomass with tapping and rail transportation, (c) biomass pellets and truck transportation, (d) biomass pellets and rail transportation. No biorefinery capacity limit is imposed for all four scenarios. The cropland usage rate changes as a function of distance from centralized storage and preprocessing facilities. The biomass processing demand is $10,000,000 \text{ Mg y}^{-1}$. Triangles represent CSP facilities and stars represent biorefinery facilities. A commonly shaded area represents one biomass supply region served by a CSP. Biorefineries source biomass from CSPs of the same color.

3.5 CONCLUSIONS

A biomass supply chain optimization (BioScope) model was developed to minimize annual biomass-ethanol production cost by selecting the optimal numbers, locations, and capacities of farms, centralized storage and preprocessing sites and biorefineries as well as identifying the optimal biomass flow patterns from farms to biorefineries. GIS were used to generate spatial data related to biomass production and the shortest transportation distances between the possible facilities using the existing road and railway network. The BioScope model was implemented to study Miscanthus-ethanol supply chain in Illinois. The baseline case was set at the demand of 2,000,000 Mg y⁻¹ using 2% of cropland for Miscanthus production. The baseline case results showed that unit Miscanthus-ethanol production costs were \$0.74 L⁻¹, and biorefinery related costs accounted for 48% of costs. The sensitivity analyses demonstrated that the optimal supply chain configuration changed for different cropland usage rates, biomass demands, transportation costs and modes, and preprocessing technologies. The unit Miscanthus-ethanol production costs decreased with increasing cropland usage rates. Rail outperformed truck transportation to ship preprocessed biomass from centralized storage and preprocessing facilities to biorefineries. Large biorefineries, supported by rail transportation, are suggested to achieve maximum economies of scale. Distributed centralized storage and preprocessing facilities are suggested to preprocess biomass locally. For the Illinois case study, ground biomass with tapping outperformed biomass pellets, largely due to the relatively low preprocessing costs of grinding and short transportation distance required. High density biomass is suggested for long distance transportation.

Note

The version of the BioScope model described here is associated with revision number 2497 on the Subversion Server maintained by the Engineering Solutions for Biomass Feedstock Production Program in the Energy Biosciences Institute. This revision of the software has been tagged for future reference.

CHAPTER 4

DYNAMIC BIOMASS-ETHANOL SUPPLY CHAIN OPTIMIZATION

This chapter describes the development of a dynamic, multiple-year, strategic planning model for biomass supply chain optimization under the changing biomass supply and demand. The model was developed to address a long-term strategic biomass supply chain planning question that how biomass supply chain configuration could be best evolved to meet the increasing cellulosic-ethanol production demand. The model could quantify the changes of biomass-biofuel production costs in an evolving system and identify the key affecting factors. The dynamic optimization model was developed based on the BioScope model, which is described in Chapter Three. The model can provide decision support on strategic level questions such as production timings, locations, and capacities of facilities given the changes of biomass supply and demand.

This chapter cannot be realized without successful teamwork, where the team members are Tao Lin, Luis Rodríguez, Yogendra Shastri, Alan Hansen, and K.C. Ting. Mr. Lin led the overall research, collected data, developed the model, and drafted the manuscript. Drs. Rodríguez, Shastri, Hansen, and Ting participated the research design and the draft revision.

The primary tasks conducted by Mr. Lin include: 1) developed constraint and objective equations of the model, 2) designed spatial related maps for results visualization, and 3) analyzed and discussed the model results.

This chapter is based on a published conference paper (Lin et al., 2012), with the expansion of updated case study design and results discussions. This chapter will be further

edited for submission to one of the following journals including Bioresource Technology, Transactions of ASABE, and GCB-bioenergy.

Abstract. *To produce 16 billion gallons of ethanol from cellulosic feedstocks by 2022, the biomass based ethanol industry will undergo significant changes in biomass supply and ethanol demand as compared to the current situation where few commercial facilities are operating. Strategic level decisions such as timings, locations, and capacities of facilities within the system will be critical for the success of the cellulosic based ethanol industry. These decisions will be impacted by biomass availability, production costs, and accessibility to transportation infrastructure. A multi-stage biomass supply chain optimization model was developed to answer these systems level questions. The model minimized the total ethanol production costs throughout the planning period (2012-2022) given the projected changes of biomass supply and ethanol demand. It was assumed that a planning decision should be made each year during the planning period. The results show that cellulosic-ethanol production costs would be reduced from \$246.1Mg⁻¹ in 2012 to \$208.7 Mg⁻¹ in 2022 for 1-year contract and from \$248 Mg⁻¹ in 2012 to \$209Mg⁻¹ in 2022 for 11-year contract. The cost savings in both scenarios are attributed to the increased economies of scale and shorten biomass transportation distances. The short-term contract scenario requires less production costs, largely due to the savings of transportation costs.*

Keywords. Supply chain optimization, dynamic, GIS, cellulosic ethanol, biofuels.

4.1 INTRODUCTION

Global climate change, shortage of the fossil fuel resources, and lack of reliable energy supply have driven many countries in the world to develop new means of energy supply. Biofuels are considered a renewable transportation fuel to reduce greenhouse gas (GHG) emissions and improve energy security (EPA, 2010). The U.S. fuel ethanol production has increased significantly in the last three decades, from 175 millions of gallons in 1980 to 13.9 billion gallons in 2011 (RFA, 2012). The first generation biofuel production, corn ethanol production, accounts for the majority of the increase. However, the increase usage of corn for fuel production has been criticized for its competition with food supply, which increased food prices and worsened the world hunger situation.

Unlike corn ethanol production, cellulosic ethanol production is considered a sustainable biofuel production because it uses renewable biomass (i.e. corn stover, forest waste, and energy crops) as its primary feedstock, which does not compete with food supply. In the U.S., cellulosic ethanol is expected to be an important component of a future renewable fuel system and its production has been target to be 16 billion gallons in 2022 (EPA, 2010). However, few commercial cellulosic ethanol facilities exist at this time due to the lack of cost-effective technologies and reliable feedstock supply. Furthermore, because of low energy density and conversion efficiency, 80 gal Mg⁻¹ as of now (Humbird et al., 2011), an annual supply of 200 million Mgs of biomass are required to meet the annual cellulosic ethanol production target in 2022. In order to transport such a large amount of biomass efficiently and effectively, a novel system infrastructure is required to ensure effective biomass feedstock provision for large-scale biofuels production. With the government support and private equity interests, cellulosic ethanol

industry is being fast developed currently. This transition feature requires a strategic planning to consider both spatial and temporal constraints to identify a system design that is best suited for large-scale cellulosic ethanol production.

Spatially, biomass yields, quality, and production costs vary due to the geographical differences in weather and soils. Geographic Information System (GIS) has been applied to quantify biomass yields and production costs at the county level (Graham et al., 2000; Khanna et al., 2008). Because of the distributed supply of biomass, the larger the biorefinery production capacity, the larger the biomass feedstock supply region, and accordingly the higher the biomass transportation costs. On the biorefinery side, large biorefinery can reduce unit production costs because of the economies of scale (Kocoloski et al., 2011). Therefore, the locations, numbers, and capacities of facilities and biomass flow patterns between the facilities within the system are critical questions on the spatial dimension.

Temporally, long-term biofuel system planning is critical when biomass supply chain system undergoes such an evolving process, expanding from nothing to a production of 16 billion gallons in 2022. The production system infrastructure will be expanded in response to the growing demand. Because of the dynamic feature of such an evolving system, several temporal issues need to be resolved, such as: 1) Whether to build new facilities or expand the existing facilities to meet the increasing demand; 2) Where to source the increasing biomass supply; 3) Will the new facilities compete biomass resources with the existing facilities?

Strategic planning of biomass supply chain network is critical to help design such a system infrastructure that can meet the increasing demand of biomass feedstock provision. Most previous studies have only considered the spatial issue of the biomass supply chain planning. Some researchers optimized the biomass supply chains that only include two stages: biomass

suppliers and biorefineries (Parker et al., 2010; Kocoloski et al., 2011; Leboreiro and Hilaly, 2011). To provide consistent quality and format of the feedstock and reduce logistics burdens, other researchers proposed a three-stage supply chain that has an addition step of centralized storage and preprocessing (CSP) to handle, receive, store, and preprocess biomass before sending raw feedstock to biorefineries (Hess et al., 2007; Shastri et al., 2012a) (Figure 4.1). However, few studies have considered the dynamic feature in the long-term strategic planning of biomass supply chain (Huang et al., 2010).

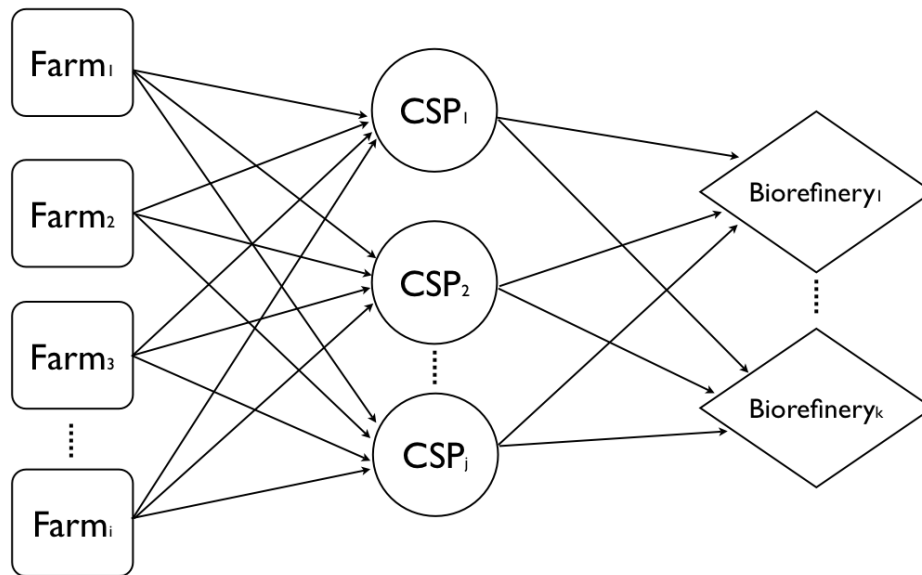


Figure 4.1: Farms, centralized storage and preprocessing (CSP) sites, and biorefineries make up a three-stage biomass-ethanol supply chain. The associated costs include biomass purchase costs, transportation costs, CSP operating costs, CSP capital related costs, biorefinery operating costs, and biorefinery capital related costs.

To achieve the overall effectiveness of such evolving biomass supply chains, a multi-period optimization model, Dynamic BioScope, was developed through incorporating both spatial and temporal dimension issues. To minimize the total system production costs within the planning horizon, the model can 1) decide the optimal timings, numbers, locations, and

capacities of facilities within the system; 2) decide whether to build new facilities or expand the existing facilities; 3) decide the optimal biomass flow patterns between facilities at each year.

4.2 OVERVIEW OF THE DYNAMIC BIOSCOPE MODEL

The system scope of this study is from biomass supply to ethanol production at biorefineries. To provide consistent quality and quantity of feedstock for large-scale cellulosic ethanol production, a three-stage supply chain was considered in this study (Figure 4.1). From a systems perspective, facility capital costs, facility operating costs, biomass purchase costs and biomass transportation costs are major cost categories for such a biomass supply chain (Hess et al., 2007; Humbird et al., 2011).

Through integrating geographic information and operations research methods, the optimization model was developed to provide decision support on the optimal biomass supply chain configurations over a planning period, under the projected biomass supply and demand changes. Annual biomass processing demands and annual cropland usage rate are the key input parameters for the dynamic optimization. County level biomass yield and production costs, transportation distances, facility capital costs, and facility operating costs are other key inputs, and the detailed description can be found in Chapter 3.

4.2.1 Mathematical model description

The dynamic optimization model is to minimize the total cellulosic ethanol production costs throughout a planning horizon, under the projected changes of biomass supply and demand. The planning horizon is divided into multiple 1-year time phases and decisions are made for each year. A list of set names, decision variables, and parameters used in the model is provided in “Nomenclature” in Tables B.1 to B.3 of Appendix B. The total cellulosic ethanol production

costs (Z) are estimated by the summation of each year production costs that are comprised of four costs: biomass procurement costs (C_b^t), transportation costs (C_v^t), CSP related costs (C_p^t), and biorefinery related costs (C_e^t) (Eq. 4.1).

$$\text{Minimize } Z = \sum_t C_b^t + C_v^t + C_p^t + C_e^t \quad (4.1)$$

Biomass supply contract is important for an emerging biofuels market, especially for dedicated energy crops where the life cycle usually lasts for more than ten years. It is assumed that if a biomass supply county is signed a contract in year tc to provide biomass feedstock, then the same amount of biomass is guaranteed to be selected from that county throughout the contract period (T^{tc}) (Eq. 4.2). The length of the contract is an input parameter determined by the user. The amount of biomass supplied from each supply site in year t ($b^{i,t}$) is estimated by summing all the biomass delivered to all the CSP facilities from all the contracts (Eq. 4.3).

$$\sum_j \sum_{tc} f^{i,j,t+1,tc} = \sum_j \sum_{tc} f^{i,j,t,tc} \quad \forall t \in T^{tc}, tc \in T, i \in I \quad (4.2)$$

$$b^{i,t} = \sum_j \sum_{tc} f^{i,j,t,tc} \quad \forall tc \in T, i \in I \quad (4.3)$$

Biomass procurement costs in year t (C_b^t) are a function of the amount of biomass provided from each supply sites in year t ($b^{i,t}$) and the county-level biomass production costs at each supply site ($c^{i,t}$) (Eq. 4.4). County-level biomass production costs ($c^{i,t}$) and biomass availability ($A^{i,t}$) are two inputs related to biomass supply. The total amount of biomass supplied from all supply counties during each year should meet the annual biomass demand (P^t) (Eq. 4.5). Moreover, the total amount of biomass output from a biomass supply site should not exceed its annual biomass availability ($A^{i,t}$) (Eq. 4.6).

$$C_b^t = \sum_i c^{i,t} \times b^{i,t} \quad \forall t \in T \quad (4.4)$$

$$\sum_i b^{i,t} = P^t \quad \forall t \in T \quad (4.5)$$

$$b^{i,t} \leq A^{i,t} \quad \forall i \in I, t \in T \quad (4.6)$$

Annual biomass transportation costs (C_v^t) are composed of variable transportation costs (V_r^t) and fixed transportation costs (V_f^t) (Eq. 4.7-4.9). The annual amounts of pre-processed biomass moved from supply counties to CSP facilities by different contracts ($f^{i,j,t,tc}$) and processed biomass moved from CSP to biorefineries ($f^{j,k,t}$) are the key decision variables for biomass transportation costs. The associated input parameters include unit variable transportation cost (T_{v1}, T_{v2}), unit fixed transportation cost (T_{f1}, T_{f2}), and the transportation distance ($d^{i,j}, d^{j,k}$). The concept of estimating annual biomass transportation costs are similar to the approach used for BioScope model, and please see the detailed equation descriptions in Chapter 3.

$$C_v^t = V_r^t + V_f^t \quad \forall t \in T \quad (4.7)$$

$$V_r^t = \sum_i \sum_j \sum_{tc} (T_{v1} \times f^{i,j,t,tc} \times d^{i,j}) + \sum_j \sum_k (T_{v2} \times f^{j,k,t} \times d^{j,k}) \quad \forall t \in T \quad (4.8)$$

$$V_f^t = \sum_i \sum_j \sum_{tc} T_{f1} \times f^{i,j,t,tc} + \sum_j \sum_k T_{f2} \times f^{j,k,t} \quad \forall t \in T \quad (4.9)$$

The costs related to CSP facilities in year t (C_p^t) are composed of annual operating costs (S_o^t) and annual capital related costs (S_c^t) (Eq. 4.10). Annual operating costs include the costs for utilities, maintenance, labor, supervision, insurance, laboratory charges, and waste treatment. In this study, it is assumed that CSP facilities with different capacities incur the same unit operating

costs (s_{op}). Therefore, annual operating costs are linearly dependent on the annual demand of biomass for CSP facilities (P^t) (Eq. 4.11).

Annual capital costs are linearly dependent on the capital investment costs where a factor α (13.7%) is used to represent its relationship. To improve the accuracy, the model adopts a piecewise linear approximation to estimate the capital investment costs for three different levels of facility capacity. Therefore, annual capital related costs are linearly dependent on the sum of fixed (s_f^l) and variable (s_v^l) capital related costs at every level of capacity at each potential location (Eq. 4.12). The binary decision variable $o_s^{j,t}$ controls whether there exists a CSP facility located in county j in year t . The binary decision variable $o_s^{j,l,t}$ controls the capacity level l of the CSP facility located in county j in year t . And, the variable $p^{j,l}$ represents the specific capacity of the CSP in county j at the capacity level l . The sum of the capacities of CSP at all levels in year t should be the same as the total CSP capacity in that county (Eq. 4.13). In the current study, it is assumed that once a facility is built in county j in year t , the facility will keep operating in the following years. The facility can be expanded later but can only be expanded to the high limit of that capacity level (Eq. 4.14). Considering the mass balance, the CSP processing capacity in county j year t should be equal to the total amount of biomass transported to county j from all supply sites by all contracts (Eq. 4.15).

$$C_p^t = S_o^t + S_c^t \quad \forall t \in T \quad (4.10)$$

$$S_o^t = s_{op} \times P^t \quad \forall t \in T \quad (4.11)$$

$$S_c^t = \alpha \times \left(\sum_j \sum_l s_v^l \times p^{j,l,t} + s_f^l \times o_s^{j,l,t} \right) \quad \forall t \in T \quad (4.12)$$

$$\sum_l p^{j,l,t} = p^{j,t} \quad \forall t \in T, j \in J \quad (4.13)$$

$$p^{j,l,t} \leq p^{j,l,t+1} \quad \forall j \in J, l \in L, t \in T \quad (4.14)$$

$$\sum_i \sum_{tc} f^{i,j,t,tc} = \sum_l p^{j,l,t} \quad \forall j \in J, t \in T \quad (4.15)$$

If there is a facility in county j , there only exists one capacity level facility during the planning period (4.16). A piecewise linear approximation approach is applied to estimate the economies of scale at different capacity levels (4.17 -4.19). The detailed description can be found in Chapter 3. The biorefinery related costs estimations and the constraints for biorefinery location, capacity, and production timing are similar to the equations provided here for CSP facilities.

$$\sum_l o_s^{j,l,t} = o_s^{j,t} \quad \forall j \in J, t \in T \quad (4.16)$$

$$\lambda_s^0 \times o_s^{j,1,t} \leq p^{j,1,t} \leq \lambda_s^1 \times o_s^{j,1,t} \quad \forall j \in J, t \in T \quad (4.17)$$

$$\lambda_s^1 \times o_s^{j,2,t} \leq p^{j,2,t} \leq \lambda_s^2 \times o_s^{j,2,t} \quad \forall j \in J, t \in T \quad (4.18)$$

$$\lambda_s^2 \times o_s^{j,3,t} \leq p^{j,3,t} \leq \lambda_s^3 \times o_s^{j,3,t} \quad \forall j \in J, t \in T \quad (4.19)$$

4.3 CASE STUDY OF ILLINOIS MISCANTHUS-ETHANOL PRODUCTION

To illustrate the use of the Dynamic BioScope model, we chose Miscanthus-ethanol supply chain in Illinois for the case study. Each county in Illinois is considered as a candidate location, thus there will be 102 candidates for each stage of the supply chain. To provide decision support on how to meet the RFS mandate, the planning period of the case study is set from 2012 to 2022.

4.3.1 Biomass demand and supply change

Based on the RFS mandate, the nationwide cellulosic ethanol production capacity will increase annually from almost nothing to 16 billion gallons in 2022 (Table 4.1). In 2011, all the corn-ethanol facilities in Illinois provided 1.23 billion gallons of ethanol, accounting for 8.3% of nationwide corn ethanol production capacity (RFA, 2012). Assuming Illinois can provide the same market share of cellulosic ethanol production biennially from 2012, the annual biomass demand for Illinois can be estimated (Table 4.1).

Table 4.1: The projected biomass demand and supply changes in Illinois from 2012 to 2022. The projected demands in Illinois are assumed based on the projected cellulosic ethanol production by RFS and the ratio of Illinois corn ethanol production capacity to nationwide ethanol production, 8.3%.

Year	The U.S. annual cellulosic ethanol production capacity [†] (Million gallons)	Illinois annual cellulosic ethanol production (Million gallons)	Illinois annual cellulosic biomass supply (Mg)	The cropland usage rate in Illinois for Miscanthus production
2012	500	41.5	530,000	1%
2013	1000	41.5	530,000	2%
2014	1750	145.3	1,850,000	4%
2015	3000	145.3	1,850,000	6%
2016	4250	352.8	4,500,000	8%
2017	5500	352.8	4,500,000	10%
2018	7000	581	7,400,000	12%
2019	8500	581	7,400,000	14%
2020	10,500	871.5	11,100,000	16%
2021	13,500	871.5	11,100,000	18%
2022	16,000	1328	17,000,000	20%

[†] The value is based on EPA (2010).

Biomass supply is a function of cropland area and biomass yield. Due to the spatially variance of weather and soils, biomass yield vary by counties (Khanna et al., 2008). To provide sufficient biomass to meet the evolving biomass demand in the next ten years, it is assumed that the cropland usage rate for Miscanthus production also increases annually (Table 4.1).

4.3.2 Facility capacity levels and capital investment costs

Facility capital investment costs are the most significant costs for cellulosic ethanol production (Humbird et al., 2011). The power law type of equation is usually applied in literature to predict capital investment cost for a particular scale based on the costs for the base, where the scaling factor usually ranges from 0.6 to 0.7 for a biomaterial and chemical processing facility (Peters and Timmerhaus, 1991). Facility capital investment costs are composed of two parts: fixed capital investment costs and variable investment costs. Large bioprocessing facilities incur higher fixed capital investment costs but lower variable investment costs as a result of economies of scale. To identify the impact of facility capacity on the supply chain configuration, three levels of centralized storage and preprocessing (CSP) facilities and biorefineries are proposed in this study, namely small (50,000 – 600,000 Mg y⁻¹), medium (600,000 – 1,250,000 Mg y⁻¹), and large (1,250,000 – 2,000,000 Mg y⁻¹). The facility capital investment costs for each capacity level of both CSP facilities and biorefineries are based on Lin et al. (2013). It is assumed that the facility expansion capital costs are the same as the facility variable capital investment costs.

4.3.3 Biomass supply contract design

The life span of dedicated energy crop usually lasts for more than ten years, which would result in an important issue on biomass supply contract design. When there does not exist a commodity

market for biomass feedstock, both farmers and biomass processors would prefer long-term contract to secure the sell and purchase of biomass feedstock, respectively. However, if there exists a commodity market, both parties would probably not prefer signing a long-term contract but seeking for a better plan for each year. To quantify the impact of the contract length on the evolving biomass market, this study considers 1-year and 11-year contract between farmers and processors. For 1-year contract, biomass processors could choose different biomass suppliers each year, whereas for 11-year contract, biomass processors would keep purchasing biomass from certain biomass suppliers once the contract is made.

4.4 RESULTS AND DISCUSSION

For one-year contract case, the least-cost planning strategy of Miscanthus-ethanol supply chain in Illinois suggests the construction of 21 centralized storage and preprocessing (CSP) facilities and 10 biorefineries from year 2012 to 2022 (Figure 4.2). CSP facilities always prefer sourcing biomass from counties nearby. The increased biomass demand would require more CSP and biorefinery facilities to be constructed, which also expands the area of biomass supply counties. During the 11 year period, 37 counties have been chosen to supply biomass, whereas 32 counties are selected to provide biomass in 2022. Some supply counties are in and out of competitive production during the planning period (Figure 4.2). The changes of supply county selection are most occurred in the years when biomass productions increase while the demands remain the same. For these years, CSP facilities would prefer sourcing more biomass from the counties in a short distance, which would drive the counties further away out of the procurement scope. The detailed results on biomass supply, CSP and biorefinery capacities are provided in Tables B.4 to B.6 of Appendix B. The total systems costs throughout the planning period are approximately

\$13.68 billions to provide a total of 5.15 billion gallons of ethanol. The average Miscanthus-ethanol production costs are $\$2.66 \text{ gal}^{-1}$, or $\$0.7 \text{ L}^{-1}$. With the increasing biomass supply and demand, larger biorefineries and CSP facilities would be built and operated in the later years of the planning period. The increased facility capacity, economies of scale, and better transportation network would reduce the annual cellulosic-ethanol production costs from $\$246.1$ per Mg of dry matter biomass in 2012, or $\$3.08$ per gallon of ethanol, to $\$208.7$ per Mg of dry matter biomass in 2022, or $\$2.61$ per gallon of ethanol (Figure 4.3).

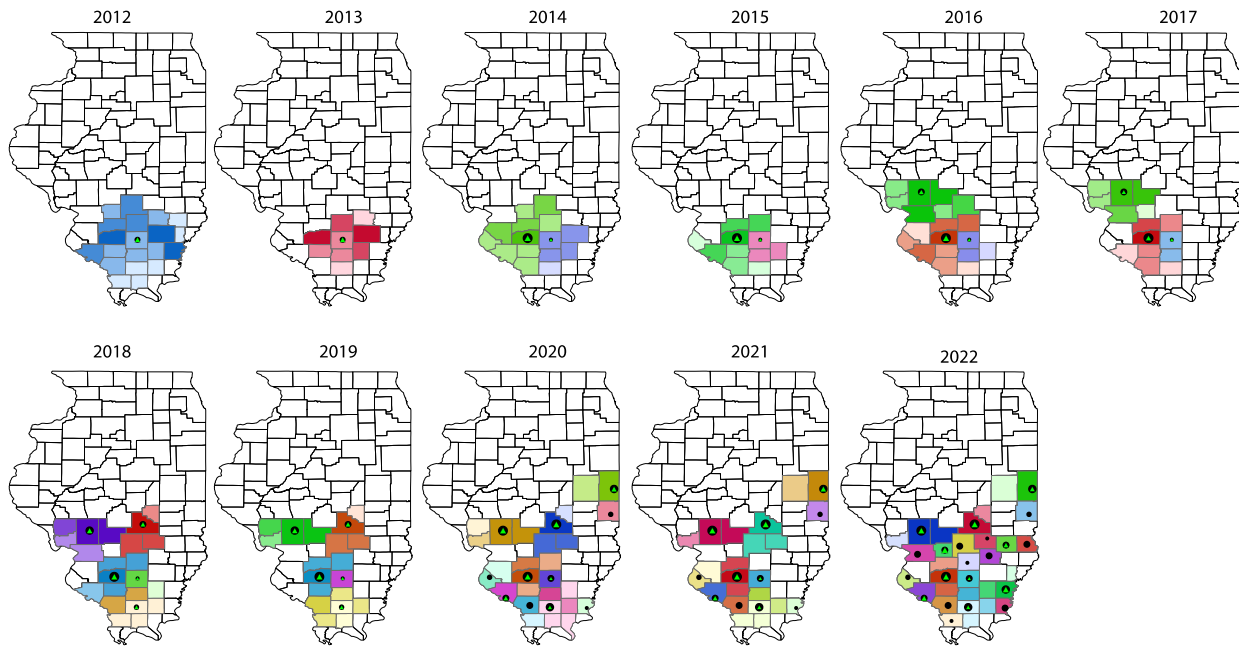


Figure 4.2: The changes of biomass supply chain configuration from 2012 to 2022 given 1-Year contract.

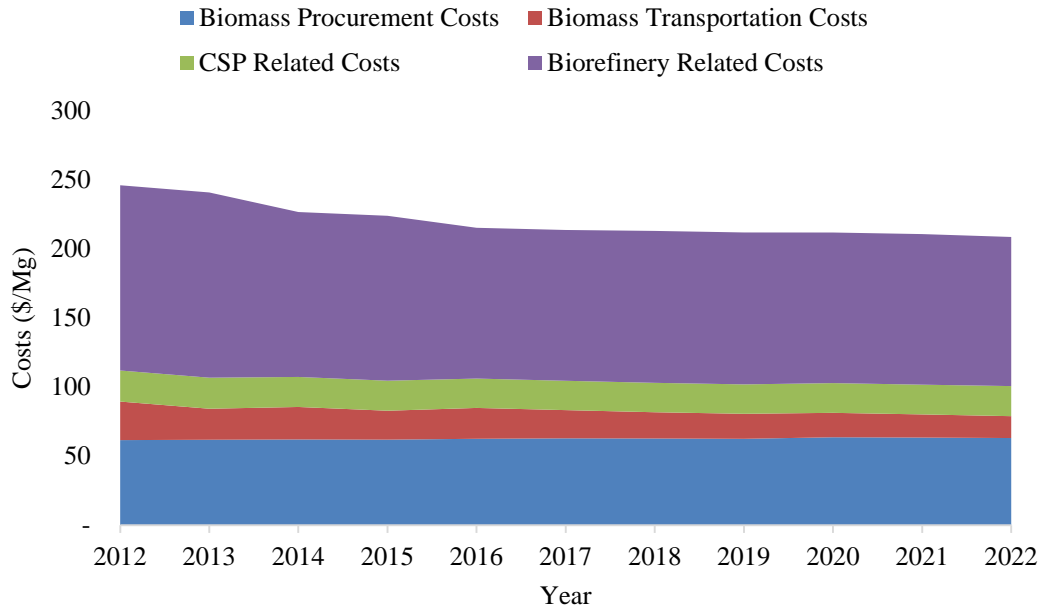


Figure 4.3: The biomass production costs changes in Illinois from 2012 to 2022 given 1-year contract.

For 11-year contract case, the least-cost planning strategy of Miscanthus-ethanol supply chain suggests the construction of 30 centralized storage and preprocessing (CSP) facilities and 11 biorefineries from year 2012 to 2022 (Figure 4.4). During this 11-year period, 33 counties have been chosen to supply biomass, and all 33 counties are selected to provide biomass in 2022 because of the long-term contract. Once a county is selected a biomass supplier, the county will always be selected as a result of the long-term contract. Although biomass supply changes annually, the supply chain configuration only changes every other year, following the changes of the demand, as a result of the long-term contract. The selected supply region remains relatively stable, which indicates the importance of the decisions at the beginning of the planning period. The detailed results on biomass supply, CSP and biorefinery capacities are provided in Tables B.7 to B.9 of Appendix B. The total systems costs throughout the planning period are approximately \$13.73 billions to providing a total of 5.15 billion gallons of ethanol. The average

Miscanthus-ethanol production costs throughout the 11-year planning period are \$2.67 gal⁻¹, or \$0.7 L⁻¹. With the evolving biomass supply and production, larger biorefineries and CSP facilities would be built and operated in the later years of the planning period. The increased facility capacity, their associated economies of scale, and better transportation network would reduce the annual cellulosic-ethanol production costs from \$248.1 per Mg of dry matter biomass in 2012, or \$3.1 per gallon of ethanol, to \$209 per Mg of dry matter biomass in 2022, or \$2.61 per gallon of ethanol (Figure 4.5).

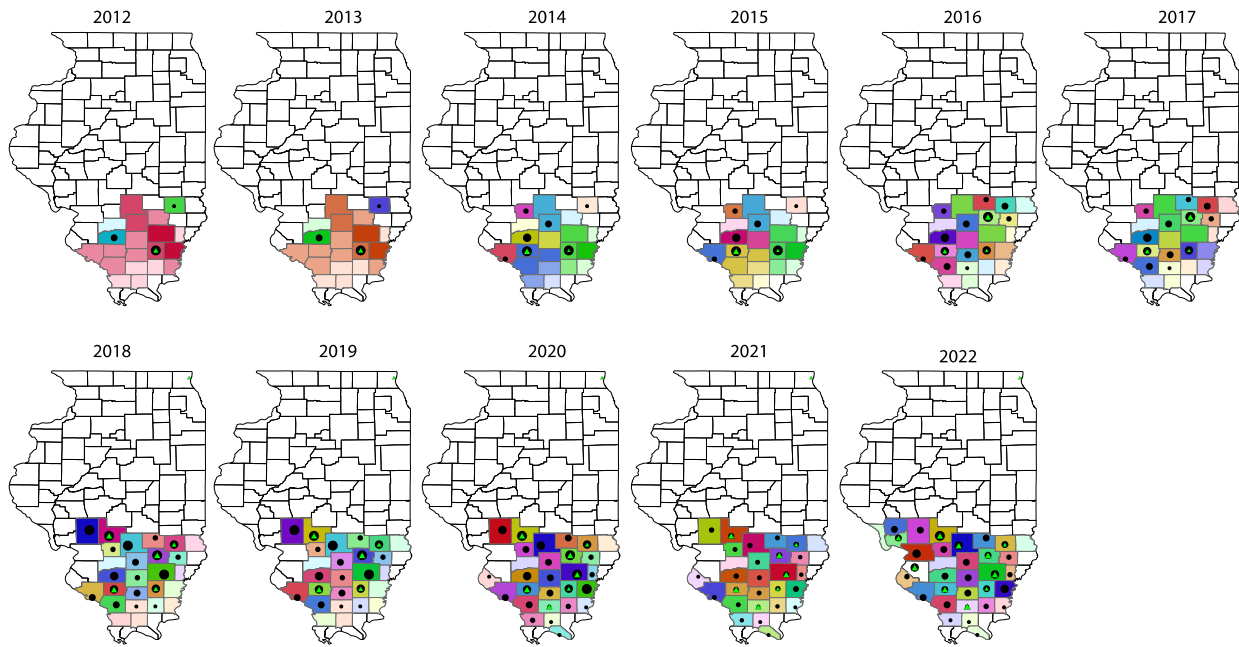


Figure 4.4: The changes of biomass supply chain configuration from 2012 to 2022 based on 11-Year contract condition.

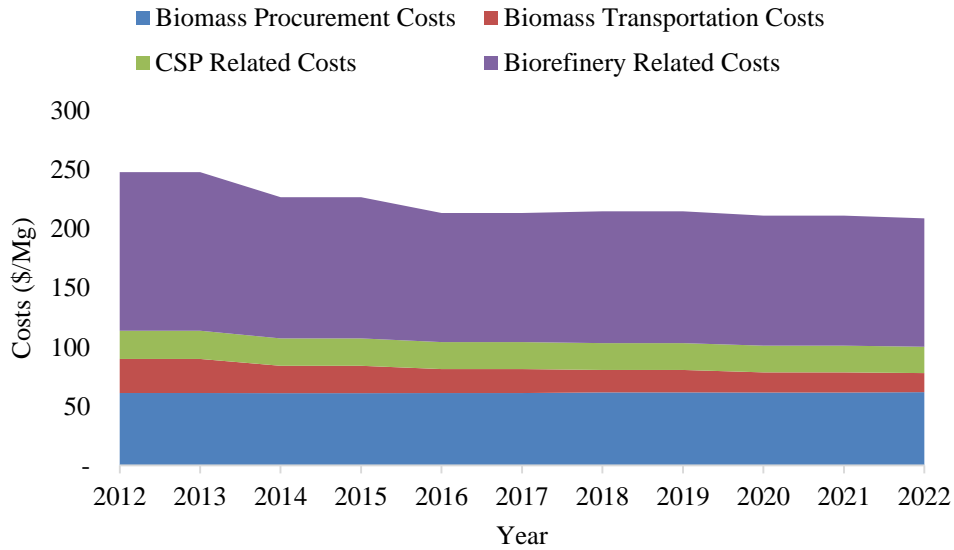


Figure 4.5: The biomass production costs changes in Illinois from 2012 to 2022 given 11-year contract.

The results of both contract scenarios show that small biorefineries and CSP facilities would be built in the early stage. With the increasing biomass supply and demand, new larger facilities would be built first to achieve economies of scale and then followed by the expansions of existing small facilities. The selected biomass supply area is more distributed for the short-term contract as compared to the long-term contract. The results show that the biomass supply area remains relatively stable under the long-term contract, where the supply counties are mainly located in southern Illinois. On the other side, the short-term contract allows the biomass supply area to be more flexible with the changes of biomass supply and demand. Some counties would be considered as the biomass supply area for a short period.

For annual cellulosic ethanol production costs, the long-term contract usually requires higher production costs in odd number years (Figure 4.6), when the demand remains the same as the previous year but with a higher biomass supply from each county. For the short-term contract, the system would prefer to source more biomass from the counties near CSP facilities

in these years, which would shrink the total supply area (Figure 4.2). The smaller biomass supply area would result in lower biomass transportation costs in the odd number years, which provides major contributions for the cost savings (Figure 4.7).

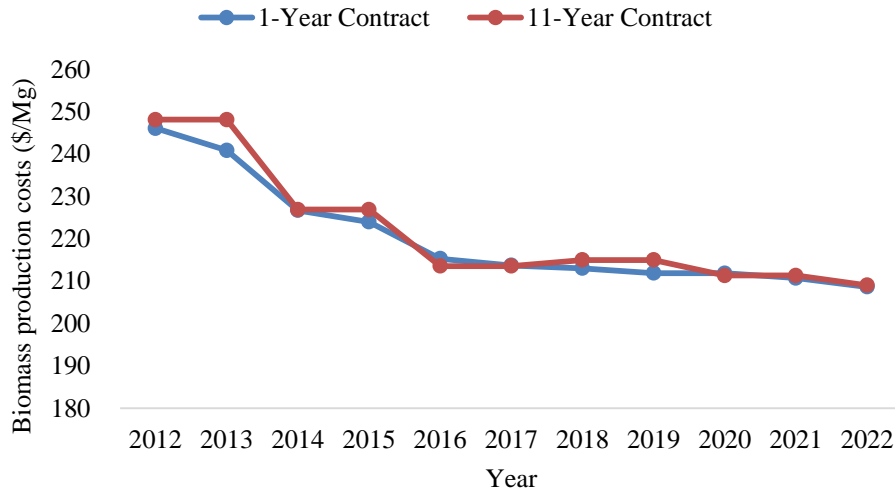


Figure 4.6: The comparison of biomass production costs from 2012 to 2022 at 1-Year and 11-Year contract conditions.

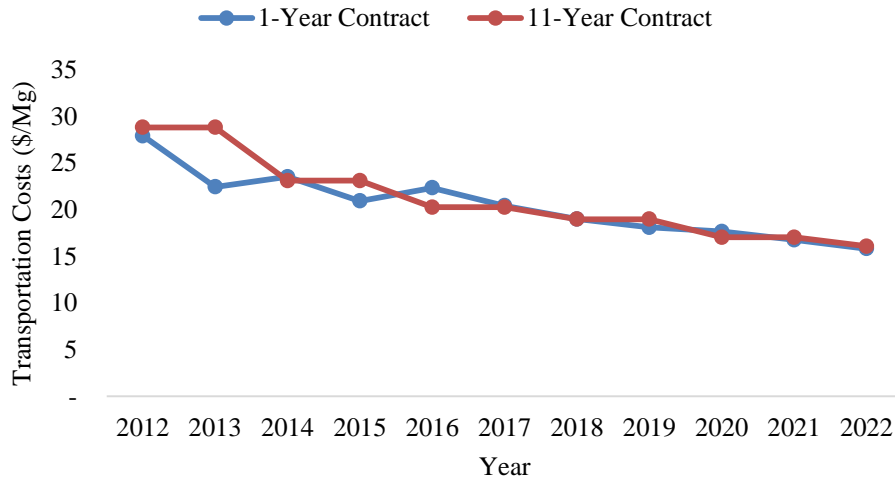


Figure 4.7: The comparison of biomass transportation costs from 2012 to 2022 at 1-Year and 11-Year contract conditions.

The contract design mainly affects the decisions on how to source biomass, which are highly related to biomass procurement and transportation costs. The results show that the short-term contract incurs lower production costs, mainly because of the flexibility of sourcing biomass in a short distance with a lower biomass procurement costs. The trend of biorefinery related costs change during the planning period are similar in both cases, which indicates that the contract design would not affect the biorefinery related decisions.

In both cases, biorefinery related costs are the most important cost factor, accounting for more than half the cellulosic-ethanol production costs. Moreover, the construction and operation of large biorefineries would drive down the unit biorefinery related costs considering the economies of scale. The magnitude of savings on biomass transportation costs is incomparable to that on biorefinery related costs (Figures 4.3 and 4.5). The decisions of building large facilities are highly dependent on the assumption of biomass demand. To better understand the dynamics of an evolving biomass-biofuel production system, more scenario analyses would be provided considering the changes on biomass demands.

4.5 CONCLUSIONS

Dynamic strategic planning helps to identify the optimal supply chain configurations suited for the transition to a future with significantly higher ethanol production from cellulosic feedstock. The strategic level decisions should consider both spatial and temporal issues. The decisions of the optimal installation/expansion timings, locations, and capacities of facilities within the system will be critical for the success of cellulosic based ethanol industry. These decisions will be impacted by biomass availability, production costs and accessibility to transportation infrastructures. The biomass-ethanol supply chain has three stages, including farms, centralized

storage and preprocessing facilities, and biorefineries. The optimization model was implemented to analyze the Miscanthus-ethanol supply chain in Illinois from the year 2012 to 2022 considering 1-year and 11-year contract scenarios. The results show that cellulosic-ethanol production costs would be reduced from \$246.1Mg⁻¹ in 2012 to \$208.7 Mg⁻¹ in 2022 for 1-year contract and from \$248 Mg⁻¹ in 2012 to \$209Mg⁻¹ in 2022 for 11-year contract. The lower production costs for the short-term contract are a result of savings on biomass transportation costs.

CHAPTER 5

INTEGRATED STRATEGIC AND TACTICAL BIOMASS SUPPLY CHAIN OPTIMIZATION

This chapter describes the development of an integrated strategic and tactical biomass supply chain optimization model. The development of the integrated model is to connect short-term decisions (e.g. harvesting and delivery schedules) to long-term decisions (e.g. facility locations and capacities) through the defined mass-balanced constraints. The integrated model can identify how strategic planning decisions would interact with tactical planning decisions for an optimal biomass provision system design. The detailed constraint equations, variables, and input data parameters are provided to better understand the biomass supply chain system. A base case study of Miscanthus production in Illinois is presented to illustrate the use of the model. Scenario analyses are conducted to quantify how the change of biomass yield rate and ethanol demand would affect the optimal biomass supply chain configuration and its associated production costs.

This study cannot be completed without successful teamwork, where the team members include Tao Lin, Luis Rodríguez, Yogendra Shastri, and K.C. Ting. Mr. Lin led the overall research, collected and analyzed data, developed the model, discussed the results, and drafted the manuscript. Dr. Rodríguez participated the research design and led the draft revision. Dr. Shastri contributed the original source code of the BioFeed model that serves as the foundation of the farm production and logistics module in the integrated model. Dr. Ting participated the research design and results discussions.

The primary tasks conducted by Mr. Lin include: 1) modified and integrated the codes of the BioFeed and BioScope models, 2) developed new constraint equations that are listed in the chapter, 3) designed a two-step workflow algorithm to speed-up computing efficiency, 4) lead the analysis of data and drove the development of conclusions.

This chapter will be further edited to submit to one of the following journals including Bioresource Technology, GCB-bioenergy, and Biofuels, Bioproducts, and Biorefining.

Abstract. *To ensure effective biomass feedstock provision for large-scale ethanol production, an integrated biomass supply chain optimization model was developed to minimize annual biomass-ethanol production costs by optimizing both strategic and tactical planning decisions simultaneously. The model is a mixed integer linear programming model and comprises four modules including farm management, logistics planning, facility allocation, and ethanol distribution. The activities optimized by the model range from biomass harvesting, packing, in-field transportation, stacking, transportation, preprocessing, and storage, to its conversion into ethanol. The numbers, locations, and capacities of biomass supply sites, CSP sites, and biorefineries and biomass and ethanol distribution patterns are key strategic decisions; while biomass production, delivery, and operating schedules as well as inventory monitoring are key tactical decisions. The model was implemented to study the Miscanthus-ethanol supply chain in Illinois. Assuming 5% of cropland is allocated for Miscanthus production to support an annual demand of 32 million gallons of ethanol in the Greater Chicago area, the results showed that unit Miscanthus-ethanol production costs were \$218.5 Mg⁻¹, or \$0.72 L⁻¹. Biorefinery related costs are the largest cost component, accounting for 62% of the total costs, followed by biomass procurement, CSP related, and transportation costs. Among the biomass procurement activities, biomass baling and harvesting are the two most expensive operations, followed by in-field transportation and stacking. The biomass delivery schedules vary by season, suggesting delivering more biomass to CSP facilities during the harvesting period to prevent biomass storage losses at farm fields. A sensitivity analysis showed a 50% reduction in biomass yield would increase biofuels production costs by 11%. Biomass procurement and transportation costs are the key factors for the cost increase.*

Keywords. Biomass, Biofuels, Supply chain, Optimization, Cost

5.1 INTRODUCTION

Cellulosic based biofuels are considered to be sustainable renewable transportation fuel. To meet a target of 16 billion gallons of cellulosic ethanol production in 2022 (EPA, 2010), more than 200 million Mg of biomass will be required annually; however, few commercial cellulosic ethanol facilities exist due to a lack of a cost-effective technology and reliable feedstock supply. Bioprocessing facility related costs and biomass procurement costs comprise the major biofuel production costs (Humbird et al., 2011; Lin et al., 2013). Biomass is produced in a distributed manner within a limited harvesting window each year; but it should be processed in a centralized facility throughout the year to gain the economies of scale. Therefore, effective and efficient provision of biomass is a key challenge for large-scale biofuel production.

Supply chain management has been proposed to facilitate effective biomass provision and, generally, three levels of decision-making are considered: strategic, tactical, and operational decisions. We seek to focus on the interplay between strategic and tactical decision-making. Strategically, biomass resource evaluation and selection of facility location and capacity are important long-term decisions. Biomass availability and associated production costs have been evaluated for feedstocks including Miscanthus (Khanna et al., 2008), switchgrass (Perrin et al., 2008), and corn stover (Kadam et al., 2003). Furthermore, considering the spatial variances of biomass availability and production costs, several models have been presented to optimize facility locations and capacities (Panichelli and Gnanasounou, 2008; Kim et al., 2011; Lin et al., 2013). These strategic planning models provide decision support based on annual biomass delivery estimations, without much consideration for tactical planning details.

Tactically, biomass can only be harvested within a limited window due to its standing dry matter loss. Biomass production, delivery, and operating schedules and inventory monitoring are key tactical decisions. Biomass procurement consists of multiple unit operations including biomass harvesting, packing, in-field transportation, and handling. Several biomass supply chain simulation and optimization models have been developed to manage biomass production and delivery activities for different feedstocks, including Miscanthus (Shastri et al., 2010), switchgrass (Kumar and Sokhansanj, 2007; Zhu et al., 2011), corn stover (Sokhansanj et al., 2006; Leboireiro and Hilaly, 2011), and cotton stalks (Tatsiopoulos and Tolis, 2003). These models, however, are based on the given strategic decisions such as determined facility locations and capacities.

Strategic decisions regarding biomass supply chain will impact subsequent tactical decisions. Without the support of biomass delivery, the processing facility cannot achieve its designed operating capacity. Few multi-scale supply chain optimization models have been developed to solve processing facility locations and capacities as well as biomass delivery schedules simultaneously (Eksioglu et al., 2009; Zhang et al., 2013). However, these studies did not consider other important tactical decisions simultaneously, such as biomass production schedules and farm management issues.

Biomass is produced within a limited time window but needs to be processed all year round. Determining how to harvest, store, and deliver biomass to support the processing activities is vital to optimizing biomass supply chains. Therefore, it is important to coordinate and optimize linkages between biomass production, logistics, and processing simultaneously. The objective of this study was to develop an integrated biomass supply chain optimization model to minimize annual biomass-biofuel production costs. The model simultaneously

optimizes both strategic decisions, such as facility locations, capacities, and resource allocations, and tactical decisions, such as biomass production, delivery and operating schedules as well as inventory monitoring.

5.2 INTEGRATED MODEL OVERVIEW

Large-scale biofuel production faces significant challenges including logistics, delivery schedules, and inconsistent feedstock formats (Hess et al., 2007). To facilitate effective biomass production, a five-stage biomass supply chain was proposed to include farms, centralized storage and preprocessing (CSP) facilities, biorefineries, ethanol blending stations, and ethanol consumption. Farmers were expected to harvest, bale, transport, and stack biomass at their farm gates for delivery. CSP facilities were expected to store, handle, and preprocess biomass, in order to provide consistent feedstock format for conversion and reduce logistics challenges (Hess et al., 2007; Eranki et al., 2011; Lin et al., 2013). After production at biorefineries, ethanol will be transported to blending stations to mix with gasoline. The mixed fuel will be transported to gas stations for end consumption. For this study, we assume current blending infrastructure and consumption stations have been well developed. The objective of an integrated model is to optimize a biomass supply chain configuration optimization based on the existing ethanol blending and consumption infrastructure.

By the nature of biomass production, spatial and temporal constraints are important for supply chain optimization. Spatially, farm number and cropland size, and biomass yield vary by county. The transportation distance between facilities varies based on their spatial distribution. These spatial features are highly related to strategic decisions such as the selection of facility locations and capacities. Temporally, the harvestable biomass yield and probability of working

day vary with time. Using these temporal constraints tactical decisions, such as when to harvest, store, and deliver biomass, can be considered. Without coordinating these activities, the loss of biomass in storage could offset the gains of the high harvestable yield.

To address spatial and temporal issues, the integrated optimization model is composed of four modules: a biomass farm management module that optimizes biomass harvesting, packing, loading, and infield transportation activities; a logistics planning module that optimizes biomass delivery schedules and transportation fleet; a location-allocation module that optimizes facility locations and capacities, transportation modes, and biomass flow patterns; and an ethanol distribution module that optimizes ethanol distribution flow patterns (Figure 5.1). The model coordinates tactical decisions, such as production and delivery schedules, with strategic decisions such as facility locations and capacities, to provide decision support on both levels accordingly. This coordination was implemented by linking delivery schedules among biomass production activities at farms, biomass utilization activities at CSP and biorefinery facilities, and ethanol demand at consumption areas (Figure 5.1).

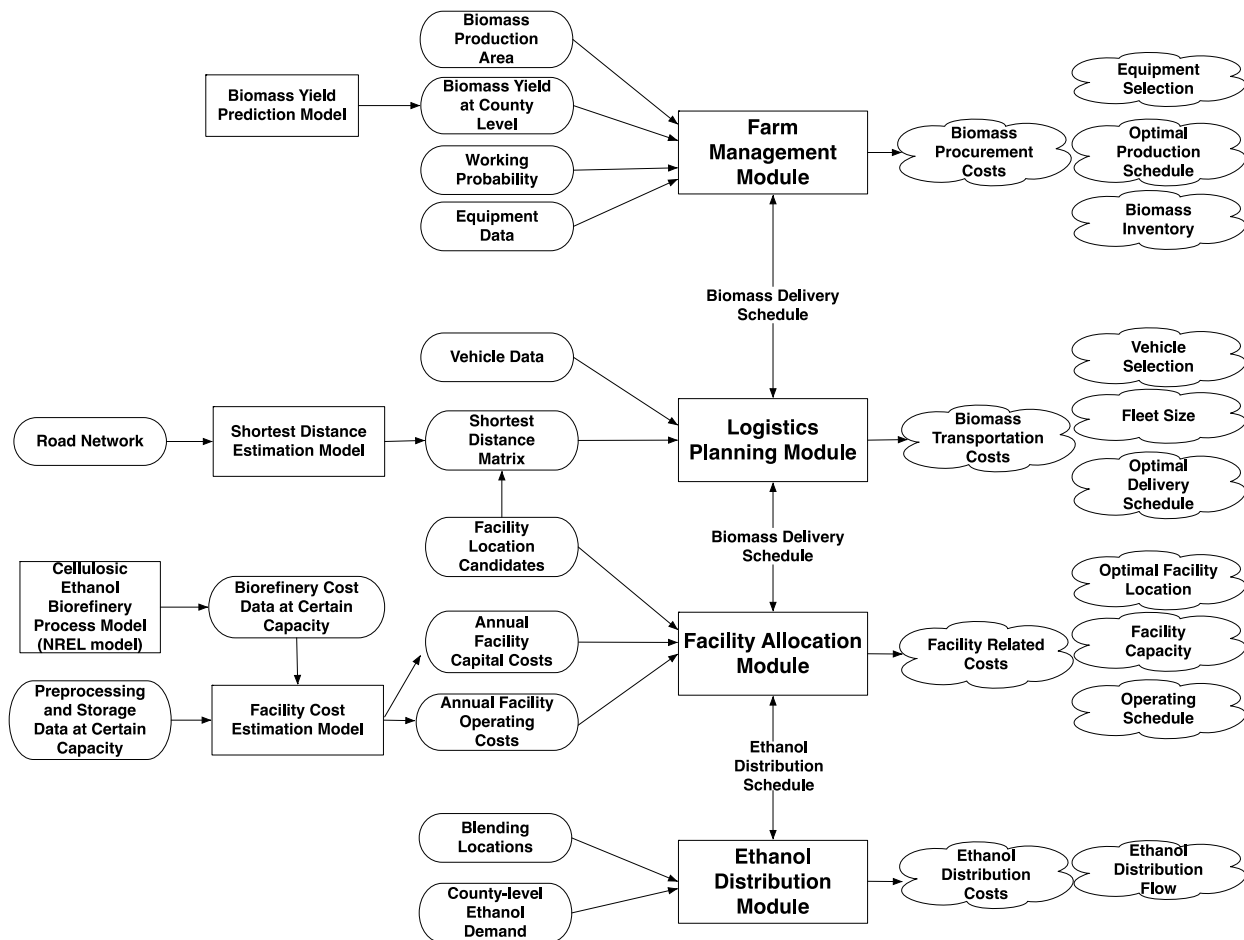


Figure 5.1: The components of the integrated optimization model and their data flow. The rounded rectangles represent source data (cropland area and farm number (USDA, 2010), biomass yield (Jain et al., 2010), land opportunity costs (Khanna et al., 2008), probability of working day (Shastri et al., 2012b), equipment and vehicle data (Shastri et al., 2010), road networks (U.S. Census Bureau, 2011), and preprocessing and storage data (Hess et al., 2007)). The rectangles represent the models used in the system (MISCANMOD (Jain et al., 2010), NREL model (Humbird et al., 2011), and Shortest Distance Estimation Model and Facility Cost Estimation Model (Lin et al., 2013)). Farm management, logistics planning, facility allocation, and ethanol distribution modules are the models developed in this study. The clouds represent output data.

The integrated optimization model is a mixed integer linear programming (MILP) model that was developed on the GAMS platform using the CPLEX solver. A list of set names, decision variables, and parameters used in the model is provided in “Nomenclature” (Tables C.1 to C.3 of Appendix C). The model was developed through the integration of key equations from the previously developed BioFeed (Shastri et al., 2010; Shastri et al., 2012b) and BioScope models (Lin et al., 2013 (or see Chapter 4)) to coordinate and optimize the entire supply chain as a single problem rather than considering strategic or tactical decisions individually. In addition to being a MILP model that optimizes strategic spatial related decisions such as farm and facility locations, the integrated model is also a discrete time optimization model that optimizes tactical temporal related decisions such as biomass harvesting and delivery schedules. The objective of the integrated model is to minimize annual biomass-ethanol production costs (Z), which consists of five parts: biomass procurement costs (Z_f), transportation costs (Z_v), CSP facility related costs (Z_p), biorefinery related costs (Z_r), and ethanol distribution costs (Z_d) (Eq. 5.1).

$$Z = Z_f + Z_v + Z_p + Z_r + Z_d \quad (5.1)$$

5.2.1 Farm management module

Biomass production on farms consists of four major unit operations: harvesting, packing, in-field transportation, and handling. Biomass procurement costs are estimated from the equipment capital related costs, operating costs, and opportunity costs of cropland allocated to energy crops (Eq. 5.2). Given the nature of crop growth and standing loss, biomass needs to be harvested in a limited time period. If more equipment can be operated during the high biomass yield period, more biomass could be harvested, which could reduce the unit biomass operating costs; however, this would increase equipment capital related costs. Different types of equipment have their

unique operating capacity and performance that could be suited for different sizes of farms.

Therefore, farm selection ($O_f^{i,j}$), equipment selection (F_f^{i,j,m_f}), and harvesting and other farm operating schedules ($P_f^{i,j,m_f,t}$) are the key decisions for farm management, where i represents biomass supply county, j represents farm number, t represents time period, and m_f represents farming equipment (e.g. harvesting and baling machines). Related to these decision variables, annualized equipment cost ($\lambda_f^{m_f}$), unit operating costs ($\mu_f^{m_f}$), farm area ($\alpha^{i,j}$), and county-level cropland opportunity costs (τ_o^i) are the key input parameters.

$$Z_f = \sum_i \sum_j \sum_{m_f} F_f^{i,j,m_f} \times \lambda_f^{m_f} + \sum_i \sum_j \sum_t \sum_{m_f} P_f^{i,j,m_f,t} \times \mu_f^{m_f} + \sum_i \sum_j \alpha^{i,j} \times O_f^{i,j} \times \tau_o^i \quad (5.2)$$

The size of farm affects the biomass production costs, where large farms could purchase and implement large equipment gaining high productivity; however the BioFeed model cannot select the appropriate farm for production (Shastri et al., 2010). Farm selection is a key strategic decision added in this integrated model, to help biofuel producers procure biomass efficiently (Eq. 5.3). The harvesting schedule is designed to monitor the cumulative harvested area of each farm by that time period ($H^{i,j,t}$). If a farm is selected for biomass production (the binary variable $O_f^{i,j}$ will be set equal to 1), all its farmland area ($\alpha^{i,j}$) needs to be harvested completely by the end of the harvesting season ($t = t^h$); whereas if a farm is not selected, its cropland will not be harvested at all.

$$H^{i,j,t=t^h} = \alpha^{i,j} \times O_f^{i,j} \quad (5.3)$$

The equations regarding farm equipment selection (F_f^{i,j,m_f}) and biomass production schedules ($P_f^{i,j,m_f,t}$) are based on the previously developed BioFeed model (Shastri et al., 2010).

The model assumes that once harvested all the biomass needs to be packed, transported, and stacked to be available for delivery at farm gate within the same time period. Therefore, given the amount of biomass required for operating during each time period, the type and number of equipment required for each unit operation can be optimized. Given the optimized harvesting schedules and the temporal changes of biomass yield, the amount of daily biomass delivered to farm gate at any time period ($B_{fg}^{i,j,t}$) can be estimated. Detailed constraints regarding farm activities can be found in Shastri et al. (2010).

The harvested biomass inventory at each farm at the end of each time period ($I_f^{i,j,t}$) is monitored based on the accumulation of the differences between the daily biomass delivered at farm gate and its daily delivery schedules to all the CSP facilities ($D^{i,j,k,t}$) while considering daily biomass losses at farms (ω_f), where Δ_t represents the length of that time interval (Eq. 5.4). Since biomass inventory cannot be negative at any time, the amount of biomass delivered from each farm is limited by biomass availability at the farm gate, which links farm management with logistics planning. The model assumes all the biomass at each farm needs to be delivered to the CSP facilities by the end of each year ($t = t^e$) (Eq. 5.5).

$$I_f^{i,j,t} = (I_f^{i,j,t-1} + (B_{fg}^{i,j,t} - \sum_k D^{i,j,k,t}) \times \Delta_t) \times (1 - \omega_f \times \Delta_t) \quad (5.4)$$

$$I_f^{i,j,t=t^e} = 0 \quad (5.5)$$

5.2.2 Logistics planning module

Biomass transportation costs (Z_v) consist of fleet equipment capital related costs (Z_{v_c}), operating costs (Z_{v_o}), and handling costs (Z_{v_h}) (Eq. 5.6-5.9). The model assumes the producers own the

fleet and can manage logistics to realize just-in-time delivery for processing. Key decisions include delivery schedules ($T^{i,j,k,m_v,t}$ and $T^{k,l,m_v,t}$) and fleet vehicle selections ($F_v^{m_v}$). Related to these decision variables, annualized vehicle costs ($\lambda_v^{m_v}$), unit operating costs ($\mu_v^{m_v}$) and handling costs (μ_{h_k} and μ_{h_l}) are key input parameters.

$$Z_v = Z_{v_c} + Z_{v_o} + Z_{v_h} \quad (5.6)$$

$$Z_{v_c} = \sum_{m_v} F_v^{m_v} \times \lambda_v^{m_v} \quad (5.7)$$

$$Z_{v_o} = \left(\sum_i \sum_j \sum_k \sum_{m_v} \sum_t T^{i,j,k,m_v,t} \times d^{i,j,k,m_v} + \sum_k \sum_l \sum_{m_v} \sum_t T^{k,l,m_v,t} \times d^{k,l,m_v} \right) \times \mu_v^{m_v} \quad (5.8)$$

$$Z_{v_h} = \sum_i \sum_j \sum_k \sum_t D^{i,j,k,t} \times \mu_{h_k} + \sum_k \sum_l \sum_t D^{k,l,t} \times \mu_{h_l} \quad (5.9)$$

Weight and volume constraints are the two major issues for biomass transportation.

Different types of vehicles have different weight ($V_w^{m_v}$) and volume capacities ($V_{vol}^{m_v}$). Based on weight and volume constraints of each type of vehicle and biomass density data ($\sigma^{i,j}$), the number of trips required for each type of vehicle during each time period ($T^{i,j,k,m_v,t}$) is estimated (Eq. 5.10 and 5.11). Similar equations will be applied to estimate the number of trips needed for each type of vehicle between CSP facilities and biorefineries ($T^{k,l,m_v,t}$). The shortest travelling distances between facilities are calculated based on the existing road networks (Lin et al., 2013). Given typical travelling speeds within the road network, the shortest travelling time between facilities for each type of vehicle (d^{i,j,k,m_v} and d^{k,l,m_v}) is estimated. Given the planned delivery schedules and travelling time as well as daily work time (η), the daily number of vehicles needed during each time period ($N_v^{m_v,t}$) is determined (Eq. 5.12). To ensure that there exist sufficient

vehicles for delivery at any time period, the total fleet size should not be smaller than the required number of vehicles at any time period (Eq. 5.13).

$$D^{i,j,k,t} \leq \sum_{m_v} V_w^{m_v} \times T^{i,j,k,m_v,t} \quad (5.10)$$

$$\frac{D^{i,j,k,t}}{\sigma^{i,j}} \leq \sum_{m_v} V_{vol}^{m_v} \times T^{i,j,k,m_v,t} \quad (5.11)$$

$$N_v^{m_v,t} \times \eta \geq \sum_i \sum_j \sum_k T^{i,j,k,m_v,t} \times d^{i,j,k,m_v} + \sum_k \sum_l T^{k,l,m_v,t} \times d^{k,l,m_v} \quad (5.12)$$

$$F_v^{m_v} \geq N_v^{m_v,t} \quad (5.13)$$

5.2.3 Facility allocation module

The costs related to CSP (Z_p) and biorefinery facilities (Z_r) are composed of annual operating and capital related costs (Eq. 5.14 and 5.15). Annual operating costs include the costs for utilities, maintenance, labor, supervision, insurance, laboratory charges, and waste treatment. In this study, it is assumed that the facilities with different capacities incur the same unit operating costs (φ_p and φ_r). Therefore, annual operating costs are linearly dependent on the amount of biomass processed. Facility capital related costs are estimated by considering fixed ($v_{p_f}^s$ and $v_{r_f}^s$) and variable ($v_{p_v}^s$ and $v_{r_v}^s$) capital costs. Because of the economies of scale, fixed and variable facility capital costs vary at different ranges of capacity. A piece-wise linear approximation approach was previously developed to estimate the associated capital costs at different capacity scales (Lin et al., 2013) and applied to this study. The key decisions for the facility module include facility capacities ($C_p^{k,s}$ and $C_r^{l,s}$) and locations (O_p^k and O_r^l) on the

strategic level and facility operating capacity ($P_p^{k,t}$ and $P_r^{l,t}$) and inventory monitoring ($I_p^{k,t}$) on the tactical level.

$$Z_p = \sum_k \sum_s (O_p^{k,s} \times v_{p_f}^s + C_p^{k,s} \times v_{p_v}^s) + \sum_k \sum_t P_p^{k,t} \times \mu_p \quad (5.14)$$

$$Z_r = \sum_l \sum_s (O_r^{l,s} \times v_{r_f}^s + C_r^{l,s} \times v_{r_v}^s) + \sum_l \sum_t P_r^{l,t} \times \mu_r \quad (5.15)$$

The amount of biomass received at a CSP facility at each time period ($A_p^{k,t}$) can be estimated based on the daily delivery schedules from all farms ($D^{i,j,k,t}$) considering biomass loss during transportation and handling (ω_v) (Eq. 5.16). The integrated model assumes that all the biomass feedstock received at a facility would be stored in a biomass input storage site first and then be handled for preprocessing. Given the differences between the amounts of biomass received and processed ($P_p^{k,t}$) at the each time period, the amount of unprocessed biomass feedstock inventory ($Q_p^{k,t}$) could be monitored at each time period considering the unprocessed biomass storage loss (ω_{p_1}) (Eq. 5.17). The designed facility capacity (C_p^k) should be greater than or equal to the amount of biomass processed at any time period (Eq. 5.18). A piece-wise linear approximation is applied to estimate the economies of scale for CSP facilities (Eq. 5.19 to 5.21), and similarly for biorefineries. The sum of the capacities at each capacity level ($C_p^{k,s}$) equals the CSP facility capacity for that county (Eq. 5.19). The facility capacity at each capacity level is constrained by the capacity range of each level ($\lambda_p^{\underline{s}}$ and $\lambda_p^{\bar{s}}$) and its capacity level selection ($O_p^{k,s}$) (Eq. 5.20). If there exists a facility in county k , the binary variable O_p^k will be set equal to one, and exactly one binary variable $O_p^{k,s}$ will be allowed to equal one (Eq. 5.21). Alternatively, if no facility exists in county k , O_p^k will be set equal to zero, and all binary variables $O_p^{k,s}$ must be

equal to zero (Eq. 5.21). Preprocessed biomass inventory at each CSP facility by the end of each time period ($I_p^{k,t}$) can be estimated by the accumulated differences between the amounts of biomass processed and biomass delivered to all biorefineries ($D^{k,l,t}$) taking into consideration the processed biomass storage loss (ω_{p_2}) (Eq. 5.22).

$$\sum_i \sum_j D^{i,j,k,t} \times (1 - \omega_v) = A_p^{k,t} \quad (5.16)$$

$$Q_p^{k,t} = (Q_p^{k,t-1} + (A_p^{k,t} - P_p^{k,t}) \times \Delta_t) \times (1 - \omega_{p_1} \times \Delta_t) \quad (5.17)$$

$$P_p^{k,t} \leq C_p^k \quad (5.18)$$

$$\sum_s C_p^{k,s} = C_p^k \quad (5.19)$$

$$\lambda_p^s \times O_p^{k,s} \leq C_p^{k,s} \leq \bar{\lambda}_p^s \times O_p^{k,s} \quad (5.20)$$

$$\sum_s O_p^{k,s} = O_p^k \quad (5.21)$$

$$I_p^{k,t} = (I_p^{k,t-1} + (P_p^{k,t} - \sum_l D^{k,l,t}) \times \Delta_t) \times (1 - \omega_{p_2} \times \Delta_t) \quad (5.22)$$

This study assumes the biorefinery adopts just-in-time operations, where the amount of biomass processed at a biorefinery facility at any time period ($P_r^{l,t}$) is estimated based on the biomass delivery schedules from all CSP facilities and accounting for biomass loss by transportation and handling (Eq. 5.23). This can be used to set a low-end constraint for a biorefinery design capacity (C_r^l) (Eq. 5.24). For each biorefinery, the amount of ethanol produced (β is the biomass-ethanol conversion rate) should be greater than or equal to the amount of ethanol transported from its facility to all blending locations (Eq. 5.25).

$$\sum_k D^{k,l,t} \times (1 - \omega_v) = P_r^{l,t} \quad (5.23)$$

$$P_r^{l,t} \leq C_r^l \quad (5.24)$$

$$\sum_t P_r^{l,t} \times \beta \geq \sum_l \sum_b D^{l,b,t} \quad (5.25)$$

5.2.4 Ethanol distribution module

Ethanol distribution costs (Z_d) are estimated based on the unit ethanol transportation cost (μ_d), ethanol transportation patterns, and the distance between biorefineries and blending stations as well as between blending stations and ethanol consumption sites (Eq. 5.26). The model assumes ethanol producers would outsource ethanol distribution to third-party logistics companies based on a unit transportation cost, in terms of \$ gal⁻¹ km⁻¹. Ethanol distribution patterns between ethanol plants and blending stations ($D^{l,b,t}$) and between blending and gas stations ($D^{b,e,t}$) are the key decision variables, whereas unit ethanol transportation cost (μ_d), transportation distances ($\theta^{l,b}$ and $\theta^{b,e}$), and county-level ethanol consumption demand (E^e) are key input parameters.

For each ethanol blending station, the total amount of ethanol received from all biorefineries should be greater than or equal to the amount of ethanol distributed to all possible ethanol consumption locations (Eq. 5.27). For each ethanol consumption site, the total amount of ethanol sourced from all possible blending stations should meet its ethanol consumption demand (E^e) (Eq. 5.28).

$$Z_d = \left(\sum_l \sum_b \sum_t D^{l,b,t} \times \theta^{l,b} + \sum_b \sum_e \sum_t D^{b,e,t} \times \theta^{b,e} \right) \times \mu_d \quad (5.26)$$

$$\sum_l \sum_t D^{l,b,t} \geq \sum_b \sum_e D^{b,e,t} \quad (5.27)$$

$$\sum_b \sum_e D^{b,e,t} = E^e \quad (5.28)$$

5.3 WORKFLOW OF THE INTEGRATED MODEL

Based on our preliminary tests, the integrated strategic and tactical optimization model requires significant computational resources and could become challenging for large-scale systems optimization. Therefore, a two-step workflow was proposed in order to develop an efficient approach to optimize a large-scale biofuels production system (Figure 5.2). The strategy behind this approach is first to select a sub-optimal supply chain region using a strategic planning model, and then to optimize both strategic and tactical planning decisions simultaneously within the sub-optimal region using the integrated optimization model.

Given an analysis region defined by users, county-level biomass production costs and biomass availability will be estimated first via the BioFeed model (Shastri et al., 2010). Biomass yield, farm size, and equipment data are the key input parameters for farm production optimization. The estimated biomass production costs and availability, together with system supply and demand requirement, will be passed as inputs to the previously developed strategic model, the BioScope model (see details in Chapter 3). The BioScope model will be executed to select the optimal biomass supply chain region to meet the defined biomass demand. Since the BioScope model was developed to optimize long-term planning decisions, only general estimations of biomass supply, processing, and storage performance are considered in the model. To ensure that the selected region would meet the targeted biomass demand in the detailed analysis, a conservative estimate of biomass provision performance, such as biomass loss rate during biomass harvesting, transportation, and storage, will be applied in the BioScope model. As a result, the selected biomass supply area from the BioScope model should require larger

areas than what the true optimal solution would select. The selected sub-optimal area will be passed as the possible biomass supply counties for the integrated strategic and tactical optimization in the second step. The strategic and tactical decisions will then be optimized simultaneously within that sub-optimal area, based on the constraint equations listed in the previous section.

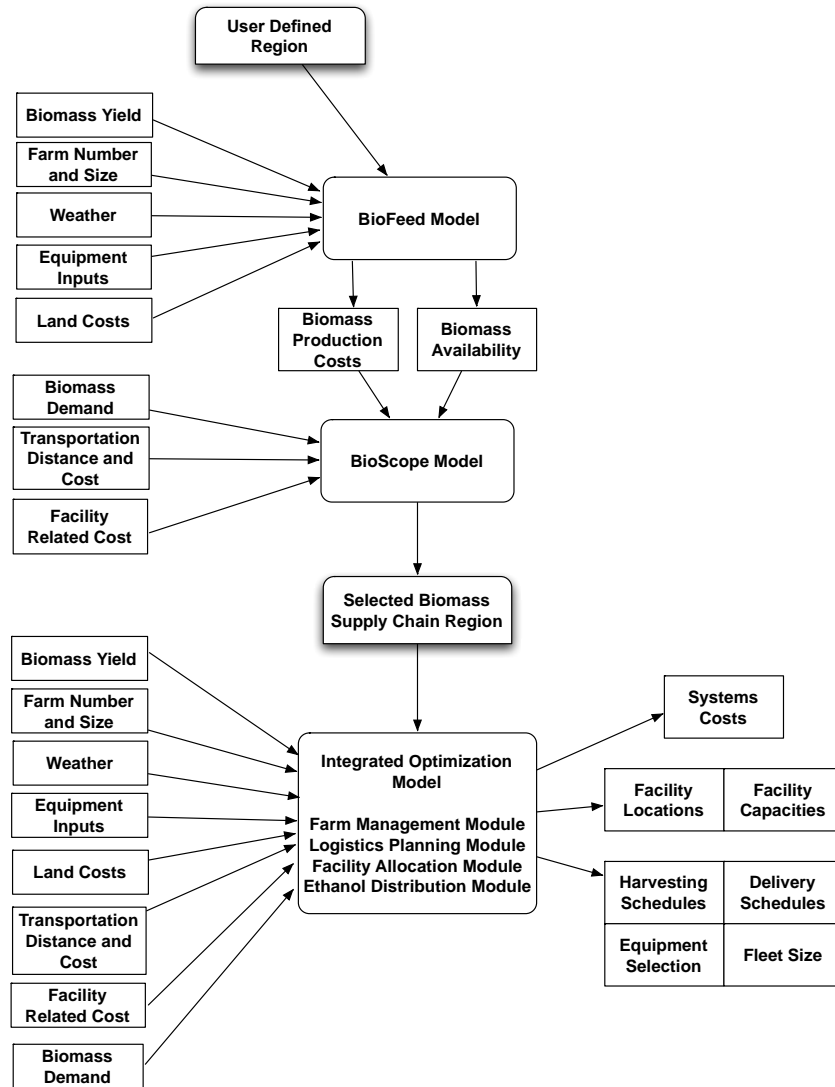


Figure 5.2: A two-step workflow of strategic and tactical supply chain optimization for large-scale biofuels production. The first step is to select a sub-optimal biomass supply area to meet the demand, and the second step is to optimize both strategic and tactical decisions within that sub-optimal area.

Through this two-step workflow, the selected potential biomass supply chain region after the first step could be much smaller than the initial user defined region. The reduced number of possible supply counties and farms would save significant computational effort in solving the integrated strategic and tactical optimization. The model is capable of providing logistics decisions from a daily basis to a weekly basis in accordance with the user's requirement.

5.4 CASE STUDY FOR MODEL APPLICATIONS

5.4.1 Basecase scenario

To illustrate the use of the integrated biomass supply chain optimization model, we chose a Miscanthus-ethanol supply chain in Illinois for a case study. In the baseline case, 5% of cropland at each of 102 counties in Illinois was assumed to be allocated for Miscanthus production. Given the number of farms and their cropland size distributions (USDA, 2010), 5% of farms in each size category in each county would be considered as potential biomass supply sites. The number of possible farms in each county of Illinois ranged from 4 to 82. The largest city in each county of Illinois was considered a candidate location for building CSP and biorefinery facilities, where either stage had 102 candidate locations. The base-case study was designed to produce sufficient ethanol to replace 1% of gasoline consumption in the eight counties of the greater Chicago area. The county-level gasoline consumption data are based on county-level populations (US Census Bureau, 2012) and per capita gasoline consumption (US EIA, 2011). The total ethanol requirement was approximately 31.7 million gallons per year for 1% gasoline replacement in the greater Chicago area (Figure 5.3), which required about 400,000 Mg of biomass annually. Among these eight counties, four counties had existing blending facilities (Figure 5.3).

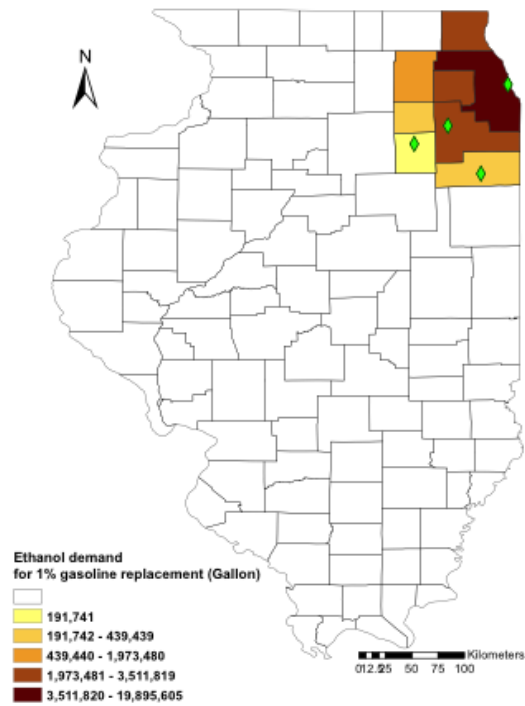


Figure 5.3: A total of 31.7 million gallons of ethanol is required for 1% gasoline replacement in the eight counties of the great Chicago area. Diamonds represent blending station locations.

Miscanthus production in Illinois reaches its peak yield in winter and peak yield data in each county were based on the MISCANMOD model (Jain et al., 2010). Miscanthus was assumed to be harvested from January to April in this study. During the harvesting season, the Miscanthus dry matter yield was reduced by approximately $0.07 \text{ Mg ha}^{-1} \text{ d}^{-1}$ from the peak yield, while the moisture content was reduced by $0.1\% \text{ d}^{-1}$ from 25% to a minimum of 15% (Shastri et al., 2010). The probability of a working day during the harvesting season varied with time as well (Shastri et al., 2012b). Given the existing interstate and state highway road network data (US Census Bureau, 2011), ArcGIS was used to calculate the shortest pathway between any potential biomass supply sites, CSP sites, and biorefinery sites. Due to the lack of specific farm location information, the transportation distance within each county from a farm to the largest

city was approximated as a stochastic number from zero to the radius of a circle with the same area as the county.

Farm management includes the following unit operations: harvesting, baling, in-field transportation, and stacking. Biomass was stacked in bales at the farm-gate for delivery. Trucks were used to serve both stages of biomass transportation, from farms to CSP facilities and from CSP facilities to biorefineries. The capital costs and operating data of farm equipment and vehicles were adopted from Shastri et al (2010). CSP facilities were designed to reduce biomass particle size through tub-grinding. The ground biomass was further tapped to increase the density to 200 kg m^{-3} , higher than 150 kg m^{-3} of baled biomass (Sokhansanj et al., 2009).

Due to the economy of scales, the facility capital investment costs for biorefineries and CSP facilities was estimated using a scaling factor of 0.7 (Lin et al., 2013). The baseline case costs were \$422 million for a biorefinery at a capacity of $2,144 \text{ Mg d}^{-1}$ (Humbird et al., 2011) and \$19 million for a CSP facility at a capacity of $2,016 \text{ Mg d}^{-1}$ (Hess et al., 2007). An annualized cost factor of 13.7% was used to estimate the annualized capital related costs (Lin et al., 2013). The capacity level and its associated capital and operating costs for both CSP and biorefinery facilities were based on Lin et al (2013).

All the costs used in this study have been converted to year 2007 using three cost indices. The costs of equipment related to farm operations and biomass size reduction were adjusted through the Index of prices paid by growers for farm machinery in the USDA's Agricultural Prices (USDA, 2007). For the equipment related to biomass handling and storage at CSP and all the equipment at the biorefinery, the Chemical Engineering Plant Cost Index was used to adjust the prices (Chemical Engineering, 2010). Labor costs were adjusted according to the Bureau of Labor Statistics index (US Department of Labor, 2010).

5.4.2 Scenario analysis of Miscanthus yield change

As would be expected with crop growth, Miscanthus yield is highly dependent on moisture stress, which varies from season to season. A sensitivity analysis was conducted to illustrate impact of changes in Miscanthus peak yield on the optimal biomass supply chain configuration. The county-level Miscanthus peak yield was considered at 100%, 75%, and 50% of the data from the MISCANMOD model (Jain et al., 2010) for each county in Illinois. 5% of cropland was allocated for producing Miscanthus and the ethanol demand was targeted for 1% of gasoline replacement in the Greater Chicago Area in all three scenarios.

5.4.3 Scenario analysis of demand change

A sensitivity analysis was conducted to illustrate the impact of the change of biomass demand on the optimal biomass supply chain configuration. Three levels of ethanol demand were considered at 1%, 2%, and 4% of gasoline consumption replacement in the Greater Chicago Area, respectively. The required biomass demand increased from 400,000 to 1,600,000 Mg per year at 4% gasoline replacement rate. A cropland area of 5% of the total available was allocated for producing Miscanthus in all three scenarios.

5.5 RESULTS AND DISCUSSION

5.5.1 Base Case Scenario

The results showed that two counties (Iroquois and Kankakee counties) were selected to support an annual demand of 31.7 million gallons of ethanol production (425,000 Mg of biomass), replacing 1% gasoline consumption in the Greater Chicago Area. The model suggested building one centralized storage and preprocessing (CSP) facility and one biorefinery in Kankakee

County. Although biomass yield is relatively high in southern Illinois counties, the selection of these two counties, which are located near the Chicago ethanol consumption area, is the result of balancing the tradeoff between biomass procurement costs and ethanol distribution costs. The optimal Miscanthus-ethanol production costs were \$218.5 Mg⁻¹ of biomass, or \$0.72 L⁻¹ (\$2.73 gal⁻¹) of ethanol. Biorefinery related costs were the largest cost component, accounting for 62% of the system costs, followed by biomass procurement, CSP related costs, biomass transportation costs, and ethanol distribution costs (Figure 5.4). Because biorefinery related costs have a significant impact on the total costs, it is worthwhile to build a large-scale facility to gain the economies of scale. The average biomass procurement costs were \$52.8 Mg⁻¹, which is in the previously observed range of \$41 to 54 Mg⁻¹ (Khanna et al., 2008). The unit biomass production cost (excluding the land opportunity costs) was \$23.1 Mg⁻¹, where baling is the most expensive farm operation, followed by harvesting, in-field transportation, and handling. The cost is lower than a cost of \$31.2 Mg⁻¹ from the baseline tactical model (Shastri et al. 2010) and \$40 Mg⁻¹ in Khanna et al. (2008), which possibly results from the large farm selection and high deliverable yield of Miscanthus in the current study. Biomass land opportunity costs, \$28.9 Mg⁻¹, accounted for more than half of the procurement costs.

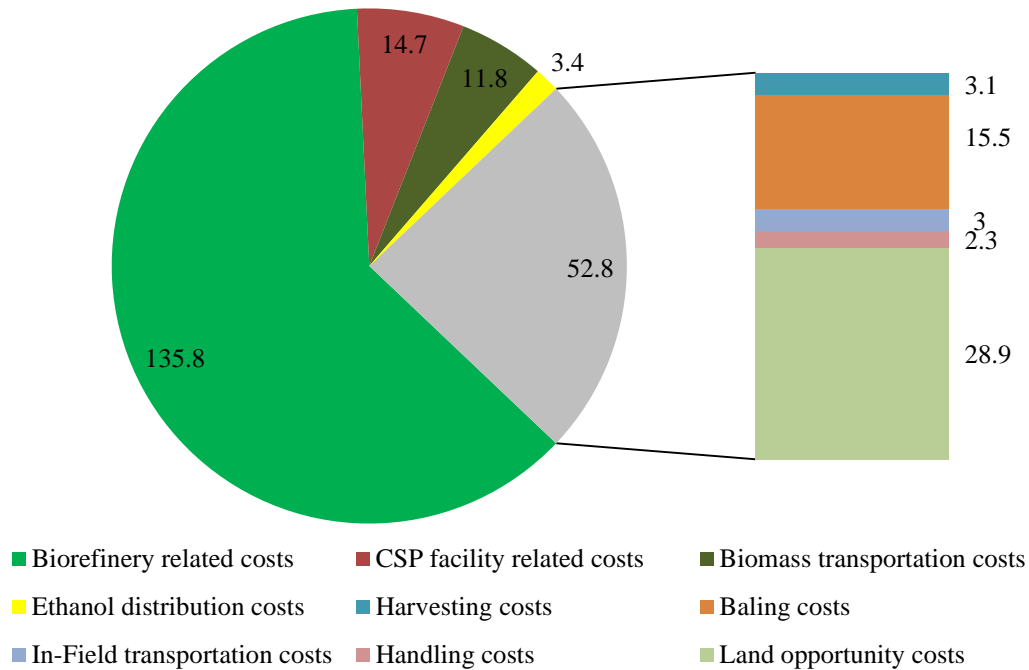


Figure 5.4: The breakdown of biofuel production costs (\$218.5 Mg⁻¹) when 5% cropland is allocated to grow Miscanthus to support an annual demand of 31.7 million gallons of ethanol.

Within the two selected counties, 40 out of 126 possible farms were selected to produce Miscanthus (Table 5.1). All the selected farms are large farms due to their relatively low biomass production costs, where the size of farms ranged from 180 to 1610 ha, or 445 to 3977 acres. The deliverable biomass yield ranged from 29.6 to 31 Mg ha⁻¹, which represents 80% of peak yield. The average deliverable yields of these two counties selected are higher than a state-level average yield of 22.3 Mg ha⁻¹ in Illinois (Khanna et al., 2008). The biomass loss on farms mainly results from three parts: standing biomass dry matter loss in the field, equipment operating loss, and storage loss. The number of pieces of farm equipment required for each farm varied significantly given the differences in their cropland areas. Based on the results, some selected farms only needed one machine for each unit operation, while some large farms needed more

than five harvesters and 10 balers to fulfill their production goals. The largest farm selected in this study could provide 34,752 Mg of biomass annually. This farm requires 5 harvesters, 14 balers, 8 in-field truck trailers, and 4 loaders.

Table 5.1: County level data regarding the number of farms selected to produce biomass, their area, biomass average deliverable yield, capture rate, and the amount of biomass supplied.

Biomass supply county	Number of farms selected in each county	Amount of selected cropland area (ha)	Average deliverable yield (Mg ha ⁻¹)	Biomass capture rate (as of peak yield)	Supply amount (Mg)
Iroquois	23 of 75	8779	28.3	80%	248,600
Kankakee	17 of 41	6584	26.9	80%	176,860

The proposed delivery schedule recommended delivering more biomass from farms to the CSP facility in the biomass harvesting season (first 120 days), to reduce biomass losses on farm fields. The CSP facility operated at a constant rate of 1136 Mg d⁻¹. The CSP biomass input rate was much larger than its preprocessing rate in the first 120 days, which resulted in an accumulation of biomass feedstock inventory (Figure 5.5). The biomass feedstock inventory peaked at the end of harvesting season with the amount of 248,285 Mg, which requires 106 acres of land for biomass feedstock storage. The accumulated baled biomass would be further preprocessed during the last 240 days of the year to maintain the design processing rate. The total operating capacity of the CSP facility was 408,915 Mgs, which is 3.7% lower than the total supply of biomass from all farms at 425,000 Mgs. The 3.7% biomass loss is a result of preprocessing operation loss and biomass feedstock storage and handling loss at CSP facilities.

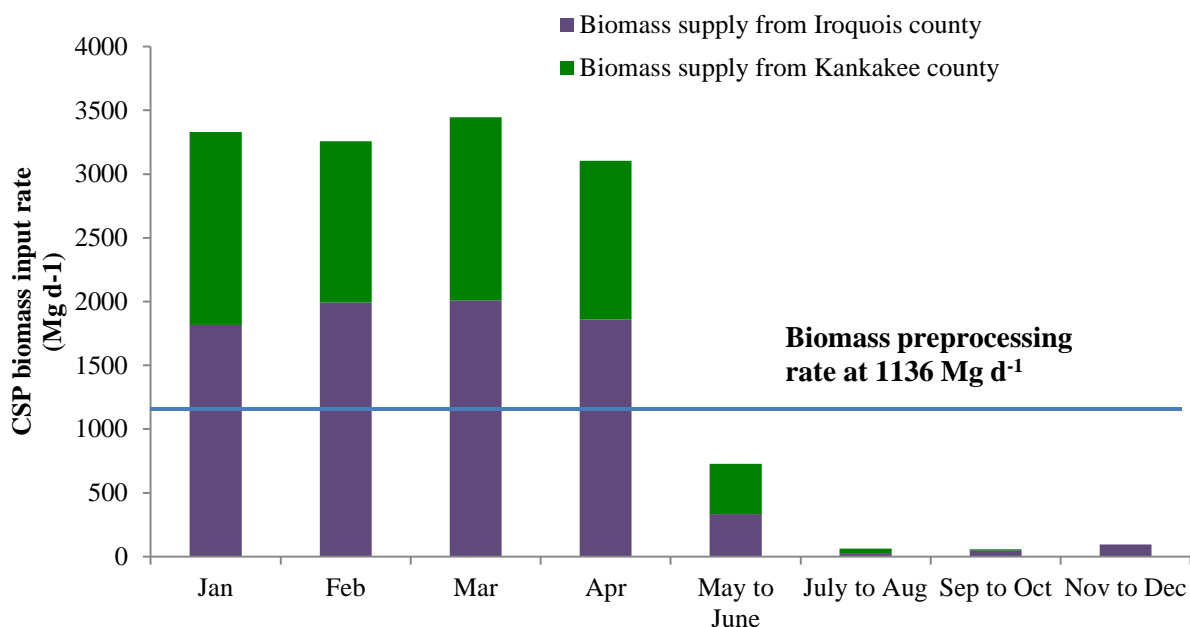


Figure 5.5: The daily CSP biomass input information from two supply counties.

The delivery rate of preprocessed biomass (ground biomass with compaction) is constant throughout the year. The system achieved just-in-time biomass delivery for a biorefinery operating at a daily operating capacity of 1,130 Mg d⁻¹. With the management of logistics planning, the system required 54 vehicles to fulfill the delivery schedules. Among them, 49 vehicles were assigned for delivery between farms and CSP facilities, as a result of distributed locations of biomass supply farms.

5.5.2 Miscanthus yield change impact

The optimal biofuel production costs increased to \$242.5 Mg⁻¹ from \$218.5 Mg⁻¹, or an 11% increase, if the Miscanthus peak yield would be 50% of that in the base case. The key factor is the increase of biomass procurement and ethanol distribution costs (Figure 5.6). The significant increase of the biomass procurement costs is largely due to the increase of the unit land

opportunity costs of growing Miscanthus. In order to convince farmers to grow Miscanthus, the model assumes that farmers would gain at least the same profit per unit area as producing corn and soybean on the same land (Khanna et al., 2008). The decreased biomass yield, therefore, would result in the increased land opportunity costs per unit biomass procured.

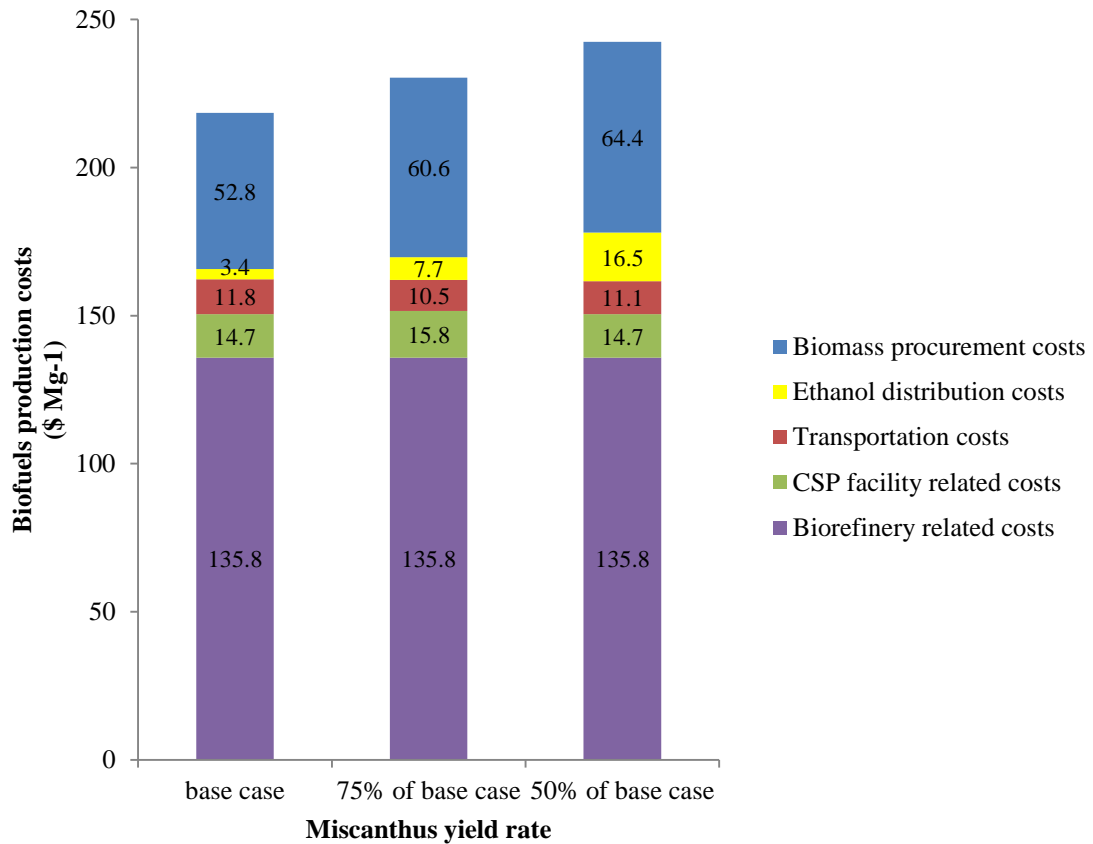


Figure 5.6: The comparison of biofuel production costs at different biomass yield rates. The base case Miscanthus yield is based on Jain et al. (2010), where the county-level peak yield ranges from 38 to 48 Mg ha⁻¹ in Illinois.

With the decrease of biomass yield, the selected biomass supply counties were moved to southern Illinois, where relatively high biomass yields were still available (Figure 5.7). The results showed that the increase of biomass procurement costs outweigh the savings of ethanol

distribution costs if biomass supply remained near the Chicago area. At low biomass yield rate, the system would choose a high biomass yield area as its supply, located in Southern Illinois.

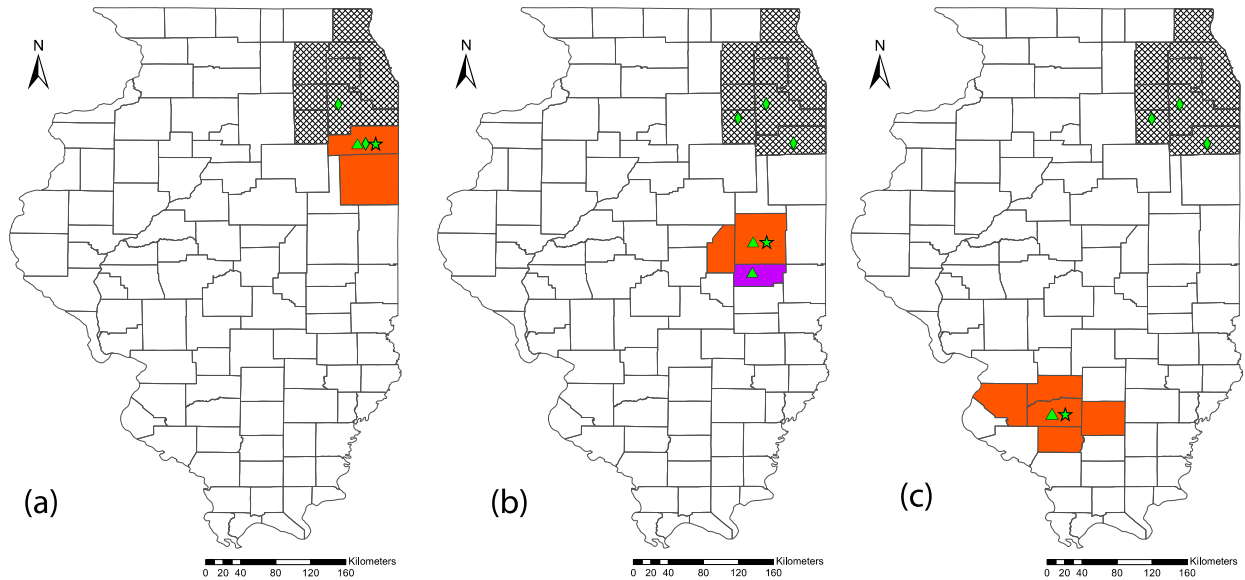


Figure 5.7: The impact of Miscanthus yield change on the optimal biomass supply chain configuration: (a) base case where peak Miscanthus yield is based on Jain et al. (2010); (b) Miscanthus peak yield rate at 75% of that in the base case; (c) Miscanthus peak yield rate at 50% of that in the base case. 5% of cropland is allocated for Miscanthus production to supply ethanol production to replace 1% gasoline consumption in eight counties of great Chicago area (greyed area). Triangles (\blacktriangle) represent CSP facilities, stars (\blackstar) represent biorefineries, and diamonds (\blacklozenge) represent blending stations. A commonly colored area represents one biomass supply region served by a CSP facility.

The required number of biomass supply counties increased from two to five, when biomass yield rate reduced to half of the base case (Table 5.2). The number of farms increased to 58 from 40 in the base case, with larger average farm size in the Southern Illinois counties. Although the projected biomass yield at each county was reduced to half of the base case, the

required production area increased to 23,453 from 15,363, representing only a 50% increase of the base case, due to the relative high biomass yield in Southern Illinois.

Table 5.2: County level data regarding the number of counties and farms selected to produce biomass, their area, and biomass average deliverable yield at different levels of biomass yield.

Scenario analysis of biomass yield	Number of selected counties	Number of farms selected	Selected cropland area (ha)	Average deliverable yield (Mg ha ⁻¹)
Base case	2	40 of 116	15,363	27.7
75% of base case	3	37 of 123	18,425	23.1
50% of base case	5	58 of 219	23,453	18.1

5.5.3 Miscanthus demand change impact

The total demand of biomass increased from 400,000 to 1,600,000 Mg annually at a 4% gasoline replacement rate. The optimal biofuel production costs were reduced with higher annual biomass demand, from \$218.5Mg⁻¹ of base case to \$195 Mg⁻¹ at an annual demand of 1.6 million Mg (Figure 5.8). In all three scenarios, the system suggested building a centralized biorefinery to gain the economies of scale, while the number of biomass supply counties and CSP facilities increased with the demand increase. Because of the economies of scale, the biorefinery related costs could be reduced by about \$27 Mg⁻¹ if biorefinery capacity was four times that of the base case. The savings in biorefinery related costs exceeded the increases in biomass procurement and transportation costs as a result of a larger biomass source area.

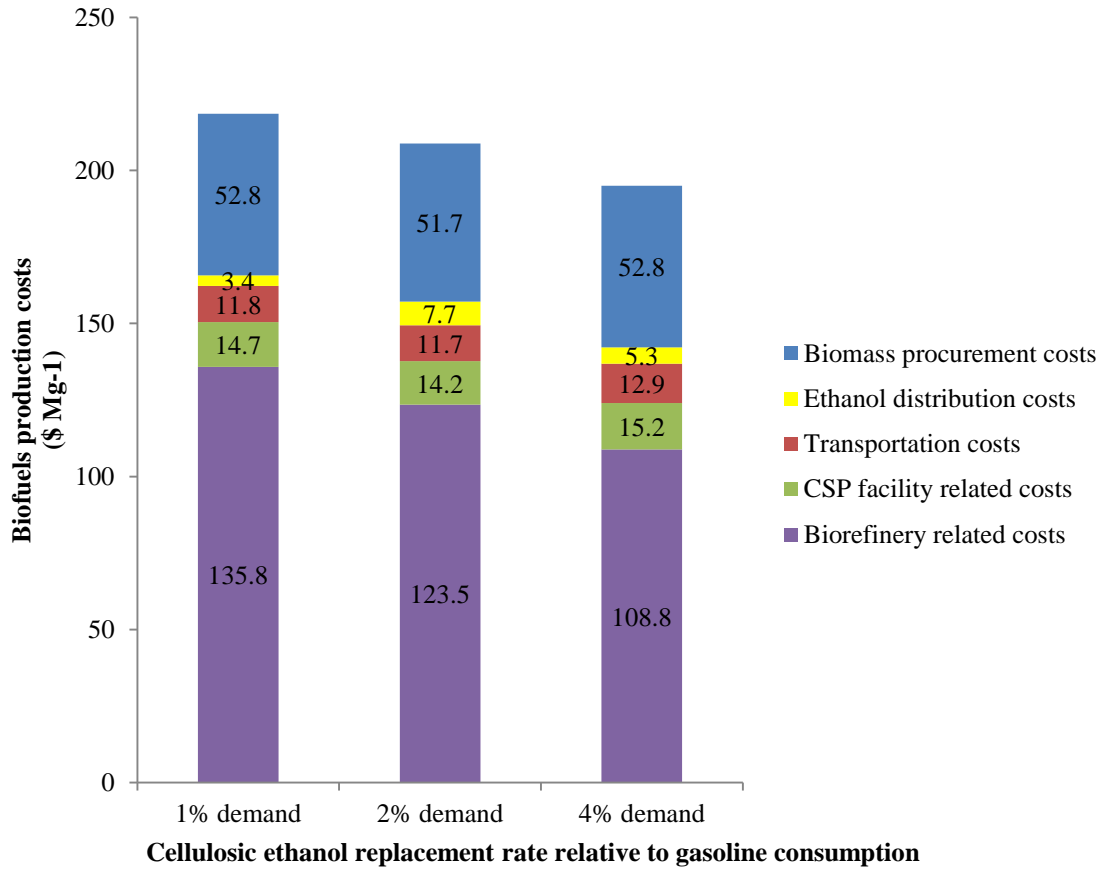


Figure 5.8: The comparison of biofuel production costs with different annual biomass demand cases.

With higher demand, the system suggested a distributed biomass supply chain configuration with more CSP facilities (Figure 5.9). The system required 203 farms from eight counties to support 4% gasoline replacement, whereas 40 and 83 farms were required for 1% and 2% gasoline replacement, respectively (Table 5.3). The total required biomass production area increased from 15,363 to 57,450 ha when the ethanol demand increased to replace 4% of gasoline consumption. The fleet size also increased from 54 vehicles for the base case to 156 vehicles for the largest demand case.

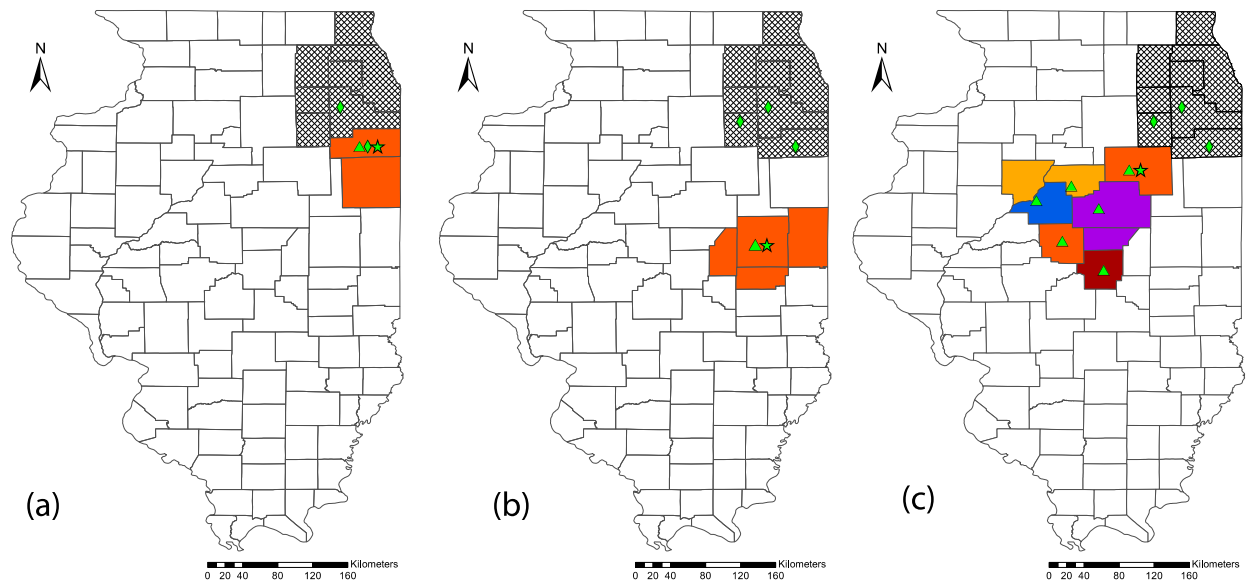


Figure 5.9: The impact of gasoline replacement rate change on the optimal biomass supply chain configuration: (a) base case at 1% gasoline replacement; (b) 2% gasoline replacement; (c) 4% gasoline replacement. 5% cropland is allocated for Miscanthus production. Triangles (▲) represent CSP facilities, stars (★) represent biorefineries, and diamonds (◆) represent blending stations. A commonly colored area represents one biomass supply region served by a CSP facility, whereas a greyed area represents the target ethanol demand market in the eight counties of Great Chicago area.

Table 5.3: County level data regarding the number of counties and farms selected to produce biomass, their area, and biomass average deliverable yield at different levels of biomass demand.

Scenario analysis of gasoline replacement rate	Number of selected counties	Number of farms selected	Selected cropland area (Ha)	Average deliverable yield (Mg Ha ⁻¹)
1%	2	40	15,363	25.8
2%	4	83	27,413	28.9
4%	8	203	57,450	27.6

5.6 CONCLUSIONS

An integrated strategic and tactical supply chain optimization model was developed to minimize biomass-biofuel production costs. The scope of a biofuel production system to be analyzed includes five major steps: biomass production, preprocessing and storage, biorefinery, blending, and end consumption. By considering spatial and temporal constraints, the model can be used to identify how long term decisions, such as facility locations and capacities, interact with short-term decisions, such as weekly biomass production and delivery schedules. A case study of Miscanthus-ethanol production in Illinois was presented to illustrate the usage of the model. The baseline case was set to replace 1% of annual gasoline consumption, or 32 million gallons, in the greater Chicago area with cellulosic ethanol and Miscanthus was assumed to be grown on 5% of cropland in Illinois. The base case results showed that unit Miscanthus-ethanol production costs were $\$0.72 \text{ L}^{-1}$ ($\$2.73 \text{ gal}^{-1}$) of ethanol, or $\$218.5 \text{ Mg}^{-1}$ of biomass. Biorefinery related costs account for 62% of the cost, followed by biomass procurement, CSP, biomass transportation, and ethanol distribution costs. To meet the proposed ethanol demand, forty large farms, providing 15,350 ha of cropland, were selected in Iroquois and Kankakee counties to grow Miscanthus. The system chose to locate a biorefinery and CSP facility in Kankakee County. Biomass delivery schedules varied seasonally, with large volumes of biomass being delivered to the CSP facility during the harvesting season. The results of scenario analyses showed that the changes of biomass yield and ethanol demand caused a significant impact on costs and supply chain configurations. When biomass yields are low, the proposed biomass supply chain system would move to southern Illinois counties to gain savings in biomass land opportunity costs due to the relatively high yields in those counties. Miscanthus-ethanol production costs increased due to the

higher land opportunity costs. When ethanol demands are high, the system would require large cropland areas to meet the demand. The savings of biorefinery related costs by achieving economies of scales exceeded the increases in transportation costs, which would drive down the system production costs.

The integrated strategic and tactical planning model developed in this study could be applied to facilitate biomass provision considering different feedstocks such as other types of energy crops and agricultural residues. The model would also be used to evaluate different preprocessing and conversion technologies by incorporating detailed processing information. For the long term, it is expected that the supply chain optimization model could be integrated with environmental and life cycle analysis tools for sustainable biomass provision analysis.

CHAPTER 6

CYBERGIS-ENABLED DECISION SUPPORT PLATFORM FOR BIOMASS SUPPLY CHAIN OPTIMIZATION

This chapter describes the development of a CyberGIS-based decision support platform for optimization of biomass feedstock provision. The platform aims to improve the computational efficiency of complex problem solving and facilitate large scale applications. The platform was developed through the integration of a web-based user interface, GISolve middleware (Wang et al., 2013), optimization models, and advanced cyberinfrastructure . A detailed workflow was presented to illustrate the major work steps of a typical service application. Model accessibility and scalability performance were evaluated through the implementation process. This implementation example could be served as a protocol for further integration development of cyberinfrastructure, operations research, and geospatial analysis and modeling.

This study cannot be completed without successful teamwork. The team includes Tao Lin, Hao Hu, Yan Liu, Luis Rodríguez, and Shaowen Wang. Mr. Lin led the overall research design, drafted the manuscript, identified the model input and output, and participated in the interface design. Mr. Hu led the interface design and spatial visualization, whereas Mr. Liu led the service integration and assisted the draft revision. Drs. Rodríguez and Wang participated in the overall research design and results discussions, and led the draft revision.

The primary tasks conducted by Mr. Lin include: 1) designed the overall workflow of the system, 2) integrated the optimization model with cyberinfrastructure the for data input and

output parsing, 3) worked together with Mr. Hu to design and implement the CyberGIS Gateway interface for model input submissions. The development of the CyberGIS Gateway is supported in part by the National Science Foundation under Grant Number 1047916. Any opinions, findings, and conclusions or recommendations expressed in the Gateway are those of the author(s) and do not necessarily reflect the views of the National Science Foundation.

This chapter will be further edited to submit to one of the possible journals including Bioresource Technology, Decision Support Systems, and GCB-bioenergy.

Abstract. *Biomass supply chain optimization models are considered to facilitate large-scale biofuels production by improving the efficiency and effectiveness of biomass feedstock provision. Most existing models are not web based, limited by the accessibility for large scale applications. A CyberGIS-enabled biomass supply chain decision support platform was developed to improve model accessibility and computational performance. The platform includes four major components: BioScope optimization model, GISolve middleware, high-performance cyberinfrastructure, and an interactive web interface. The workflow and functions of each component are provided to illustrate the development and usage of the platform. High performance and high throughput computational evaluations were conducted to demonstrate the utility of the CyberGIS-enabled decision support platform. The results showed that by leveraging cyberinfrastructure resources, computational efficiency could be improved for both single and multiple job submissions. The improved computational performance could support the decision support platform for group-based applications.*

Keywords. Biomass feedstock provision, cyberinfrastructure, cyberGIS, decision support, GIS, optimization

6.1 INTRODUCTION

Biofuels are considered as an important component of renewable energy, which could improve energy independence, reduce greenhouse gas emissions, and improve rural economics. Biomass feedstock, however, is distributed and has low energy and bulk density. How to supply biomass efficiently and effectively is one of major challenges for large-scale biofuels production.

Biomass supply chain optimization is important to the development of large-scale biomass provision systems. Recently, several biomass supply chain optimization and simulation models have been developed to minimize biomass production costs by determining optimal supply chain network designs (Panichelli and Gnanasounou, 2008; Kim et al., 2011) as well as biomass production and delivery schedules (Shastri et al., 2011; Zhang et al., 2013). Most existing optimization models have been developed using the mixed integer linear programming method, which requires significant computational resources for large-scale problem solving. Several studies have been proposed to develop and apply approximation methods to improve computational efficiency and scalability, including Lagrangean relaxation (Fisher, 1985), Lagrangean decomposition (Chen and Pinto, 2008), and bi-level decomposition (You et al., 2010). However, the reduction of computational time by using approximation methods is at the expense of result quality. Moreover, most optimization models are developed based on sequential computing and for single user access, not for online sharing, which limits the model accessibility.

Visualization is another major challenge for interpreting and understanding results of complex spatial decision-making problems. Biomass production and distribution is spatially explicit, as influenced often by weather and soil differences. Therefore, spatial visualization

facilitates the understanding of biomass supply chain analysis. Several models have been developed to apply Geographic Information Systems (GIS) to manage biomass availability (Jain et al., 2010), production costs (Khanna et al., 2008), and visualize numerical results from optimization models on maps (Tittmann et al., 2010).

To improve model accessibility and result visualization and sharing, several web-based spatial decision support platforms have appeared in literature for renewable energy development: including strategic planning of wind farm (Simao et al., 2009; Mari et al., 2011) and woody based biomass production (Frombo et al., 2009). However, most of these platforms have not addressed any significant computational challenges.

It is expected that model accessibility and throughput as well as visualization and sharing of modeling results are key limiting factors for large-group decision-making applications. Cyberinfrastructure (CI) is designed to integrate computing systems, data storage systems, advanced instruments, and visualization environments together by software and high performance networks to facilitate complex problem solving (Stewart et al., 2010). GIS based on advanced CI – defined as CyberGIS – provides a seamless integration of CI, GIS, and spatial modeling analysis, which is becoming important to facilitate large-scale problem solving, model accessibility, and visualization capabilities (Wang et al., 2012). The GISolve middleware is an important element of CyberGIS software, which is composed of service-oriented GIS components, spatial middleware, a suite of parallel and distributed GIS algorithms, and a set of user-interface and collaboration services (Wang, 2010). GISolve has been applied to various research areas, including for example analysis of climate change impact (Wang and Zhu, 2008) and ecological modeling (Tang and Wang, 2009).

In order to improve model accessibility and computational performance for complex optimization problem solving, there is a need to develop an integrated system 1) to facilitate complex optimization model solving through the support of high-performance distributed computational infrastructure; 2) to integrate optimization tools with CyberGIS to improve model accessibility and understanding of spatial relationships embedded in modeling results through intuitive online visualization. The proposed CyberGIS-enabled decision support platform is designed to achieve the following user-centered design: 1) allow users to upload their source data to evaluate the system performance; 2) manage historical scenarios analyses; 3) provide spatial visualization tools for better result interpretation; 4) reduce computational times in terms of single job or multiple job submissions.

This study describes the development of CyberGIS-enabled decision support platform for the optimization of biomass feedstock provision. The content of this study is organized as follows: Section Two describes the components and current workflow of the BioScope model, with discussions of existing computational and application limitations. Section Three describes the components and workflow of the proposed CyberGIS-enabled decision support platform. Section Four presents the computational performance evaluation of the BioScope model application on the CyberGIS platform.

6.2 OVERVIEW AND CHALLENGES OF BIOSCOPE

To minimize annual biomass-ethanol production costs for a three-stage biomass supply chain, a BioScope model was developed to select the optimal numbers, locations, and capacities of biomass supply sites, centralized storage and preprocessing sites, and biorefineries and identify the most efficient biomass flow patterns within the system (Lin et al., 2013). The BioScope

model is a mixed integer linear programming model that was developed on the GAMS platform using the CPLEX solver (GAMS, 2013). GIS was used to store, manage, and retrieve geospatial information, including county level biomass availability, biomass production costs, and transportation distances between facilities in the supply chain, and to visualize the optimized supply chain configuration on maps.

6.2.1 Workflow of BioScope model application

Data collection, mathematic modeling, and result visualization comprise the three major steps of the current workflow of the BioScope model application (Figure 6.1). Since the BioScope model optimizes a three-stage biomass supply chain configuration, candidate locations of each stage are key input information. Furthermore, county-level biomass availability and farm-gate prices for the supply candidate locations, transportation distances, annual facility capital costs, and annual facility operating costs are the other major inputs for BioScope model. (The details of required input data information can be found in Chapter 3.) These data will be saved into multiple common separate value (csv) files that can be read by BioScope model to instantiate parameters and constraints for analyses. The numerical results from BioScope model will be exported into csv files. ArcGIS software (ESRI, 2013) will be further applied to correlate numerical results with the corresponding spatial information and visualize the results on the maps.

The major challenge of the current model application is that the linkages among data collection, model solving, and result visualization have not been well integrated, which requires certain knowledge and efforts on data transferring, processing, and spatial visualization.

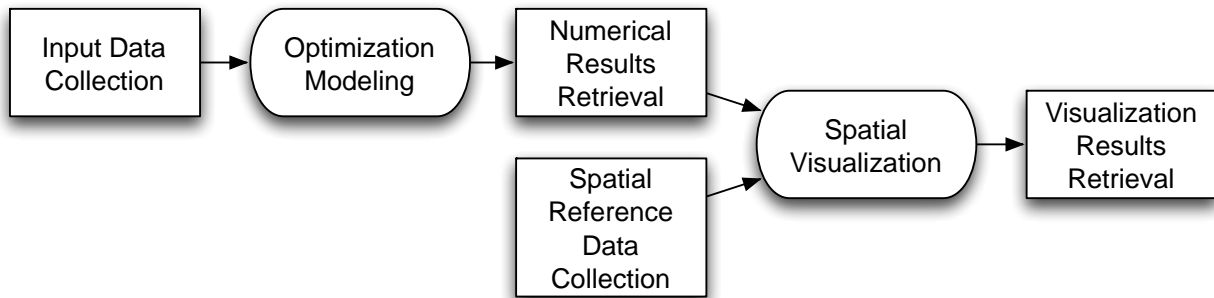


Figure 6.1: The workflow of the BioScope model

6.2.2 Application limitations

In addition to the lack of an integrated workflow for problem solving and result visualization, the application of the Bioscope model has three major limitations: 1) significant computational time and memory requirement for complex problem solving, 2) limited model accessibility, and 3) lack of high throughput computational capability for scenario analyses by a large group of users.

The BioScope model is based on mixed integer programming, which is classified as an *NP*-Hard problem. Significant computational challenges could be foreseen for complex problem solving. How to design and implement scalable computing by leveraging CI resources would be a key to reduce computing challenges.

The source code of the BioScope model is currently available upon request for research and non-profit uses; however, it can only be executed through the GAMS software. Therefore, the application of the model requires the installation of the GAMS software and ability with GAMS programming. Lack of graphic user interface on the GAMS platform further constraints the application accessibility of the model.

Our previous study showed that an optimal biomass supply chain configuration is highly dependent on several input parameters, such as cropland usage rate, biomass yield rate, and

transportation cost rate (Lin et al., 2013). In order to provide a solid decision support for a new biomass supply chain configuration, many scenario analyses should be conducted to evaluate the system performance under various conditions. Currently, the model is operated on a single desktop computer where scenario analyses can only be conducted sequentially. The problem solving time for a solid decision support case study would be highly dependent on the number of scenarios under consideration. Implementation of a high-throughput problem solving workflow is effective to reducing computational time of scenario analyses, and this will be even more important for large group-based applications.

6.3 INTEGRATION OF MODEL, USER INTERFACE, AND INFRASTRUCTURE

6.3.1 The structure of proposed systems integration approach

To facilitate large-scale complex problem solving and improve model accessibility and throughput, a CyberGIS-enabled decision support platform has been developed. The platform includes four major components: 1) a high performance CI for optimization problem solving, 2) the BioScope optimization model where is deployed on the cyberinfrastructure; 3) GISolve middleware that includes a set of Open Service APIs and web server PHP functions; and 4) an interactive web-based user interface on the CyberGIS Gateway (Wang and Liu, 2009) (Figure 6.2).

A web-based user interface is developed to support user management, input data submission, job status updating, and geospatial visualization. The design of the web interface provides dynamic and interactive functions based on Web 2.0 and HTML5. With its connection

to the GISolve middleware, the interface manages to submit user defined input parameters and files, retrieve the message of problem solving status in a real time, and provide data and result visualization requests.

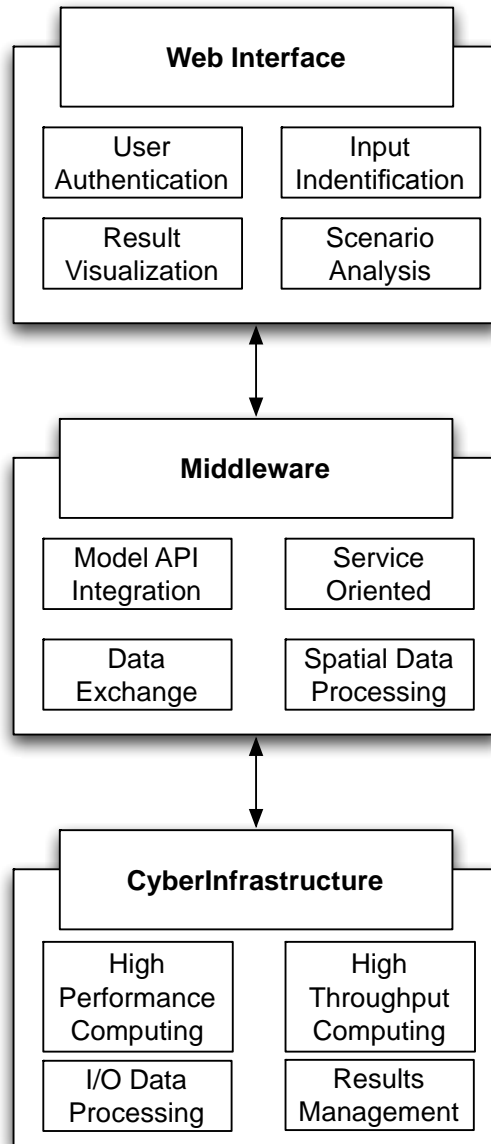


Figure 6.2: The abstract diagram of a three-tier platform integration of web interface, middleware, and cyberinfrastructure. The BioScope model is deployed on cyberinfrastructure to leverage high performance and high throughput computing resources.

To better integrate web client requests with cyberinfrastructure, GISolve middleware manages the complexity of accessing low-level operating software and standards, security, and communication protocols to facilitate data interactions, communications, and sharing (Wang et al., 2005). The design of GISolve is based on an open service integration framework that supports the three integration levels across toolkit, cyberinfrastructure, and web interface by managing data and software functions as web services and providing programming interfaces for service developers and consumers. This framework provides a unified approach to streamlining the encapsulation of CyberGIS data and functions and transparent access to CI for high-performance computation and large-scale data handling. Functions in the framework are established using widely adopted REST services with JSON/XML as the format of service request and response messages based on the GISolve open-service APIs. CI provides powerful and advanced computational capabilities for large complex models solving and data storage and handling. Supported by a queuing and resource management system, CI provides not only high-performance computing, exploiting large numbers of processors through specialized, high-speed interconnections for a job solving, but also high throughput computing, allocating multiple job submissions to available computational resources simultaneously.

6.3.2 Workflow of an integrated platform development

The integration of web interface, middleware, model, and cyberinfrastructure requires a systematic workflow approach. A typical workflow includes three major steps: job submission, job status query, and results management, where the realization of each step requires an integration across the three layers of the system (Figure 6.3).

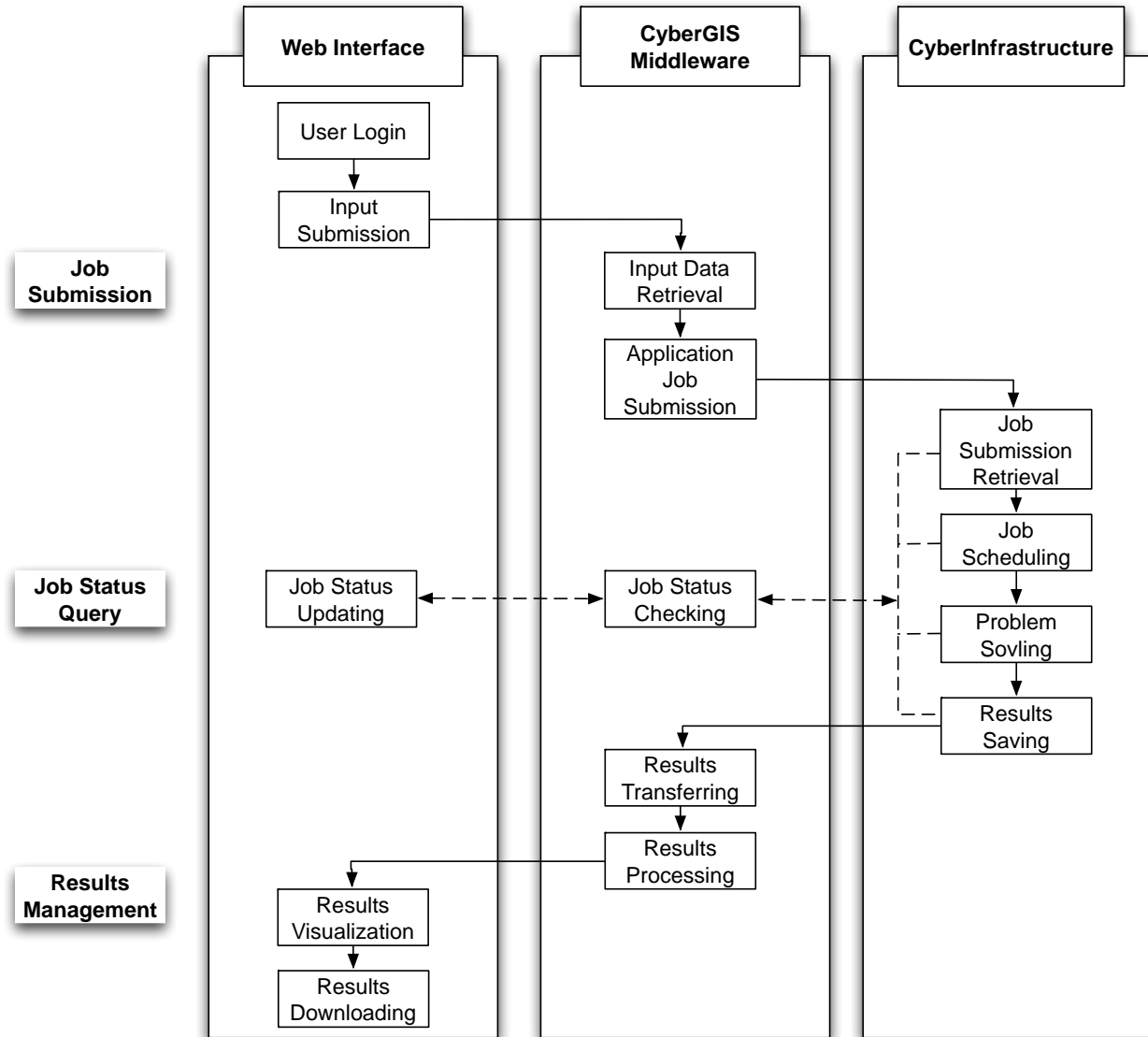


Figure 6.3: A workflow diagram of the integrated platform.

The proposed platform was implemented by integrating the following components: a dynamic web interface was developed using EXT JS, a JavaScript based web platform development framework. AJAX was applied to create asynchronous web applications that communicate with a server in the background, without interfering with the current stage of the Web page. In the current AJAX implementation, JSON format was used for the interchange of data. OpenLayers, an open source JavaScript library for displaying map data, and Keyhole

Markup Language (KML) were applied to visualize geospatial related input and output information on web-based maps.

To operate the system, the user first needs to register to the system to get an appropriate user privilege for application usage. Once the user logs in to online environment, the introduction panel page would be popped up for the overview of the platform (Figure 6.4). The introduction panel describes the objective and procedures of the application.

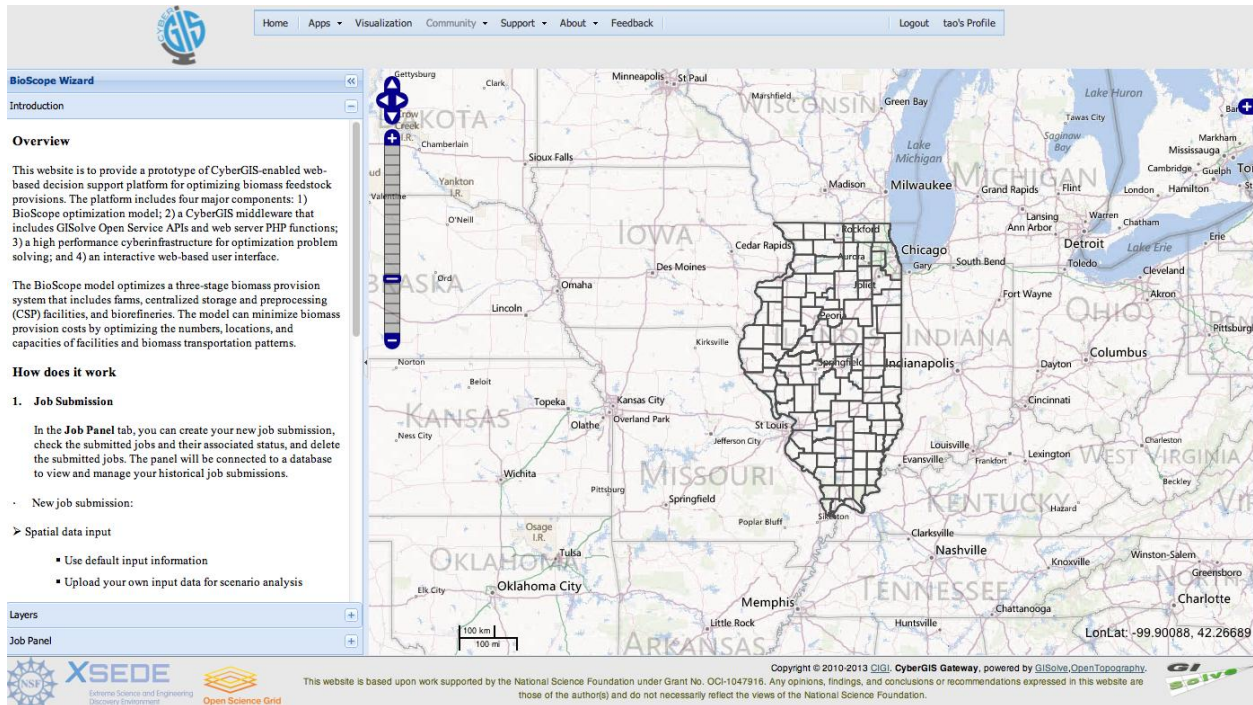


Figure 6.4: The user interface of the CyberGIS-enabled decision support platform.

In the job panel of the web interface, the user can submit new scenario analysis or retrieve previously submitted job information (Figure 6.5). To create a new analysis by clicking the green “New” button, the user will be asked whether to use existing data source provided by the system or upload required input files to instantiate a new job submission. For the BioScope model, it requires seven key input files that include the candidate locations of biomass supply counties,

centralized storage and preprocessing facility, and biorefinery, county-level biomass yield, biomass production costs, and transportation distances between supply counties and CSP facilities and between CSP facilities and biorefineries. Furthermore, biomass demand rate, cropland usage rate, yield rate, and transportation cost rate are the four key parameters that need to be defined for a scenario analysis.

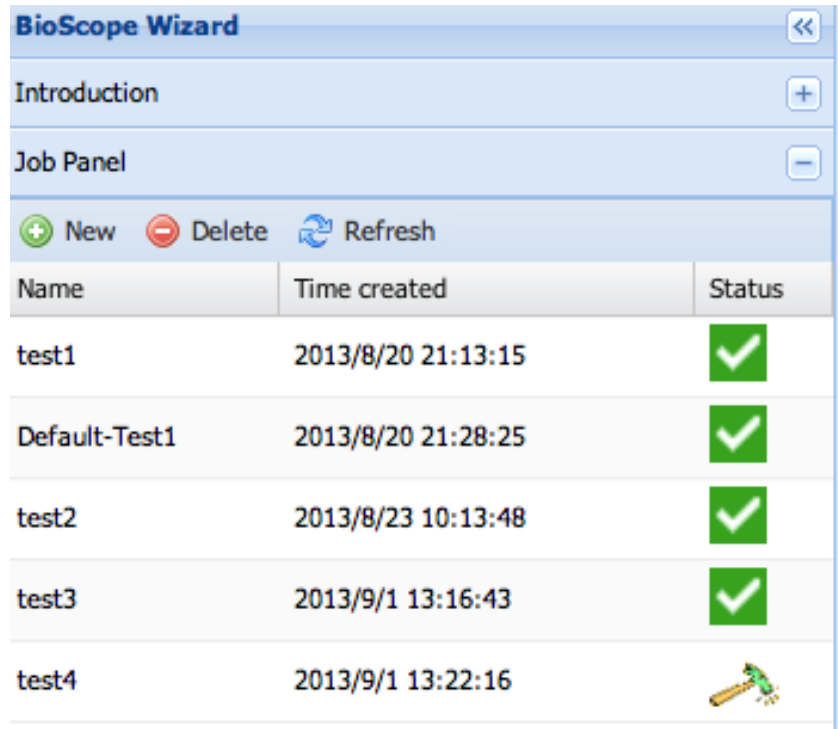


Figure 6.5: The job panel of the CyberGIS-enabled decision support platform.

If a user chooses to create a new scenario analysis, an upload data window will be displayed to let the user define the new job name, upload required input files, and determine the critical input parameters (Figure 6.6). If a user chooses to use the existing data source in the system, the user would need to define the job name and modify the values for the critical input parameters, but cannot upload the input files. The user can download the input files by clicking the file tab for the information share and verification (Figure 6.7).

New Job [X]

New Job Name

You Job Name:

Spatial Data

Default Illinois Data User Upload Data

Supply Locations: Browse... CSP Locations: Browse...

Biorefinery Locations: Browse... Distance Matrix 1: Browse...

Distance Matrix 2: Browse... Cropland Area: Browse...

Biomass Yield: Browse... Production Costs: Browse...

Decision Parameters

Total Demand: Conversion Rate:

Yield Rate: Transporation Cost Rate:

Reset Submit

Figure 6.6: New job submission panel for using the user uploaded data.

New Job [X]

New Job Name

You Job Name:

Spatial Data

Default Illinois Data User Upload Data

Decision Parameters

Total Demand: Conversion Rate:

Yield Rate: Transporation Cost Rate:

Reset Submit

Figure 6.7: New job submission panel for using the existing Illinois case study data.

Once the user completes data submission, GISolve middleware will retrieve these data and notify the user of successful job submission. The uploaded data and files will then be converted and packaged as a public URL. The middleware will submit a job request to the CI through a JSON format that includes the data source URL. Once receiving the job submission request, the platform retrieves all the necessary data and file from the web server based on the url provided in the JSON message.

Once the job is submitted, the interface will automatically change to a job status panel, where the user can view the current job status. The current system provides seven different status for users (Figure 6.8). Each status is visualized as an animation picture on the interface for better understanding. The status is updated in a real time manner through the linkage between interface, middleware, and CI. Furthermore, in the job status panel, users can also review the status of all job submissions (Figure 6.6).







Icon	Status	Icon	Status
	Analysis submitted for computation		Results created
	Analysis waiting to be executed		Results ready for visualization
	Analysis running	No Icon	Computation problem
	Computation done		

Figure 6.8: The description of status icon for visualizing the current job status (Image courtesy of CIGI laboratory).

GISolve schedules jobs based on the first-in first-out principle while sending status request to CI resources to check job running status. Once a job is completed on CI, GISolve automatically transfers the results from CI and process the numerical results for geospatial

visualization. Currently, optimization results are exported into csv files. By referencing to geospatial data, the selected supply counties, CSP, and bioreifnery locations are converted into geospatial formats such as as Keyhole Markup Language (KML). The CyberGIS-enabled platform supports the mapping of these KML files on web browers.

In the layers panel, user can visualize resluts from previously completed jobs. Each completed job has its unique folder named by the job name, which has three layers including biomass supply counties, CSP facilities, and bioreifnery faciliities. Users can check the box next to the layers on the web interface to see the optimization model results on a web-based map once the job is completed (Figure 6.9). The results map is interactive, where the amount of biomass supply from each selected county can be presented by clicking a highlighted county. The results are also available for users to download to their own disk for detailed evaluation.

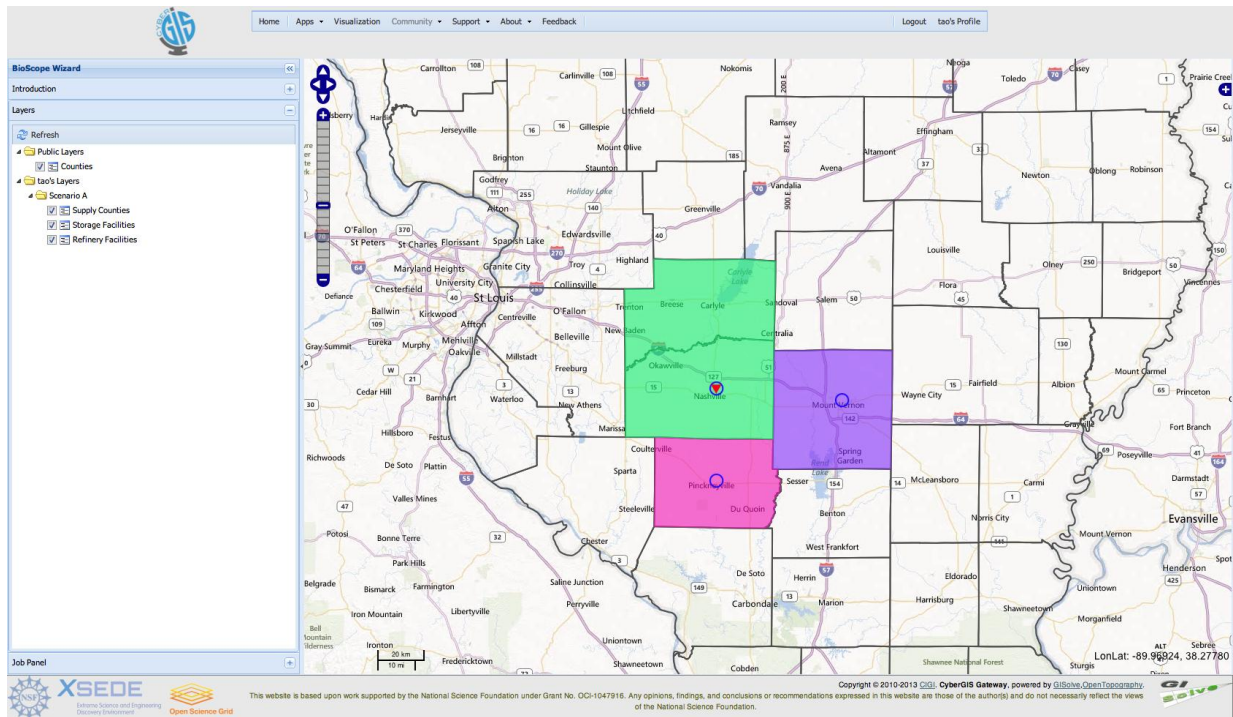


Figure 6.9: Results visualization panel of CyberGIS-enabled decision support platform interface. The colored areas represent biomass supply counties where each colored area represents the supply counties sharing the same CSP facility, the circles represent the proposed locations of CSP facilities, and the triangle represents the proposed location of the biorefinery facility.

6.4 COMPUTATIONAL PERFORMANCE EVALUATION

Both high performance and high throughput computing have been employed in the platform. High performance computing aims to reduce the computational time for a submitted job by leveraging multiple computing resources of a single high performance computer, usually related to parallel programming, High throughput computing aims to reduce total computational time for a set of submitted jobs by leveraging more computing nodes or machines, usually related to distributed computing.

To evaluate computational performance of the BioScope model, we chose a three-stage Miscanthus-ethanol supply chain in Illinois for a case study. This mixed integer linear programming problem had a total of 26,625 variables, including 816 binary variables. Miscanthus annual processing demand, cropland usage rate, and Miscanthus yield rate are three major input factors affecting the optimal supply chain configuration (Lin et al., 2013). Miscanthus yield rate is the percentage of the projected yield by the MISCANMOD model (Khanna et al., 2007). The complexity of the problem solving is increased with higher Miscanthus demand and lower cropland usage and Miscanthus yield rates.

6.4.1 High-performance computing evaluation

High-performance computing was evaluated by the computational time for a scenario analysis when Miscanthus demand was $2,000,000 \text{ Mg y}^{-1}$ and 2% of cropland was allocated for Miscanthus production at the projected yield. The CPLEX solver recently provided a multi-thread approach to improve computational efficiency for complex problem solving (GAMS, 2013). To evaluate the multi-thread computing performance, we tested four scenarios using the number of threads from one to eight. By increasing the number of threads from one to four, the results showed that the computational time could be reduced significantly, from 1675 seconds using one thread to 477 seconds using eight threads (Figure 6.10).

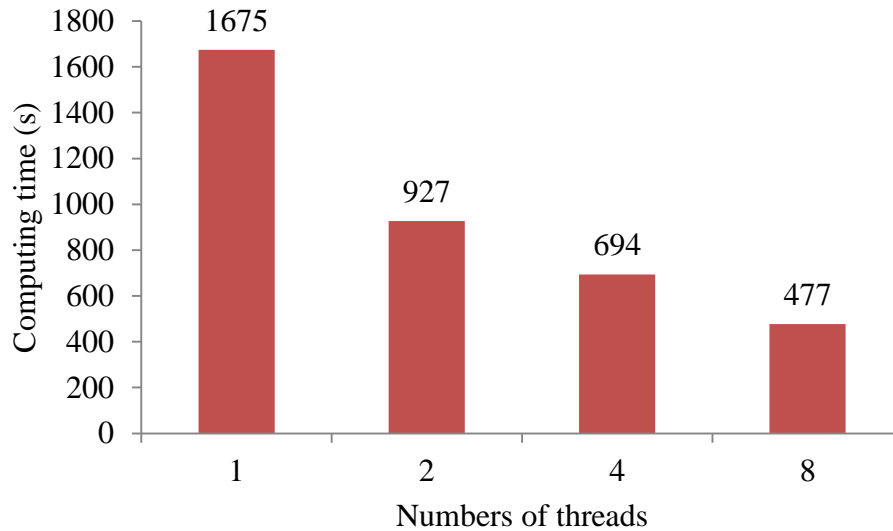


Figure 6.10: High-performance computing evaluation using different numbers of threads for one scenario analysis by the BioScope model application on the CyberGIS platform

6.4.2 High-throughput computing evaluation

A thorough decision support should be provided with the consideration of multiple scenario analyses, given the uncertainty of biomass supply and demand changes. High-throughput computing was evaluated by the computational time for a group of 60 different scenario analyses. The analyses considered ten levels of annual Miscanthus demand ranged from 1,100,000 to 2,000,000 Mg y⁻¹, three levels of cropland usage rate at 4%, 5%, and 6%, and two levels of Miscanthus yield rate at 80% and 100% of the projected yield. The evaluation was conducted by leveraging the number of machines nodes from 1, 2, 4, to 8. Each individual scenario analysis was solved using single thread computing. By increasing the number of machine nodes, the computing time of these 60 scenario analyses could be reduced significantly, from 4411 seconds using one node to 894 seconds using eight nodes (Figure 6.11).

With more available computing nodes, multiple scenario analyses could be conducted simultaneously, rather than solving the problems sequentially using one computing node. The computational time of each individual scenario analysis ranged from seven seconds, when Miscanthus demand is 1,100,000Mg y⁻¹ at 6% cropland usage rate and 100% Miscanthus yield rate, to 114 seconds, when Miscanthus demand is 2,000,000Mg y⁻¹ at 4% cropland usage rate and 80% Miscanthus yield rate.

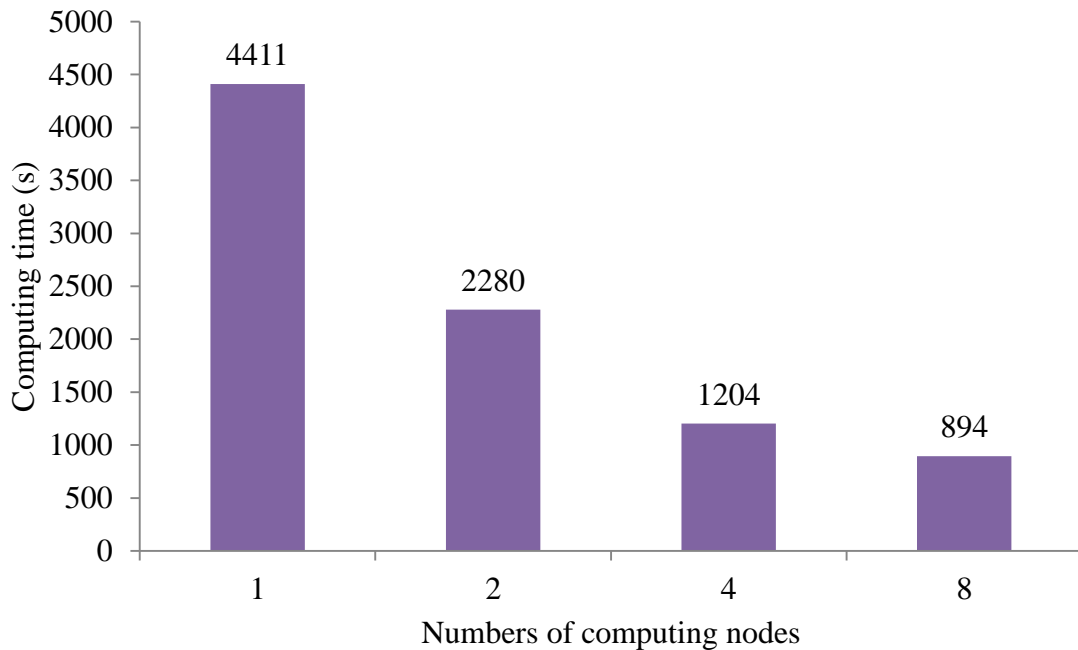


Figure 6.11: High-throughput computing evaluation using different numbers of computing nodes for 60 scenario analyses by the BioScope model application on the CyberGIS platform.

6.5 CONCLUSIONS

Biomass supply chain optimization models are considered to facilitate large-scale biofuels production by improving biomass provision efficiency and effectiveness. Most existing models are limited by the computational efficiency and lack of accessibility for large scale applications.

A CyberGIS-enabled biomass supply chain decision support platform was developed to improve optimization model accessibility and computational performance. The platform is composed of four major components, including the BioScope optimization model, GISolve middleware, hybrid cyberinfrastructure and an interactive CyberGIS Gateway user interface. The workflow and functions of each component are presented to illustrate the development and usage of the platform. The results of computing performance evaluations demonstrate that the CyberGIS platform can support interactive decision-making analysis for a group of users on solving computationally intensive and complex models for biomass supply chain optimization.

CHAPTER 7

CONCLUSIONS

Biomass feedstock provision has been considered as a key limiting factor for large-scale biofuels production. Spatially, biomass availability, production costs, and transportation distances vary geographically. Temporally, biomass can be only harvested in a short time window but needs to be processed throughout the year. Concurrent Science, Engineering, and Technology (ConSEnT) concept was proposed to take a systems approach to improve biomass provision efficiency and effectiveness. Three comprehensive optimization modeling tools have been developed to optimize both long-term supply chain configurations and short-term operations management for large-scale biofuels production. A CyberGIS-enabled web decision support platform has been developed to improve model accessibility and computing performance of the optimization model.

Two strategic-level optimization models, BioScope and Dynamic BioScope, have been developed to address long-term decisions for a three-stage biomass supply chain system. The system includes biomass supply sites, centralized storage and preprocessing (CSP) facilities, and biorefineries. BioScope, a mixed integer linear programming model, was developed to minimize annual biomass-biofuel production costs by optimizing decisions including the numbers, locations, and capacities of facilities and biomass distribution patterns. Built upon the BioScope model considering spatial related constraints, the Dynamic BioScope model, a multi-period optimization model, was developed to incorporate temporal constraints on the changes of biomass supply and changes over time. The Dynamic BioScope model aims to provide decisions on how a biomass provision system would best evolve to meet the increasing biofuel demand.

Both strategic-level models were applied to address long-term decisions for Illinois Miscanthus-ethanol production. BioScope model was applied to evaluate different scenarios including different cropland usage rates, annual biomass demands, and transportation modes; while Dynamic BioScope model was applied to evaluate how the changes of biomass supply contract length would affect the optimal supply chain configurations.

BioScope model has been applied to quantify the cost differences between two different preprocessing technologies including biomass grinding and pelletization. It is expected that with more data available on different feedstocks and preprocessing and conversion technologies, BioScope model can quantify the cost changes as a result of technology improvement.

Integrated strategic and tactical planning model was developed to identify how strategic planning decisions, such as facility locations and capacities, would interact with tactical planning decisions, such as biomass harvesting and delivery schedules. The integrated model is composed of four major modules including farm management, logistics planning, facility allocation, and ethanol distribution. A base case study of Miscanthus-ethanol production in Illinois showed that biorefinery related costs are the largest cost component, followed by biomass procurement, CSP related, and transportation costs. The biomass delivery and operating schedules vary by season, suggesting preprocessing more biomass during the harvesting period to prevent biomass storage losses at farm fields. Scenario analysis showed that when biomass yields are low, the proposed biomass supply chain system would move to southern Illinois counties to gain savings in biomass land opportunity costs due to their relatively high yields.

A CyberGIS-based decision support platform was developed to improve BioScope model accessibility and throughput and knowledge sharing. The platform was developed through the integration of a web-based user interface, GISolve middleware, BioScope model, and high

performance distributed cyberinfrastructure. The computational efficiency and throughput performance can be significantly improved by leveraging high performance cyberinfrastructure and service oriented middleware. Web-based maps are provided to visualize the numerical results to facilitate decision support, eliminating the space and hardware constraints of complex problem solving.

The developed optimization tools in this dissertation can serve a solid foundation for a comprehensive software suite of Biomass Implementation Optimization Modeling Analysis Simulation Software (BIOMASS). Through the integration of optimization models and high-performance cyberinfrastructure, a CyberGIS-enabled decision support platform would facilitate decision making for large-scale biofuel production.

CHAPTER 8

FUTURE WORK

Systems informatics, modeling and analysis, and decision support platform compromise the three major components of the concept of Concurrent Science Engineering and Technology (ConSEnT). This dissertation provides a protocol of the application of ConSEnT on biofuels production, with the focus on the strategic and tactical planning of biomass feedstock provision. The depth and width of the systems analysis of biofuels production could be improved if we can achieve the following objectives.

8.1 DATA AND INFORMATICS

All the modeling tools and analysis are driven by the data. Most of case studies in this dissertation provide analysis for biomass-biofuel production system in Illinois, arguably the most important reason is due to the data availability and quality. It would be great if we can develop a one-stop biomass-biofuel data center by collecting nation-wide data related to biofuels production. The key data includes county-level biomass yield for different feedstock types such as Miscanthus, switchgrass, sweet sorghum, energy cane, and crop residues. Biomass transportation costs are not negligible based on our previous studies. Nation-wide transportation infrastructure data including road, rail, and waterway would be collected and stored in a database for regional and national biomass transportation costs evaluation. Operating data of farming equipment will be collected from literatures and on-going experimental research from our colleagues. The improved farming operating data would facilitate farming management.

8.2 MODELING AND ANALYSIS

Long distance biomass or ethanol transportation could be anticipated as we approaching to 16 billion gallons annual production target in 2022. Many studies have indicated the importance of biomass sourcing and transportation costs, but there exist no complete study on the quantitative analysis of long distance biomass/ethanol movement. We are planning to conduct a comprehensive study of long distance transportation by using BioScope model. Several key data are required for the study: 1) comprehensive understanding of various preprocessing technologies such as capital investment requirements, operating costs, product density (Figure 8.1); 2) estimation of unit transportation costs for different formats of biomass feedstock. The unit transportation costs of biomass would be related to product density, weight and volume limits of transportation mode, and value of the product (unit rail transportation costs have been estimated (see Figure 8.2)); 3) transportation distance data of road, rail, and waterway; and 4) biomass yield, availability, and production cost data at different regions.

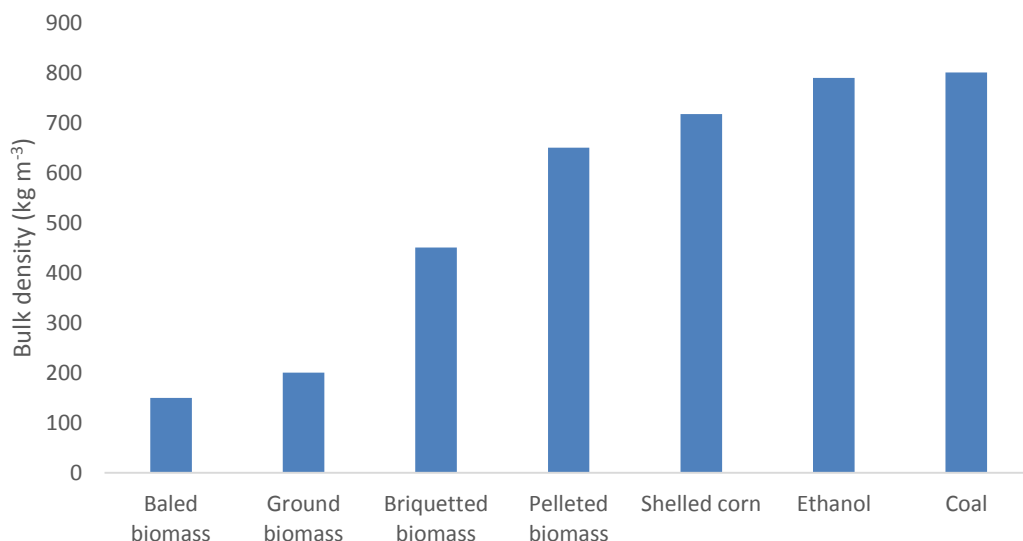


Figure 8.1: Product density information on different types of biomass formats, shelled corn, ethanol, and coal.

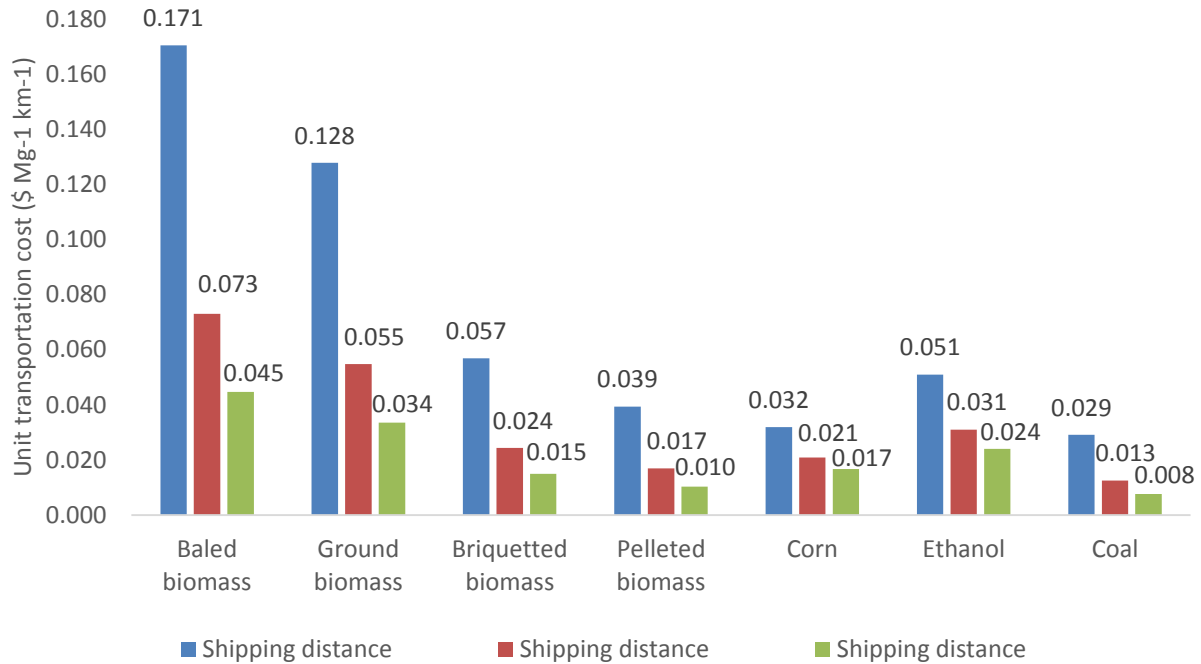


Figure 8.2: Unit transportation cost data of different commodities at three levels of shipping distance. Four types of preprocessed biomass transportation cost are based on its density difference as compared to the transportation cost of coal (Surface Transportation Board, 2009).

The approach of the long-distance biomass transportation study would be suggested as follow: 1) identify and collect all the required data; 2) define the level of biomass transportation distance, including short distance (<800 km), medium distance (800-1600 km), and long distance (>1600 km); 3) estimate the biomass transportation costs for different formats at different distance levels, 4) quantify the differences of sourcing biomass locally versus long-distance biomass sourcing, which would be related to biorefinery location issue that is whether to build a biorefinery near the consumption area (i.e. California) or near a high biomass availability area (i.e. Midwest area).

It is also anticipated that different preprocessing technology may affect biomass conversion rate. BioScope model can be further integrated with detailed biomass conversion

processing models to quantify the impact of preprocessing format on the whole supply chain configuration.

Dynamic BioScope model was developed to understand how the whole biomass provision system would best evolve to meet the increasing biofuel demand. It is highly possible that such a large system might not be controlled or managed by one single entity. Therefore, different entities would compete for goods and resources. The Dynamic BioScope model would be changed to optimize the system in a sequential approach by minimizing each year production costs rather than minimizing the total production costs throughout the planning period. The results would be discussed to understand how the optimal supply chain configuration would change considering resource competition. Furthermore, the design of biomass supply contract would be improved by considering the relationship among purchases prices, contract length, and supply amount.

We have developed strategic and tactical planning models for large-scale biofuels production. A detailed operational planning on farm management is proposed to develop to understand and optimize farm production activities based on the field operating data. Biomass production costs account for more than one third of system production costs. Equipment selection, technology improvement, and better operating management would facilitate to reduce biomass production costs. A biomass harvesting research group at the Energy Biosciences Institute is developing a real-time sensing and control system to improve harvesting efficiency. We are working with them to develop a detailed farm operating management model to quantify the cost reduction by implementing novel control technologies in biomass harvesting.

In addition to new model development, how to validate the existing developed models would be also important. Since there exists no commercial cellulosic biofuel facility, it would be

difficult to validate the model on a large system scale. However, by working with some existing pilot facilities, the model could be applied to evaluate whether the modeling results would improve their operating efficiency and effectiveness. Moreover, the computational tools developed in this dissertation could be cross-validated by evaluating the same system using the tools developed from other research groups such as IBSAL model (Kumar and Sokhansanj, 2007).

8.3 DECISION SUPPORT PLATFORM

The integration of BioScope application and CyberGIS-enabled decision support platform facilitates model accessibility and improve computational efficiency through the utilization of high performance cyberinfrastructure.

The web-based platform will be further integrated with a spatial-supported database that includes regional biomass production related data. Spatial-enabled interactive functions will be incorporated into the platform to allow user to define their region of study and candidates as model inputs directly from the web-based interactive map.

Developed optimization tools such as BioFeed and integrated strategic and tactical planning model will be further integrated with the platform. The web-based user interface will be further modified to improve user experience, including better results analysis and visualization tools development, historical scenario analysis results management, and raw data and results sharing function.

REFERENCES

- Aden, A., M. Ruth, K. Ibsen, J. Jechura, K. Neeves, J. Sheehan, B. Wallace, L. Montague, A. Slayton, and J. Lukas. 2002. *Lignocellulosic Biomass to Ethanol Process Design and Economics Utilizing Co-Current Dilute Acid Prehydrolysis and Enzymatic Hydrolysis of Corn Stover*. National Renewable Energy Laboratory. Report NREL/TP-510-32438, Golden, CO.
- Bhargava, H. K., D. J. Power, and D. Sun. 2007. Progress in Web-based decision support technologies. *Decision Support Systems* 43(4): 1083-1095.
- Brown, T. R. and R. C. Brown. 2013. A review of cellulosic biofuel commercial-scale projects in the United States. *Biofuels, Bioproducts and Biorefining* 7(3): 235-245.
- Brummer, E., C. Burras, M. Duffy, and K. Moore. 2000. Switchgrass production in Iowa: economic analysis, soil suitability, and varietal performance. *Iowa State University, Ames, Iowa*.
- Campbell, K. 2007. A feasibility study guide for an agricultural biomass pellet company. *Agricultural Utilization Research Institute, USA*.
- Chemical Engineering. 2010. *Chemical Engineering Plant Cost Index*. Available at: <http://www.che.com>. Accessed 3 June 2012.
- Chen, C. and Y. Fan. 2012. Bioethanol supply chain system planning under supply and demand uncertainties. *Transportation Research Part E: Logistics and Transportation Review* 48(1): 150-164.

Chen, P. and J. M. Pinto. 2008. Lagrangean-based techniques for the supply chain management of flexible process networks. *Computers & Chemical Engineering* 32(11): 2505-2528.

Church, R. L., A. T. Murray, M. A. Figueroa, and K. H. Barber. 2000. Support system development for forest ecosystem management. *European Journal of Operational Research* 121(2): 247-258.

Dwivedi, P., J. R. Alavalapati, and P. Lal. 2009. Cellulosic ethanol production in the United States: Conversion technologies, current production status, economics, and emerging developments. *Energy for Sustainable Development* 13(3): 174-182.

Ebadian, M., T. Sowlati, S. Sokhansanj, L. Townley-Smith, and M. Stumborg. 2012. Modeling and analysing storage systems in agricultural biomass supply chain for cellulosic ethanol production. *Applied Energy* 102:840-849.

Eksioglu, S. D., A. Acharya, L. E. Leightley, and S. Arora. 2009. Analyzing the design and management of biomass-to-biorefinery supply chain. *Computers & Industrial Engineering* 57(4): 1342-1352.

EPA. 2010. *Renewable Fuel Standard*. Washington, DC: US EPA. Available at: <http://www.epa.gov/otaq/fuels/renewablefuels/index.htm>. Accessed 5 December 2011.

Eranki, P. L., B. D. Bals, and B. E. Dale. 2011. Advanced Regional Biomass Processing Depots: a key to the logistical challenges of the cellulosic biofuel industry. *Biofuels, Bioproducts and Biorefining* 5(6): 621-630.

ESRI. 2013. ArcGIS Desktop, Release 10. Redlands, CA.: Environmental Systems Research Institute.

Fisher, M. L. 1985. An applications oriented guide to Lagrangian relaxation. *Interfaces* 15(2): 10-21.

Fleisher, D. H., K. C. Ting, and G. A. Giacomelli. 2002. Decision Support Software for Phytoremediation Systems Using Rhizofiltration Processes. *Transactions of the CSAE* 18: 210-215.

Frombo, F., R. Minciardi, M. Robba, F. Rosso, and R. Sacile. 2009. Planning woody biomass logistics for energy production: A strategic decision model. *Biomass and Bioenergy* 33(3): 372-383.

GAMS. 2013. GAMS for windows, Version 23.7. Washington, D.C.: GAMS Development Corporation.

Goodchild, M. F. 2000. Part 1 Spatial analysts and GIS practitioners. The current status of GIS and spatial analysis. *Journal of Geographical Systems* 2: 5-10.

Graham, R. L., B. C. English, and C. E. Noon. 2000. A Geographic Information System-based modeling system for evaluating the cost of delivered energy crop feedstock. *Biomass and Bioenergy* 18(4): 309-329.

Huang, Y., C. Chen, and Y. Fan. 2010. Multistage optimization of the supply chains of biofuels. *Transportation Research Part E: Logistics and Transportation Review* 46(6): 820-830.

Hess, J. R., C. T. Wright, and K. L. Kenney. 2007. Cellulosic biomass feedstocks and logistics for ethanol production. *Biofuels, Bioproducts and Biorefining* 1:181-190.

Humbird, D, R. Davis, L. Tao, C. Kinchin, D. Hsu, A. Aden, P. Schoen, J. Lukas, B. Olthof, M. Worley, D. Sexton, and D. Dudgeon. 2011. *Process design and economics for biochemical conversion of lignocellulosic biomass to ethanol: Dilute-acid pretreatment and enzymatic hydrolysis of corn stover*. Report NREL/TP-5100-47764, Golden, CO.: National Renewable Energy Laboratory.

Jain, A. K., M. Khanna, M. Erickson, and H. Huang. 2010. An integrated biogeochemical and economic analysis of bioenergy crops in the Midwestern United States. *GCB Bioenergy* 2(5): 217-234.

Kadam, K. L. and J. D. McMillan. 2003. Availability of corn stover as a sustainable feedstock for bioethanol production. *Bioresource Technology* 88(1): 17-25.

Khanna, M., B. Dhungana, and J. Clifton-Brown. 2008. Costs of producing miscanthus and switchgrass for bioenergy in Illinois. *Biomass and Bioenergy* 32(6): 482-493.

Kim, J., M. J. Realff, J. H. Lee, C. Whittaker, and L. Furtner. 2011. Design of biomass processing network for biofuel production using an MILP model. *Biomass and Bioenergy* 35(2): 853-871.

Kocoloski, M., W. Michael Griffin, and H. Scott Matthews. 2011. Impacts of facility size and location decisions on ethanol production cost. *Energy Policy* 39(1): 47-56.

Kumar, A. and S. Sokhansanj. 2007. Switchgrass (*Panicum virgatum*, L.) delivery to a biorefinery using integrated biomass supply analysis and logistics (IBSAL) model. *Bioresource Technology* 98(5): 1033-1044.

Kumar, A., J. B. Cameron, and P. C. Flynn. 2005. Pipeline transport and simultaneous saccharification of corn stover. *Bioresource Technology* 96(7): 819-829.

Leboreiro, J. and A. K. Hilaly. 2011. Biomass transportation model and optimum plant size for the production of ethanol. *Bioresource Technology* 102(3): 2712-2723.

Leduc, S., F. Starfelt, E. Dotzauer, G. Kindermann, I. McCallum, M. Obersteiner, and J. Lundgren. 2010. Optimal location of lignocellulosic ethanol refineries with polygeneration in Sweden. *Energy* 35(6): 2709-2716.

Liao, Y. 2011. *Decision support for biomass feedstock production enabled by concurrent science, engineering and technology (ConSEnT)*. University of Illinois, Champaign, IL.

Lin, T., L. F. Rodríguez, Y. N. Shastri, A. C. Hansen, and K. C. Ting. 2012. *Biomass-ethanol supply chain optimization: dynamic facility location planning under changing supply and demand*. 2012 ASABE Annual International Meeting, Dallas, TX.

Lin, T., L. F. Rodríguez, Y. N. Shastri, A. C. Hansen, and K. C. Ting. 2013. GIS-enabled biomass-ethanol supply chain optimization: Model development and *Miscanthus* application. *Biofuels, Bioproducts and Biorefining* 7(3): 314-333.

- Mahmudi, H. and P. C. Flynn. 2006. Rail vs truck transport of biomass. *Applied Biochemistry and Biotechnology* 129-13288-103.
- Mari, R., L. Bottai, C. Busillo, F. Calastrini, B. Gozzini, and G. Gualtieri. 2011. A GIS-based interactive web decision support system for planning wind farms in Tuscany (Italy). *Renewable Energy* 36(2): 754-763.
- Miao, Z., Y. Shastri, T. E. Grift, A. C. Hansen, and K. C. Ting. 2012. Lignocellulosic biomass feedstock transportation alternatives, logistics, equipment configurations, and modeling. *Biofuels, Bioproducts and Biorefining* 6(3): 351-362.
- Morrow, W. R., W. M. Griffin, and H. S. Matthews. 2006. Modeling switchgrass derived cellulosic ethanol distribution in the United States. *Environmental Science & Technology* 40(9): 2877-2886.
- Noon, C. E., F. B. Zhan, and R. L. Graham. 2002. GIS-based analysis of marginal price variation with an application in the identification of candidate ethanol conversion plant locations. *Networks and Spatial Economics* 2(1): 79-93.
- Panichelli, L. and E. Gnansounou. 2008. GIS-based approach for defining bioenergy facilities location: A case study in Northern Spain based on marginal delivery costs and resources competition between facilities. *Biomass and Bioenergy* 32(4): 289-300.
- Park, J. B. 1984. *Biomaterials and Science and Engineering*, Wiley-Interscience: New York.

- Parker, N., P. Tittmann, Q. Hart, R. Nelson, K. Skog, A. Schmidt, E. Gray, and B. Jenkins. 2010. Development of a biorefinery optimized biofuel supply curve for the Western United States. *Biomass and Bioenergy* 34(11): 1597-1607.
- Perimenis, A., H. Walimwipi, S. Zinoviev, F. Müller-Langer, and S. Miertus. 2011. Development of a decision support tool for the assessment of biofuels. *Energy Policy* 39(3): 1782-1793.
- Perrin, R., K. Vogel, M. Schmer, and R. Mitchell. 2008. Farm-scale production cost of switchgrass for biomass. *BioEnergy Research* 1(1): 91-97.
- Peters, M. S. and D. K. Timmerhaus. 1991. *Plant Design and Economics for Chemical Engineers*. McGraw-Hill: New York.
- Prindezis, N. and C. Kiranoudis. 2005. An internet-based logistics management system for enterprise chains. *Journal of Food Engineering* 70(3): 373-381.
- Ray, J. J. 2007. A web-based spatial decision support system optimizes routes for oversize/overweight vehicles in Delaware. *Decision Support Systems* 43(4): 1171-1185.
- RFA, 2012. *2012 Ethanol Industry Outlook*. Washington, DC: Renewable Fuels Association. Available at: http://ethanolrfa.3cdn.net/d4ad995ffb7ae8fbfe_1vm62ypzd.pdf. Accessed on 4 April 2012.
- Rodríguez, L., S. Kang, and K. Ting. 2003. Top-level modeling of an als system utilizing object-oriented techniques. *Advances in Space Research* 31(7): 1811-1822.

- Santos, L., J. Coutinho-Rodrigues, and C. H. Antunes. 2011. A web spatial decision support system for vehicle routing using Google Maps. *Decision Support Systems* 51(1): 1-9.
- Searcy, E., P. Flynn, E. Ghafoori, and A. Kumar. 2007. The relative cost of biomass energy transport. *Applied Biochemistry and Biotechnology* 137(1-12): 639-652.
- Shastri, Y. N., A. C. Hansen, L. F. Rodríguez, and K. C. Ting. 2010. Optimization of miscanthus harvesting and handling as an energy crop: BioFeed model application. *Biological Engineering* 3(2): 37-69.
- Shastri, Y. N., A. C. Hansen, L. F. Rodríguez, and K. C. Ting. 2011. Development and application of BioFeed model for optimization of herbaceous biomass feedstock production. *Biomass and Bioenergy* 35(7): 2961-2974.
- Shastri, Y. N., L. F. Rodríguez, A. C. Hansen, and K. C. Ting. 2012a. Impact of distributed storage and pre-processing on Miscanthus production and provision systems. *Biofuels, Bioproducts and Biorefining* 6(1): 21-31.
- Shastri, Y. N., A. C. Hansen, L. F. Rodríguez, and K. C. Ting. 2012b. Impact of probability of working day on planning and operation of biomass feedstock production systems. *Biofuels, Bioproducts and Biorefining* 6(3): 281-291.
- Simao, A., P. J. Densham, and M. Haklay. 2009. Web-based GIS for collaborative planning and public participation: An application to the strategic planning of wind farm sites. *Journal of Environmental Management* 90(6): 2027-2040.

Sokhansanj, S. and A. Turhollow. 2004. Biomass densification-cubing operations and costs for corn stover. *Applied Engineering in Agriculture* 20(4): 495-502.

Sokhansanj, S., A. Kumar, and A. F. Turhollow. 2006. Development and implementation of integrated biomass supply analysis and logistics model (IBSAL). *Biomass and Bioenergy* 30(10): 838-847.

Sokhansanj, S., S. Mani, A. Turhollow, A. Kumar, D. Bransby, L. Lynd, and M. Laser. 2009. Large-scale production, harvest and logistics of switchgrass (*Panicum virgatum* L.)—current technology and envisioning a mature technology. *Biofuels, Bioproducts and Biorefining* 3(2): 124-141.

Stewart, C. A., S. Simms, B. Plale, M. Link, D. Y. Hancock, and G. C. Fox. 2010. What is cyberinfrastructure. In *Proceedings of the 38th annual fall conference on SIGUCCS*, 37-44. ACM.

Sugumaran, V. and R. Sugumaran. 2007. Web-based Spatial Decision Support Systems (WebSDSS): evolution, architecture, examples and challenges. *Communications of the Association for Information Systems* 19:844-875.

Tang, W. and S. Wang. 2009. HPABM: A Hierarchical Parallel Simulation Framework for Spatially-explicit Agent-based Models. *Transactions in GIS* 13(3): 315-333.

Tatsiopoulou, I. P. and A. J. Tolis. 2003. Economic aspects of the cotton-stalk biomass logistics and comparison of supply chain methods. *Biomass and Bioenergy* 24(3): 199-214.

Ting, K.C., D. H. Fleisher, and L. F. Rodríguez. 2003. Concurrent science and engineering for phytomation systems. *農業氣象* 59(2): 93-101.

Tittmann, P., N. Parker, Q. Hart, and B. Jenkins. 2010. A spatially explicit techno-economic model of bioenergy and biofuels production in California. *Journal of Transport Geography* 18(6): 715-728.

USDA. 2007. *Agricultural Prices, Prices Paid: Indexes by Farm Type by Year, US*. Washington, D.C.: USDA National Agricultural Statistics Service. Available at: www.nass.usda.gov. Accessed 23 April 2012.

USDA. 2010. *2007 Census Report. The Census of Agriculture*. Washington, D.C.: USDA National Agricultural Statistics Service. Available at: www.agcensus.usda.gov. Accessed 23 April 2012.

US Census Bureau. 2011. *2010 Topologically Integrated Geographic Encoding and Referencing system*. Washington, D.C.: U.S. Census Bureau. Available at: www.census.gov/geo/tiger/. Accessed 3 May 2012.

US Census Bureau. 2012. 2010 Census. Washington, D.C.: U.S. Census Bureau. Available at: www.census.gov. Accessed 10 May 2012.

US Department of Labor. 2010. *Employment, Hours, and Earnings*. Washington, D.C.: US Department of Labor, Bureau of Labor Statistics. Available at: www.bls.gov/data. Accessed 7 June 2012.

US EIA, 2011. State Energy Data System. Washington, D.C.: US EIA. Available at: www.eia.gov/state/seds. Accessed 6 June 2012.

Walther, G., A. Schatka, and T. S. Spengler. 2012. Design of regional production networks for second generation synthetic bio-fuel—A case study in Northern Germany. *European Journal of Operational Research* 218(1): 280-292.

Wang, S. 2010. A CyberGIS framework for the synthesis of cyberinfrastructure, GIS, and spatial analysis. *Annals of the Association of American Geographers* 100(3): 535-557.

Wang, S., L. Anselin, B. Bhaduri, C. Crosby, M. F. Goodchild, Y. Liu, and T. L. Nyerges. 2013. CyberGIS software: a synthetic review and integration roadmap. *International Journal of Geographical Information Science* DOI:10.1080/13658816.2013.776049.

Wang, S., M. P. Armstrong, J. Ni, and Y. Liu. 2005. GISolve: A Grid-based Problem Solving Environment for Computationally Intensive Geographic Information Analysis. In *Proceedings of the 14th International Symposium on High Performance Distributed Computing (HPDC-14) – Challenges of Large Applications in Distributed Environments (CLADE) Workshop*, 3-12. Research Triangle Park, North Carolina, USA: IEEE Press.

Wang, S., and Y. Liu. 2009. TeraGrid GIScience Gateway: Bridging Cyberinfrastructure and GIScience. *International Journal of Geographical Information Science* 23 (5): 631-656.

Wang, S., N. R. Wilkins-Diehr, and T. L. Nyerges. 2012. CyberGIS – Toward Synergistic Advancement of Cyberinfrastructure and GIScience: A Workshop Summary. *Journal of Spatial Information Science* 4: 125-148.

Wang, S. and X. Zhu. 2008. Coupling cyberinfrastructure and geographic information systems to empower ecological and environmental research. *Bioscience* 58(2): 94-95.

Yan, J., M. K. Cowles, S. Wang, and M. P. Armstrong. 2007. Parallelizing MCMC for Bayesian spatiotemporal geostatistical models. *Statistics and Computing* 17(4): 323-335.

You, F., I. E. Grossmann, and J. M. Wassick. 2010. Multisite capacity, production, and distribution planning with reactor modifications: MILP model, bilevel decomposition algorithm versus Lagrangean decomposition scheme. *Industrial & Engineering Chemistry Research* 50(9): 4831-4849.

Zhang, J., A. Osmani, I. Awudu, and V. Gonela. 2013. An integrated optimization model for switchgrass-based bioethanol supply chain. *Applied Energy* 102:1205-1217.

Zhu, X., X. Li, Q. Yao, and Y. Chen. 2011. Challenges and models in supporting logistics system design for dedicated-biomass-based bioenergy industry. *Bioresource Technology* 102(2): 1344-1351.

APPENDIX A

SUPPLEMENTARY MATERIALS FOR BIOSCOPE

MODEL

Table A.1: A list of model inputs with each description, unit, value, and source

Symbol	Description	Unit	Value	Source
b^i	Biomass availability at county level	Mg	Figure 3.3	USDA (2010) and Jain et al (2010)
c^i	Biomass purchase cost at county level	\$ Mg ⁻¹	Figure 3.4	Shastri et al (2010) and USDA (2010)
P	Total biomass required for processing	Mg	2,000,000	User defined
$d^{i,j}$	Distance between biomass supply sites and centralized storage and preprocessing (CSP) sites	km		US Census Bureau (2011)
$d^{j,k}$	Distance between CSP sites and biorefinery sites	km		US Census Bureau (2011)
s_{op}	Unit operating costs for CSP	\$ Mg ⁻¹	9.95	Hess et al (2007)
s_v^l	Variable capital costs for CSP at different levels	\$ Mg ⁻¹	Table A.3	
s_f^l	Fixed capital costs for CSP at different levels	\$	Table A.3	
λ_s^l	High-end capacity limit of a CSP at capacity level l	Mg	Table A.3	
α	Annualized cost factor		13.7%	User defined
β	Biomass loss rate at CSP		5%	User defined
e_{op}	Unit operating costs for a biorefinery	\$ Mg ⁻¹	48	Humbird et al (2011)

Table A.1 (cont.)

e_v^l	Variable capital costs for a biorefinery at different levels	\$ Mg ⁻¹	Table A.4
e_f^l	Fixed capital costs for a biorefinery at different levels	\$	Table A3.4
λ_e^l	High-end capacity limit of a biorefinery at capacity level l	Mg	Table A3.4

Table A.2: A list of decision variables in the model, with the nomenclature used in equations, a description of the type of variable, and a description of the meaning of each variable

Symbol	Type	Description
$f^{i,j}$	Non-negative continuous variable	Amount of biomass flow from supply to CSP
$f^{j,k}$	Non-negative continuous variable	Amount of biomass flow from CSP to biorefinery
p^j	Non-negative continuous variable	The total centralized storage and preprocessing (CSP) facility capacity in county j
o_s^j	Binary variable	Indicates whether there is a CSP facility located in county j
$p^{j,l}$	Non-negative continuous variable	The CSP facility capacity in county j at level l
$o_s^{j,l}$	Binary variable	Indicates whether there is a CSP facility located in county j at level l
q^k	Non-negative continuous variable	The total biorefinery capacity in county k
o_s^k	Binary variable	Indicates whether there is a biorefinery facility located in county k
$q^{k,l}$	Non-negative continuous variable	The biorefinery capacity in county k at level l
$o_e^{k,l}$	Binary variable	Indicate whether there is a biorefinery facility located in county k at level l

Table A.3: Estimated capital investment costs for centralized storage and preprocessing (CSP) are estimated using a piecewise linear approximation of the power law with a scaling factor of 0.7. Three capacity level ranges are defined for each linear approximation: small, medium, and large. Fixed and variable costs are defined as a function of the capacity level.

Capacity level of a CSP facility	Lower limit of the range (λ_s^0) (Mg y ⁻¹)	Upper limit of the range (λ_s^l) (Mg y ⁻¹)	Variable capital investment costs (\$ Mg ⁻¹)	Fixed capital investment costs (\$)
Small ($l=1$)	50,000	600,000	24.31	2,521,900
Medium ($l=2$)	600,000	1,300,000	16.94	6,697,000
Large ($l=3$)	1,300,000	2,000,000	14.32	9,996,800

Table A.4: Estimated capital investment costs for biorefineries are estimated using a piecewise linear approximation of the power law with a scaling factor of 0.7. Three capacity level ranges are defined for each linear approximation: small, medium, and large. Fixed and variable costs are defined as a function of the capacity level.

Capacity level of a biorefinery	Lower limit of the range (λ_e^0) (Mg y ⁻¹)	Upper limit of the range (λ_e^l) (Mg y ⁻¹)	Variable capital investment costs (\$ Mg ⁻¹)	Fixed capital investment costs (\$)
Small ($l=1$)	50,000	600,000	518.83	53,823,000
Medium ($l=2$)	600,000	1,300,000	361.6	142,928,000
Large ($l=3$)	1,300,000	1,900,000	308.31	209,270,000

To consider a scenario where variable cropland usage rates might occur, several new constraint equations were defined. In this case, up to 10% of cropland usage rate is assumed for a supply county if it lies within a distance of 80 km served by a centralized storage and preprocessing (CSP) facility, up to 7% at a distance between 80 and 160 km, and 5% at a distance beyond 160 km. To enable the study of variable cropland usage rates the previous approach to determining biomass availability (Eq. 3.4) is replaced with the approach defined here (Table A.5, Eq. A.4a-A.4f).

Table A.5: The nomenclature and definition of additional binary variables for the study of variable cropland usage rates within supply counties, as a function of its distance to a CSP facility.

Symbol	Type	Description
$\delta_1^{i,j}$	Binary variable	Indicates whether supply county i is located within a distance of 160 km to a CSP facility located in county j
ϕ_1^i	Binary variable	Indicates whether supply county i is located within a distance of 160 km to a CSP facility that serves
$\delta_2^{i,j}$	Binary variable	Indicates whether supply county i is located within a distance of 80 km to a CSP facility located in county j
ϕ_2^i	Binary variable	Indicates whether supply county i is located within a distance of 80 km to a CSP facility that serves
η^i	Binary variable	The cropland usage rate for supply county i

Distances from the supply sites to the CSP ($d^{i,j}$), calculated via ArcGIS using existing road network data, are used to determine whether a supply county is close to a CSP facility. If so, the supply county is labeled ($\delta_1^{i,j}$) if it is located with 160 km (Eq. A.4a). If the supply county is also within 80 km (Eq. A.4c) it is labeled ($\delta_2^{i,j}$) as being both with 80 and 160 km. It is possible

that a supply county may serve more than one CSP facility, thus it is necessary to ensure that if it is within the range of at least one CSP facility, at either 80 or 160 km, then it is necessary to ensure that its cropland usage rate is allowed to vary to the rate associated with the closest CSP (Eq. A.4b and A.4d). Therefore, cropland usage rate (η^i) is estimated (Eq. A.4e) and used to adjust biomass availability (b^i) within each county (Eq. A.4f).

$$\delta_1^{i,j} \leq \left(\frac{160}{d^{i,j}}\right) * o_s^j \quad (\text{A.4a})$$

$$\sum_j \delta_1^{i,j} \geq \phi_1^i \quad (\text{A.4b})$$

$$\delta_2^{i,j} \leq \left(\frac{80}{d^{i,j}}\right) * o_s^j \quad (\text{A.4c})$$

$$\sum_j \delta_2^{i,j} \geq \phi_2^i \quad (\text{A.4d})$$

$$\eta^i = 0.05 + 0.02\phi_1^i + 0.03\phi_2^i \quad (\text{A.4e})$$

$$\sum_j f^{i,j} \leq b^i * \eta^i \quad (\text{A.4f})$$

APPENDIX B

SUPPLEMENTARY MATERIALS FOR DYNAMIC BIOSCOPE MODEL

Table B.1: A list of sets and indices used in the model

Index	Set name and element labels
<i>i</i>	Biomass supply county, where $i \in I$
<i>j</i>	CSP facility location, where $j \in J$
<i>k</i>	Biorefinery facility location, where $k \in K$
<i>t</i>	Biomass delivery time, where $t \in T$.
<i>tc</i>	Contract signed time, where $tc \in T$.
<i>l</i>	Capacity scale for a facility, where $l \in L$

The biomass delivery time during a contract period (T^{tc}) is a subset of T and it is related to the contract signing time and the length of the contract. For example, if $T = 2012, 2013, \dots, 2022$, a 11-yr contract signed in year 2014 ($tc = 2014$), then $T^{tc} = 2014, 2015, \dots, 2022$.

Table B.2: A list of decision variables

Decision Variables	Description
$f^{i,j,t,tc}$	The amount of biomass supplied from supply county i to CSP facility j during year t by the contract signed in year tc
$b^{i,t}$	The amount of biomass from supply county i during year t
$f^{j,k,t}$	The amount of biomass supplied from CSP facility j to biorefinery k during year t
$p^{j,l,t}$	The annual production capacity of a CSP facility at capacity level l located in county j during year t
$P^{j,t}$	The annual production capacity of a CSP facility located in county j during year t
$o_s^{j,t}$	Binary variable: whether a CSP facility is located in county j during year t
$o_s^{j,l,t}$	Binary variable: whether a capacity level l of the CSP facility is located in county j during year t

Table B.3: A list of model inputs with each description and source

Input Parameters	Description	Source for case study
$c^{i,t}$	Biomass procurement costs in county i during year t (\$ Mg ⁻¹)	Lin et al., 2013
P^t	The total system biomass demand during year t (Mg)	User defined
A^i	Cropland area in county i (ha)	USDA, 2010
Y^i	Biomass yield in county i (Mg ha ⁻¹)	Jain et al., 2010
$U^{i,t}$	Cropland usage rate in county i during year t	User defined
T_{v1}	Unit variable transportation cost for unprocessed biomass between biomass supply counties and CSP facilities (\$ Mg ⁻¹ km ⁻¹)	Kumar et al., 2005
T_{v2}	Unit variable transportation cost for processed biomass between CSP facilities and biorefineries (\$ Mg ⁻¹ km ⁻¹)	Lin et al., 2013
T_{f1}	Unit fixed transportation cost for unprocessed biomass between biomass supply counties and CSP facilities (\$ Mg ⁻¹)	Kumar et al., 2005
T_{f2}	Unit fixed transportation cost for processed biomass between CSP facilities and biorefineries (\$ Mg ⁻¹)	Lin et al., 2013
$d^{i,j}$	Transportation distance between biomass supply counties and CSP facilities (km)	US Census Bureau, 2011
$d^{j,k}$	Transportation distance between CSP facilities and biorefineries (km)	US Census Bureau, 2011
s_f^l	Fixed capital investment costs for a CSP facility at capacity scale l (\$)	Lin et al., 2013
s_v^l	Variable capital investment costs for a CSP facility at capacity scale l (\$ Mg ⁻¹)	Lin et al., 2013

Table B.4: The amount of biomass supply from all selected biomass supply counties during the period from 2012 to 2022 for the 1-year contract scenario.

	2012	2013	2014	2015	2016	2017	2018	2019	2020	2021	2022	Grand Total
Bond	29,105		116,420		232,841	134,886					582,101	1,095,353
Champaign									360,222	249,000	137,778	747,000
Clay	25,955	33,058									519,107	578,121
Clinton	36,149		144,596	216,894	289,192	361,490	433,788	506,086	578,384	650,681	439,817	3,657,075
Crawford											503,162	503,162
Edgar									393,459	393,459	393,459	1,180,377
Edwards	15,307										11,201	26,508
Effingham							353,063	411,907	470,751	529,595	588,439	2,353,756
Fayette	36,545		146,182		269,068		438,545	511,635	584,726	603,184	730,908	3,320,792
Franklin	28,893	57,787	115,574	173,361	231,148	247,327	346,722	324,063	462,296	520,082	577,869	3,085,122
Gallatin									34,715	34,715	558,459	627,889
Greene					235,200	294,000	352,799	406,063	179,930			1,467,991
Hamilton	30,118	60,236	120,472	180,707	72,714		185,332		94,283		602,358	1,346,218
Jackson	28,448		113,791	170,687	227,582	284,478	341,373	398,269	455,164	512,060	568,955	3,100,806
Jasper											600,000	600,000
Jefferson	28,267	56,535	113,069	169,604	226,139	282,673	339,208	395,743	452,277	508,812	565,347	3,137,674
Jersey					177,008	221,260	265,512	309,764	354,016	350,689	167,432	1,845,679
Johnson	8,700						104,400	121,800	139,200	156,600	174,000	704,702
Macoupin					377,091	471,364	565,637	659,910	754,183	848,456	942,729	4,619,371
Madison					322,857	403,571	280,772				600,000	1,607,199
Marion	31,654	63,307	126,614	189,922	253,229	316,536	379,843	426,529	377,253		200,000	2,364,887
Monroe			88,359	39,733	176,719				353,437	397,617	441,796	1,497,661
Montgomery					355,936	444,920	533,904	622,888	711,872	800,856	889,839	4,360,213
Moultrie							251,621	23,328	173,660		405,016	853,625
Perry	26,813	53,626	107,252	160,878	214,504	268,130	321,755	375,381	429,007	482,633	536,259	2,976,238
Pope									81,801			81,801
Randolph	31,389		125,554	188,331	251,108	169,560	271,467		502,217	564,994	600,000	2,704,620
Richland	503											503
Saline	15,694						188,328	219,716	251,104	282,492	313,880	1,271,213
Shelby							578,147	674,505	770,863	867,221	963,579	3,854,314
St-Clair			168,541		107,821				88,359	44,180		408,901
Union	12,335						148,015	172,684	197,354	222,023	246,692	999,103
Vermilion									889,778	1,001,000	1,112,222	3,003,000
Washington	49,429	98,858	197,716	296,573	395,431	494,289	593,147	692,004	790,862	889,720	988,578	5,486,606
Wayne	42,745	85,490	123,653									251,888
White	41,399										827,982	869,381
Williamson	10,552	21,104	42,207	63,311	84,414	105,518	126,622	147,725	168,829	189,932	211,036	1,171,250
Grand Total	530,000	530,000	1,850,000	1,850,000	4,500,000	4,500,000	7,400,000	7,400,000	11,100,000	11,100,000	17,000,000	67,760,000

Table B.5: The changes of capacities of all CSP facilities during the period from 2012 to 2022 for the 1-year contract scenario.

	2012	2013	2014	2015	2016	2017	2018	2019	2020	2021	2022	Grand Total
Bond											600,000	600,000
Clay											519,107	519,107
Crawford											503,162	503,162
Edgar									393,459	393,459	393,459	1,180,377
Effingham											70,043	70,043
Fayette											600,000	600,000
Gallatin									34,715	34,715	558,459	627,889
Jackson									568,955	568,955	568,955	1,706,866
Jasper											600,000	600,000
Jefferson	530,000	530,000	530,000	530,000	530,000	530,000	530,000	530,000	530,000	530,000	530,000	5,830,000
Macoupin					1,970,000	1,970,000	1,998,624	1,998,624	2,000,000	2,000,000	2,000,000	13,937,248
Madison											600,000	600,000
Marion											200,000	200,000
Monroe									441,796	441,796	441,796	1,325,389
Randolph									600,000	600,000	600,000	1,800,000
Shelby							1,621,376	1,621,376	2,000,000	2,000,000	2,000,000	9,242,752
Union											242,403	242,403
Vermilion									1,250,000	1,250,000	1,250,000	3,750,000
Washington			1,320,000	1,320,000	2,000,000	2,000,000	2,000,000	2,000,000	2,000,000	2,000,000	2,000,000	16,640,000
White											1,441,541	1,441,541
Williamson							1,250,000	1,250,000	1,281,075	1,281,075	1,281,075	6,343,225
Grand Total	530,000	530,000	1,850,000	1,850,000	4,500,000	4,500,000	7,400,000	7,400,000	11,100,000	11,100,000	17,000,000	67,760,000

Table B.6: The changes of capacities of all biorefineries facilities during the period from 2012 to 2022 for the 1-year contract scenario.

	2012	2013	2014	2015	2016	2017	2018	2019	2020	2021	2022	Grand Total
Bond											1,900,000	1,900,000
Jasper											1,607,696	1,607,696
Jefferson	503,500	503,500	503,500	503,500	503,500	503,500	503,500	503,500	503,500	503,500	503,500	5,538,500
Macoupin					1,871,500	1,871,500	1,898,693	1,898,693	1,900,000	1,900,000	1,900,000	13,240,385
Randolph									1,530,214	1,530,214	1,727,518	4,787,946
Shelby							1,540,307	1,540,307	1,900,000	1,900,000	1,900,000	8,780,615
Vermilion									1,561,286	1,561,286	1,561,286	4,683,858
Washington			1,254,000	1,254,000	1,900,000	1,900,000	1,900,000	1,900,000	1,900,000	1,900,000	1,900,000	15,808,000
White											1,900,000	1,900,000
Williamson							1,187,500	1,187,500	1,250,000	1,250,000	1,250,000	6,125,000
Grand Total	503,500	503,500	1,757,500	1,757,500	4,275,000	4,275,000	7,030,000	7,030,000	10,545,000	10,545,000	16,150,000	64,372,000

Table B.7: The amount of biomass supply from all selected biomass supply counties during the period from 2012 to 2022 for the 11-year contract scenario.

	2012	2013	2014	2015	2016	2017	2018	2019	2020	2021	2022	Grand Total
Bond			116,420	116,420	232,841	232,841	349,261	349,261	465,681	465,681	582,101	2,910,507
Calhoun											134,820	134,820
Clay	25,955	25,955	25,955	25,955	207,643	207,643	311,464	311,464	415,285	415,285	519,107	2,491,713
Clinton	15,274	15,274	15,274	15,274	15,274	15,274	15,274	15,274	15,274	15,274	111,643	264,383
Crawford					102,722	102,722	102,722	102,722	102,722	102,722	102,722	719,057
Edwards	15,307	15,307	15,307	15,307	15,307	15,307	77,877	77,877	244,918	244,918	306,148	1,043,582
Effingham					235,376	235,376	353,063	353,063	470,751	470,751	588,439	2,706,820
Fayette	36,545	36,545	105,355	105,355	292,363	292,363	438,545	438,545	584,726	584,726	730,908	3,645,974
Franklin	28,893	28,893	115,574	115,574	231,148	231,148	292,172	292,172	462,296	462,296	577,869	2,838,035
Gallatin	27,923	27,923	27,923	27,923	27,923	27,923	27,923	27,923	101,579	101,579	101,579	528,121
Greene											587,999	587,999
Hamilton	30,118	30,118	120,472	120,472	240,943	240,943	361,415	361,415	481,886	481,886	602,358	3,072,024
Jackson	28,448	28,448	113,791	113,791	227,582	227,582	341,373	341,373	455,164	455,164	568,955	2,901,672
Jasper	31,080	31,080	31,080	31,080	248,639	248,639	372,958	372,958	497,278	497,278	621,597	2,983,665
Jefferson	28,267	28,267	113,069	113,069	226,139	226,139	339,208	339,208	452,277	452,277	565,347	2,883,268
Jersey											442,520	442,520
Johnson	8,700	8,700	34,800	34,800	42,207	42,207	42,207	42,207	139,200	139,200	174,000	708,230
Macoupin							565,637	565,637	565,637	565,637	942,729	3,205,278
Madison											807,141	807,141
Marion	31,654	31,654	126,614	126,614	253,229	253,229	379,843	379,843	506,458	506,458	633,072	3,228,669
Massac									172,075	172,075	215,093	559,243
Monroe									150,895	150,895	441,796	743,585
Montgomery							533,904	533,904	711,872	711,872	889,839	3,381,390
Perry	26,813	26,813	107,252	107,252	214,504	214,504	321,755	321,755	429,007	429,007	536,259	2,734,922
Randolph	22,869	22,869	125,554	125,554	251,108	251,108	339,072	339,072	502,217	502,217	600,000	3,081,641
Richland					219,110	219,110	328,665	328,665	438,220	438,220	547,775	2,519,763
Saline	15,694	15,694	62,776	62,776	125,552	125,552	159,393	159,393	251,104	251,104	313,880	1,542,918
St-Clair											842,704	842,704
Union	12,335	12,335	49,338	49,338	98,677	98,677	98,677	98,677	197,354	197,354	246,692	1,159,452
Washington	49,429	49,429	197,716	197,716	395,431	395,431	438,121	438,121	770,993	770,993	770,993	4,474,371
Wayne	42,745	42,745	137,926	137,926	341,959	341,959	512,938	512,938	683,917	683,917	854,897	4,293,865
White	41,399	41,399	165,596	165,596	169,910	169,910	169,910	169,910	662,386	662,386	827,982	3,246,385
Williamson	10,552	10,552	42,207	42,207	84,414	84,414	126,622	126,622	168,829	168,829	211,036	1,076,284
Grand Total	530,000	530,000	1,850,000	1,850,000	4,500,000	4,500,000	7,400,000	7,400,000	11,100,000	11,100,000	17,000,000	67,760,000

Table B.8: The changes of capacities of all CSP facilities during the period from 2012 to 2022 for the 11-year contract scenario.

	2012	2013	2014	2015	2016	2017	2018	2019	2020	2021	2022	Grand Total
Bond			116,420	116,420	232,841	232,841	234,363	234,363	465,681	465,681	582,101	2,680,710
Clay					721,506	721,506	721,506	721,506	721,506	721,506	721,506	5,050,541
Edwards									244,918	244,918	306,148	795,984
Effingham					235,376	235,376	235,376	235,376	368,333	368,333	588,439	2,266,608
Fayette							600,000	600,000	600,000	600,000	875,623	3,275,623
Franklin					292,172	292,172	292,172	292,172	462,296	462,296	577,869	2,671,150
Gallatin									101,579	101,579	101,579	304,737
Greene											587,999	587,999
Hamilton	434,217	434,217	530,000	530,000	530,000	530,000	530,000	530,000	530,000	530,000	600,000	5,708,435
Jackson					326,259	326,259	326,259	326,259	455,164	455,164	568,955	2,784,319
Jasper	31,080	31,080	31,080	31,080	351,361	351,361	475,681	475,681	600,000	600,000	600,000	3,578,403
Jefferson							218,978	218,978	404,163	404,163	565,347	1,811,630
Jersey											577,339	577,339
Johnson									139,200	139,200	174,000	452,401
Macoupin							565,637	565,637	565,637	565,637	600,000	2,862,549
Madison											807,141	807,141
Marion			257,924	257,924	282,464	282,464	282,464	282,464	506,458	506,458	600,000	3,258,619
Massac									172,075	172,075	215,093	559,243
Monroe									150,895	150,895	441,796	743,585
Montgomery							600,000	600,000	711,872	711,872	1,232,568	3,856,311
Perry			462,962	462,962	462,962	462,962	462,962	462,962	600,000	600,000	600,000	4,577,775
Randolph			125,554	125,554	251,108	251,108	339,072	339,072	502,217	502,217	600,000	3,035,904
Richland					234,417	234,417	234,417	234,417	234,417	234,417	469,695	1,876,198
Saline							101,579	101,579	251,104	251,104	313,880	1,019,245
St-Clair											949,955	949,955
Union									197,354	197,354	246,692	641,399
Washington	64,703	64,703	326,059	326,059	410,705	410,705	410,705	410,705	600,000	600,000	600,000	4,224,344
Wayne							600,000	600,000	683,917	683,917	857,254	3,425,089
White									662,386	662,386	827,982	2,152,753
Williamson					168,829	168,829	168,829	168,829	168,829	168,829	211,036	1,224,009
Grand Total	530,000	530,000	1,850,000	1,850,000	4,500,000	4,500,000	7,400,000	7,400,000	11,100,000	11,100,000	17,000,000	67,760,000

Table B.9: The changes of capacities of all biorefineries facilities during the period from 2012 to 2022 for the 11-year contract scenario.

	2012	2013	2014	2015	2016	2017	2018	2019	2020	2021	2022	Grand Total
Clay					1,900,000	1,900,000	1,900,000	1,900,000	1,900,000	1,900,000	1,900,000	13,300,000
Fayette											1,900,000	1,900,000
Hamilton	503,500	503,500	503,500	503,500	503,500	503,500	600,000	600,000	600,000	600,000	600,000	6,021,000
Jasper							600,000	600,000	600,000	600,000	600,000	3,000,000
Jersey											1,520,000	1,520,000
Lake							130,000	130,000	130,000	130,000	130,000	650,000
Montgomery							1,900,000	1,900,000	1,900,000	1,900,000	1,900,000	9,500,000
Perry			1,254,000	1,254,000	1,871,500	1,871,500	1,900,000	1,900,000	1,900,000	1,900,000	1,900,000	15,751,000
St-Clair											1,900,000	1,900,000
Wayne									1,900,000	1,900,000	1,900,000	5,700,000
Williamson									1,615,000	1,615,000	1,900,000	5,130,000
Grand Total	503,500	503,500	1,757,500	1,757,500	4,275,000	4,275,000	7,030,000	7,030,000	10,545,000	10,545,000	16,150,000	64,372,000

APPENDIX C

SUPPLEMENTARY MATERIALS FOR INTEGRATED OPTIMIZATION MODEL

Table C.1: A list of sets and indices used in the model

Set	Set name and element labels
I	Biomass supply county, where $i \in I$
J	Farm, where $j \in J$
K	CSP facility location, where $k \in K$
L	Biorefinery location, where $l \in L$
B	Blending location, where $b \in B$
E	Ethanol consumption county, where $e \in E$
T	Time period, where $t \in T$. t^h is an element representing the end of the harvesting season and t^e is an element representing the end of the simulation cycle.
M	Type of equipment, where $m \in M$. m_f is a subset of M representing farming equipment and m_v is a subset of M representing road vehicles.
S	Capacity scale for a facility, where $s \in S$

Table C.2: A list of decision variables used in the model

Decision Variables	Description
F_f^{i,j,m_f}	The number of each type of equipment required for farm j in county i
$P_f^{i,j,m_f,t}$	The operating hours of each type of equipment required for farm j in county i at time period t
$B_{f_g}^{i,j,t}$	The amount of biomass delivered to the gate of farm j in county i at time period t (Mg d ⁻¹)
$H^{i,j,t}$	The cumulative harvested area for farm j in county i until the end of time period t (km ²)
$I_f^{i,j,t}$	The biomass inventory data for farm j in county i at the end of time period t
$D^{i,j,k,t}$	The amount of biomass delivered from farm j in county i to CSP facility k at time period t (Mg d ⁻¹)
$F_v^{m_v}$	The required fleet size of each type of vehicle
$T^{i,j,k,m_v,t}$	The number of trips required from farm j in county i to CSP facility at county k by vehicle type m_v at time period t
$T^{k,l,m_v,t}$	The number of trips required from CSP facility in county k to biorefinery in county l at time period t by vehicle type m_v
$N_v^{m_v,t}$	The number of vehicle type m_v required at time period t
$C_p^{k,s}$	The capacity of CSP facility in county k at the capacity scale s (Mg d ⁻¹)
$A_p^{k,t}$	The amount of biomass received by CSP facility in county k during time period t (Mg d ⁻¹)
$P_p^{k,t}$	The amount of biomass preprocessed by CSP facility in county k during time period t (Mg d ⁻¹)
$Q_p^{k,t}$	The unprocessed biomass feedstock inventory for CSP facility located in county k at the end of time period t
$I_p^{k,t}$	The preprocessed biomass inventory data for CSP facility located in county k at the end of time period t

Table C.2 (cont.)

$D^{k,l,t}$	The amount of biomass delivered from CSP facility in county k to biorefinery in county l at time period t (Mg d ⁻¹)
$P_r^{l,t}$	The amount of biomass processed by the biorefinery in county l at time period t (Mg d ⁻¹)
C_r^l	The capacity of biorefinery in county l (Mg d ⁻¹)
$D^{l,b,t}$	The amount of ethanol delivered from biorefinery in county l to blending station in county b at time period t (Mg d ⁻¹)
$D^{b,e,t}$	The amount of ethanol delivered from blending station in county b to ethanol consumption site in county e at time period t (Mg d ⁻¹)
$O_f^{i,j}$	Binary variable: Whether farm j in county i is selected for biomass production
O_p^k	Binary variable: Whether a CSP facility is located in county k
O_r^l	Binary variable: Whether a biorefinery is located in county l
$O_p^{k,s}$	Binary variable: Whether a CSP facility is located in county k at the capacity scale s
$O_r^{l,s}$	Binary variable: Whether a biorefinery is located in county l at the capacity scale s

Table C.3: A list of input parameters used in the model

Input Parameters	Description
$\mu_f^{m_f}$	The unit operating cost of each type of equipment ($\$ \text{h}^{-1}$)
$\lambda_f^{m_f}$	The annual capital related cost of each type of equipment
$\alpha^{i,j}$	The size of each farm j in county i (km^2)
τ_o^i	The unit cropland opportunity cost in county i ($\$ \text{km}^{-2}$)
η	Operating hours per day
d^{i,j,k,m_v}	The travelling time from farm j in county i to CSP facility in county k during time period t using vehicle type m_v (h)
d^{k,l,m_v}	The travelling time CSP facility in county k during time period t to biorefinery in county l using vehicle type m_v (h)
$V_w^{m_v}$	The weight limit of each type of vehicle (Mg)
$V_{vol}^{m_v}$	The volume limit of each type of vehicle (m^3)
$\lambda_v^{m_v}$	The annual capital related cost of each type of vehicle
$\mu_v^{m_v}$	The unit operating cost of each type of vehicle ($\$ \text{h}^{-1}$)
μ_{h_k}	The unit biomass handling cost at CSP facilities ($\$ \text{Mg}^{-1}$)
β	Ethanol conversion rate (gal Mg^{-1})
$\theta^{l,b}$	The distance between biorefinery location in county l to ethanol blending station in county b (km)
$\theta^{b,e}$	The distance between ethanol blending station in county b and ethanol consumption in county e (km)
$\sigma^{i,j}$	The density of delivered biomass from farm j in county i (Mg m^{-3})
$v_{p_f}^s$	The fixed capital cost to build a CSP facility at the capacity scales
$v_{p_v}^s$	The unit variable capital cost to build a CSP facility at the capacity scale s ($\$ \text{Mg}^{-1}$)
$v_{r_f}^s$	The fixed capital cost to build a biorefinery at the capacity scale s
$v_{r_v}^s$	The unit variable capital cost to build a biorefinery at the capacity scale s ($\$ \text{Mg}^{-1}$)

Table C.3 (cont.)

ω_f	The biomass loss rate occurred at farms
ω_v	The biomass loss rate occurred during transportation and handling
ω_{p1}	The unprocessed biomass loss rate during storage at CSP
ω_{p2}	The processed biomass loss rate during storage at CSP facilities
μ_r	Unit operating cost of ethanol production ($\$ \text{Mg}^{-1}$)
μ_p	Unit operating cost of preprocessing ($\$ \text{Mg}^{-1}$)
μ_{h1}	The unit biomass handling cost at biorefineries ($\$ \text{Mg}^{-1}$)
μ_d	The unit ethanol distribution cost ($\$ \text{gal}^{-1} \text{km}^{-1}$)
